UNIVERSITÀ DEGLI STUDI DI MILANO

FACOLTÀ DI SCIENZE E TECNOLOGIE

Doctorate School in Chemical Science - XXIX Cycle

Natural products as building blocks and lead compounds for API production

PhD Thesis of

Cristina MARUCCI

R10607

Tutor: Prof. Daniele Passarella

Cotutor: Dott. Marcello Luzzani

Academic Year: 2015/2016

Ai miei genitori

Summary

Abstract

This dissertetion describes the relevance of natural products as building blocks for production of active pharmaceutical ingredients (API) and as lead compounds.

Chapter 1 offers an introduction on the use of natural products as an effective therapeutic and its role on inspiring the discovery of new drugs.

Chapter 2 focuses on the importance of natural products as lead compounds for active pharmaceutical ingredients (API) production. In the first part of this chapter the synthesis of vincamine, the major indole alkaloid presents in *Vinca minor L.*, will be discussed. In particular the design of experiment (DOE) applied to the synthesis of vincamine starting from vincadifformine will be described. In the second part of this chapter the semi-synthesis of two lignan derivatives, oxomatairesinol and (-)-7-(*R*)-hydroxymatairesinol, will be reported.

Chapter 3 will focus on the isolation and structural characterization of natural products. The first part describes the isolation and structural characterization of ten indole alkaloids from *Voacanga africana* (Apocynaceae) seeds. Then the semisynthesis of two cytisine derivatives, *N*-formyl and *N*-methyl cytisine, will be described.

Chapter 4 describes the role of natural products as lead compounds. The first section illustrate a project that was performed in the laboratory of Prof. Karl-Heinz Altmann (ETH-Zurich, Switzerland) in the frame of COST Action CM1407 (Challenging Organic Synthesis Inspired By Nature: From Natural Product Chemistry To Drug Discovery). It is related to the synthesis of an analogue of the natural product doliculide, a 16-membered depsipeptide, that has been isolated in 1994 from the Japanese sea hare *Dolabella auricularia*. The second section will focus on the design and synthesis of hybrid compounds. Particularly it will describe the synthesis of pironetin-dumetorine hybrid compounds whose structures are representative of an optimizable lead scaffold for the discovery of new tubulin binders. Another topic here discussed will be the production of bivalent compounds linking two different units, a pironetin-dumetorine hybrid compound and a drug able to bind β-tubulin, in order to have a duble action with the aim to limit the the protein-protein interaction between α and β-tubulin.

Chapter 5 offers an overview on the role of natural products in drug discovery, in particular related to cancer stem cells (CSCs). In a recent review we summarized the natural products that demonstrate activity against CSCs. Forty-nine different natural products grouped into several structural classes (such as flavonoids, polyketides, terpenes, alkaloids and many others) will be described. Their structure diversity could suggest the synthesis of libraries of new compounds for a huge exploration of the chemical space of CSCs inhibitors.

1. Natural products in drug discovery

1.1. Role of nature in drug discovery

Nature is continually providing interesting inspirations for the discovery, design and synthesis of novel drugs.[1] In fact, it offers a tremendous variety of small molecules that possess fascinating structure and potent medicinal properties. The biological origin of these small molecules is as diverse as their chemical composition (Figure 1).

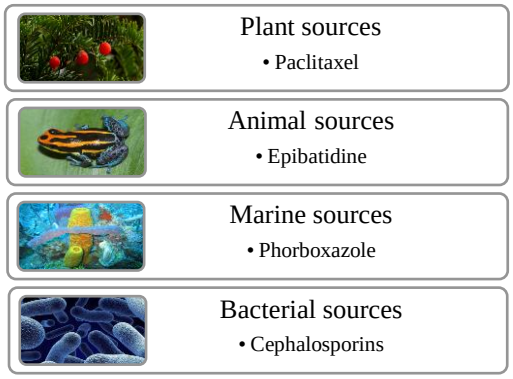

Figure 1: Examples of natural product sources

The term natural products refers to: (a) pure bioactive compounds (alkaloids, lignans, flavonoids, sugars, etc.) isolated from plants, microorganisms or animals; (b) an entire organism, for example plant or microorganism, that has not been submitted to any kind of treatment or processing except a simple process of preservation, such as drying; (c) an extract of an organism or part of an organism; (d) part of an organism (leaves or seeds of a plant).

The importance of natural products in the treatment of different human diseases is well documented. This is a demonstration of the continuing and valuable contributions of nature as a source not only of potential therapeutic agents but also of lead compounds that inspire the semisynthesis or total synthesis of effective new drugs.

[1] (a) Martin, M. E. *Org. Biomol.Chem.* **2015**, *13*, 5302–5343; (b) Cordier, C.; Morton, D.; Murrison, S.;Nelson, A.; O'Leary-Steele, C. *Nat. Prod.Rep.* **2008**, *25*, 719–737; (c) Grabowski, K.; Baringhaus,K.-H.; Schneider, G. *Nat. Prod. Rep*. **2008**, *25*, 892–904; (d) Vasilevich, N. I.; Kombarov, R. V.; Genis, D. V.; Kirpichenok, M. A. *J. Med. Chem*. **2012**, *55*, 7003–7009.

In a recent review, Cragg *et al.*[2] reported an extensively analysis of the role of natural products in the drug discovery and development process, covered the period from 1981 to 2014. In this paper, the drugs were classified as N (natural product); NB (natural product "botanical drug"); ND (a modified natural product); S (totally synthetic drug); S* (a synthetic compound with a natural product pharmacophore); S*/NM (a synthetic compound with a natural product pharmacophore showing competitive inhibition of the natural product substrate); V (vaccine); and S/NM (a synthetic compound showing competitive inhibition of the natural product substrate).

They reported that for example, in the area of cancer, the 13% of the 174 anticancer drugs approved or in clinical trials from 1981 to 2014 are classifiable into the "S" category (totally synthetic drug), while the 38.22% of the anticancer drugs are derived from a natural product using generally a semisynthetic modification (Figure 2).

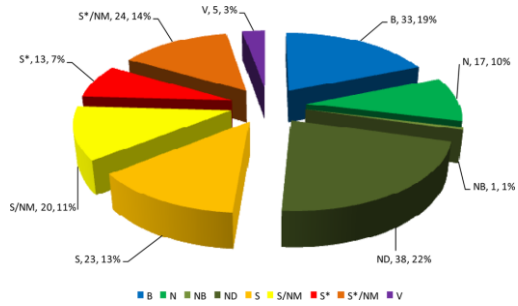

Figure 2: All anticancer drugs covering the years 1981-2014

In 2012 the Food and Drug Administration (FDA) approved two plant-derived agents, omacetaxine mepesuccinate, formerly named as homoharringtonine or HHT, for the treatment of chronic myeloid leukemia, and ingenol mebutate, named also Picato, for the topical treatment of actinic keratosis, a precancerous condition, that if untreated may turn into a type of cancer called squamous cell carcinoma (Figure 3). As natural products derivatives ("ND" category), abiraterone was approved in 2011 under the trade names Zytiga, Abiratas, Abretone, Abirapro, together with Adcetris, a dolastatin 10 derivative, which was approved in the same year. In 2012, the aminolevulinic acid hydroclochloride

[2] Newman, D.J.; Cragg, G. M. *J. Nat. Prod.* **2016**, *79*, 629−661.

Ameluz was approved for photodynamic therapy and in the same year was also approved carfilzomib under the trade name Kyprolis, for use in patients with multiple myeloma (Figure 3).

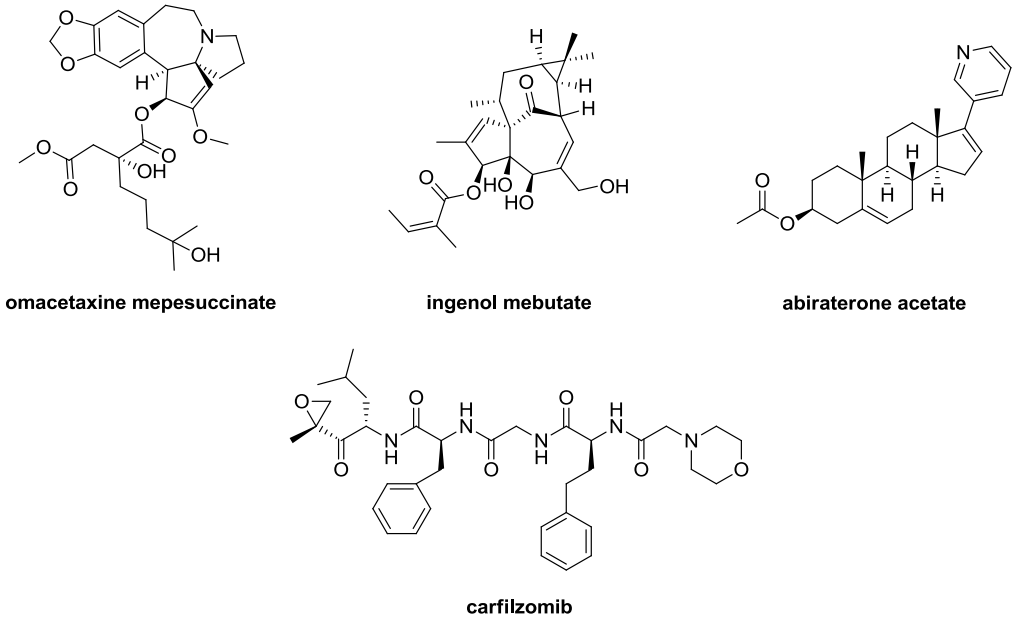

Figure 3: Novel drugs inspired by natural products

In other areas, the influence of natural product structures is quite marked, wit the anti-infective area being dependent on natural products and their structures.

Concerning the new drugs approved by FDA from 1981 until 2014, the 27% of the drugs are totally synthetic compounds, while the 21% of the drugs are natural products analogues (Figure 4).

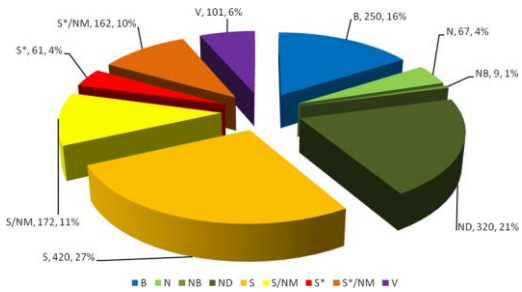

Figure 4: All new drugs from 1981 till 2014

In addition in this review it is possible to find a list of antibacterial, antifungal, antiviral, anticancer and antidiabetic drugs (filled up to 2014) arising from natural sources, illustrating in this way the continuing contribution of natural products to the expansion of the chemotherapeutic space.

Metabolomics and metagenomics are useful tools to indentify new classes of natural products.

The term metabolomics refers to the qualitative and quantitative analysis of all metabolites contained in an organism under a given set of conditions and at a specific time.[3] This stategy provides indirect monitoring of the biochemical and genetic status of an organism by examining its biochemical profile. A combination of metabolomics and genomics can be used to optimize a biosynthetic pathway to selectively produce biologically active secondary metabolites.

While metabolite analysis has been conducted for decades, recent improvements in metabolomics technologies reveal the unequivocal role of metabolomics tools in gene-function systems biology, analysis and diagnostic platforms.

Metabolomic may have diverse applications. For example, it could be used during the isolation, purification and structural elucidation of bioactive secondary metabolites for identifying the fractions for further purification, leading to save time and resources in isolating the target compounds.

[3] Hur, M.; Campbell, A. A.; Almeida-de-Macedo, M.; Li, L.; Ransom, N.; Jose, A.; Crispin, M.; Nikolau, B.J.; Wurtele, E.S. *Nat. Prod. Rep.* **2013**, *30*, 565–583.

Metabolomics can also be applied to recognize and sustain the production of interesting secondary metabolites during cultivation and production processes, and to optimize fermentation, thus assisting in improving the biosynthesis of desired products.

Along with the OSMaC (one strain, many compounds, an approach to activate metabolic pathways that can be combined with genomics scanning) approach, metabolomics can be used to explore and statistically validate relationships between culture methods, diversity, bioactivity and metabolome evolution in a microbial isolate.

Continued advancements in metabolomic technologies will give additional improvements in the utility of metabolomics tools as applied toward both medical and scientific research. With advanced spectroscopic and mass analysis, rapid accurate metabolite profiles will continue to enhance metabolomics data repositories and lead to new drug therapies, more effective diagnostics and improved disease prognosis.

Genomics and metagenomics are also interesting tools in the target-directed search of new bioactive secondary metabolites and microorganisms from different geographical areas.[4] Metagenomics approaches have now become important tools for defining, elucidating, and controlling biosynthetic pathways. The aim of these approaches is to develop an efficient heterologous gene expression platform that will facilitate the production of particular target secondary metabolites or various new natural product.

An example of the usefulness of this approach is related to the epothilones, naturally occurring polyketide macrolides originally isolated from *Sorangium cellulosum*. They posses anticancer activity and are able to act as microtubule disruptors, similarly to taxanes. Several epothilone analogues (Figure 5) are currently undergoing clinical trials: patupilone (also named as EPO-906 or epothilone B) has been through Phase III trials in the United States, and Phase III trials are ongoing in Spain, United Kingdom and Greece for the treatment of ovarian cancer.

Ixabepilone (Ixempra; Bristol-Myers Squibb), an analogue of epothilone B, has been approved by the FDA in 2007 for the treatment of breast cancer.[5] The biosynthetic gene

[4] Wilson, M. C.; Piel, J. *Chem. Biol.* **2013**, 20, 636–647.
[5] Alvarez, R. H.; Valero, V.; Hortobagyi, G. N. *Ann. Med.* **2011**, *43*, 477–486.

clusters of epothilones have been extensively studied.[6] Recently, a 56-kb epothilone biosynthetic gene cluster was reassembled using unique restriction sites (which allowed for future module interchangeability) in the guanine- and cytosine-rich host *Myxococcus xanthus*.

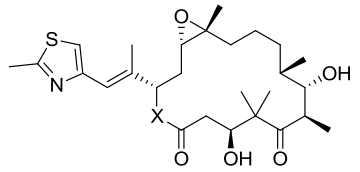

X= O : Epothilone B
X= NH : Ixabepilone

Figure 5: Epothilone B and Ixabepilone structures

To increase production yield, and to efficiently derivatize a variety of analogues with improved bioactivity, the epothilone biosynthetic gene cluster from *Sorangium cellulosum* was redesigned and reassembled for expression in *Myxococcus xanthus*.[7]
Although natural products have been extensively used in traditional medicine, there are still many resources that need to be investigated in modern natural-product research.
In addition, microorganisms demonstrate a large biodiversity that exceedes those of eukaryotes, and can have exceptional metabolic adaptability. Nevertheless, less than 1% of this huge biodiversity has been investigated, mainly due to non-cultivability in the laboratory. Using metagenomic and heterologous-expression techniques, we can increase the diverse microbial community and so potentially, we can have the advantage to access to a source of novel bioactive compounds.

[6] Molnar, I.; Schupp, T.; Ono, M.; Zirkle, R. E.; Milnamow, M.; Nowak-Thompson, B.; Engel, N.; Toupet, C.; Stratmann, A.; Cyr, D. D.; Gorlach, J.; Mayo, J. M.; Hu, A.; Goff, S.; Schmid, J.; Ligon, J. M. *Chem. Biol.* **2000**, *7*, 97–109.
[7] Osswald, C.; Zipf, G.; Schmidt, G.; Maier, J.; Bernauer, HS.; Müller, R.; Wenzel, SC. *ACS Synth. Biol.* **2012**, *3*, 759–772.

2. Natural products as building blocks for production of API

2.1. Industrial synthesis of vincamine

2.1.1. Introduction

The genus *Vinca* (Apocynaceae), also referred as *Lochnera*, *Pervinca*, *Catharanthus* and *Ammocallis*, is distributed in Europe, Northwest Africa, and South-west Asia. The most important species are *Vinca major* L. and *Vinca minor* L. (Figure 6). *Vinca minor* was first investigated by Lucas in 1859, but the first *Vinca* alkaloids whose structure became known, were reserpine, sarpagine and akuammine, which had previously been isolated from *Rauvolfia* and *Catharanthus* species. After the isolation of reserpine many research groups examined apocynaceaous plants in order to find new alkaloids and now over 90 *Vinca* alkaloids are known.

Figure 6: *Vinca minor L.*

The Apocynaceae plant family includes a great number of so-called eburnamine–vincamine alkaloids. The same foundamental C9-C10 unit characterizes this family of alkaloids. Variation of this unit, in combination with tryptamine, formally elaborate the three significantly different groups of complex indole alkaloids: *Coryananthe*, *Iboga* and *Aspidosperma* (Figure 7). With three exception (vincoridine, vincamidine and pleiocarpiamine chloride), all of the other *Vinca minor* alkaloids contain the carbon skeleton type II and III in Figure 7.

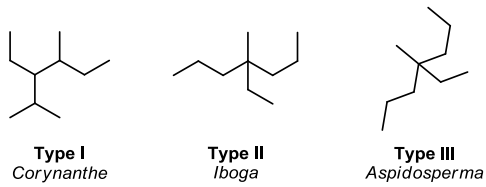

Figure 7: Terpenoid skeleton of Vinca alkaloids

Very different are the *Vinca* major alkaloids, where the majority of compounds derive from "unrearranged" ten-carbon units (structure I in Figure 7), such as ajmaline and sarpagine

alkaloids type. The *Vinca* major alkaloids, which contain a rearranged non-tryptophan unit (structure II and III in Figure 7), are represented by vincamine, vincadifformine and vincine. Pharmacological investigation on *Vinca* alkaloids and their derivatives, such as vincristine, vinorelbine, vinblastine and vindesine, mainly regard their anticancer properties.

Among *Vinca* alkaloids, vincamine (Figure 8) is the most frequently observed alkaloids in this genus plants. It was first isolated from *Vinca minor L.* (Apocyanaceae) by Zabolotnaya[8] and independently by Schilitter and Furlenmeyer.[9] However, only in 1961 its structure was elucidated by Trojanek.[10]

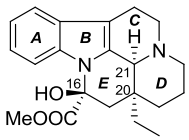

Figure 8: Vincamine

Vincamine, a monoterpenoid indole alkaloid, is an attractive synthetic target, because it showed to be pharmacologically active in both cardiovascular and central nervous system. Nevertheless, its activity is mainly on the vessels of the brain. By increasing the cerebral blood flow vincamine is able to improve the metabolism of essential nutrients and oxygen utilization in the brain. The above properties make vincamine of particular interest for the treatment of some important neurodegenerative conditions such as Parkinson's and Alzheimer diseases.[11]

Vincamine is sold as drug in Europe under the trade name Oxybral SR, for the treatment of primary degenerative and vascular dementia, while in US it is sold as "smart drug" or nootropics to support cerebral metabolism and cognitive function and to improve memory and concentration.

Vincamine (98.0%) is commercially available from Sigma-Aldrich and some companies supply vincamine (≥ 98.5%) to the pharma industry.

[8] Zabolotnaya, E.S. *Moscow* **1950**, *10*, 29–33.

[9] Schlittler, E.; Furlenmeier, R. *Helv. Chim. Acta* **1953**, *36*, 2017.

[10] Trojànek, J.; Ŝtrouf, O.; Holubeck, J.;Ĉekan, Z. *Tetrahedron Lett.* **1961**, *20*, 702–706.

[11] (a) Karpati, E.; Biro K.; Kukorelli, T. *Acta Pharma. Hung.* **2002**, *72*, 25-36; (b) Vas, A.; Gulyas, B. *Med.Res.Rev.***2005**, *25*, 737-757; (c) Vereczkey, L. *Drug. Metab. Pharmacokinet.* **1985**, *10*, 89-103.

Chemical identification of vincamine:

CAS registry No.	1617-90-9
Iupac name	Methyl(3α,16 α)-14,15-Dihydro-14βhydroxyeburnaminenine-14-carboxylate
Other name	(+)-vincamine; vincamine (6CI,8CI); 1H-Indolo [3,2,1*de*] pyrido [3,2,1-*ij*][1,5] naphthyridine, eburnamenine-14-carboxylic acid deriv.; (+)-cis-Vincamine
Molecular formula	$C_{21}H_{26}N_2O_3$
Molecular weight	354.44 g/mol
Melting point	231.5 °C
Appearance	White crystalline powder
Specific optical rotation	Between +39.0 and +43.5 (dry basis)
Solubility	Soluble in chloroform, slightly soluble in alcohol, insoluble in water
Storage	Sealed container and protected from light

2.1.2. Biosynthesis

The eburnamine-vincamine group of alkaloids[12] is an interesting family that has received considerable attention concerning the biosynthetic pathway. Structural analysis of different members shows that these alkaloids may be related biosynthetically to the *Aspidosperma* family.[13]

In 1965, Wenkert[14] proposed a simple mechanism for the biosynthesis of vincamine **E** that takes into account the implication of the Aspidosperma intermediate **A** and its rearrangement via **B, C,** and **D** (Scheme1).

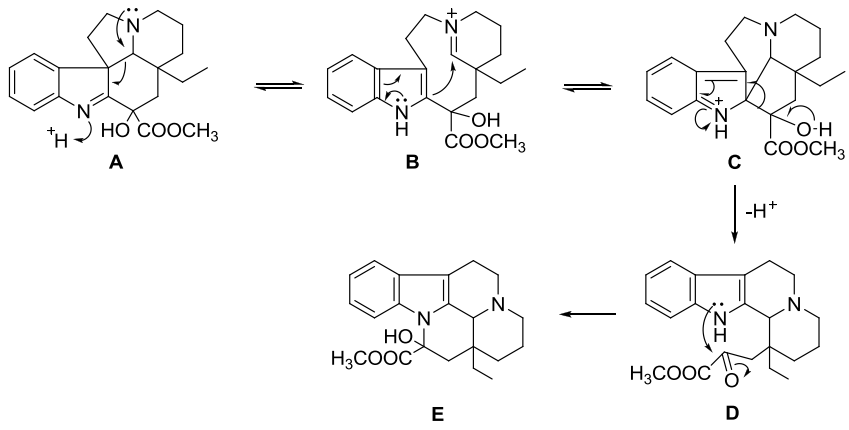

Scheme 1: Biomimetic conversion of vincadifformine into vincamine

Kutney and co-workers reported an extensively investigation on eburnamine-vincamine alkaloids biosynthesis.[15] They observed the incorporation of various intermediates, such as tryptophan, stemmadenine, tabersonine and secodine, into *V. minor* L. However, these results suggested but *did not prove* that the eburnamine-vincamine group of alkaloids may be derived from the corynantheinoid family *via* the *strychnos* and *aspidosperma* bases as outlined in Scheme 1.

[12] W. I. Taylor, *Alkaloids* **1968**, *11*,125.
[13] A. I. Scott , *Accounts Chem. Res.***1970**, *3*, 151.
[14] E. Wenkert and B. Wickberg, J.*Amer. Chem. Soc.***1965**, *87*, 1580.
[15] (a) Kutney, J. P.; Ehret, C.; Nelson, V**.** R.; Wigfield, D. C. *J.Amer.Chem.Soc.* **1968**, *90*, 5929; (b) Kutney, J. P.; Ehret, C.; Nelson, V**.** R.; Wigfield, D. C. *J. Amer. Chem. Soc.* **1971**, *93*, 255-257.

Recently, O'Konnor's group,[16] discovered the cytochrome P450 16T3O (16-methoxytabersonine 3-oxygenase) which is required for the biosynthesis of vindoline. This enzyme catalyzes the formation of epoxide **F**, which first opens to imine alcohol **G** and then can undergo rearrangement to give the vincamine–eburnamine backbone.The evidence of the action of 16T3O in inducing a rearrangement of **F** to **H** suggests that a16T3O homolog is implicated in the biosynthesis of vincamine and related alkaloids (Scheme 2). Therefore, the discovery of this enzyme can be useful in order to elucidate the biosynthetic pathway of vincamine starting from tabersonine.

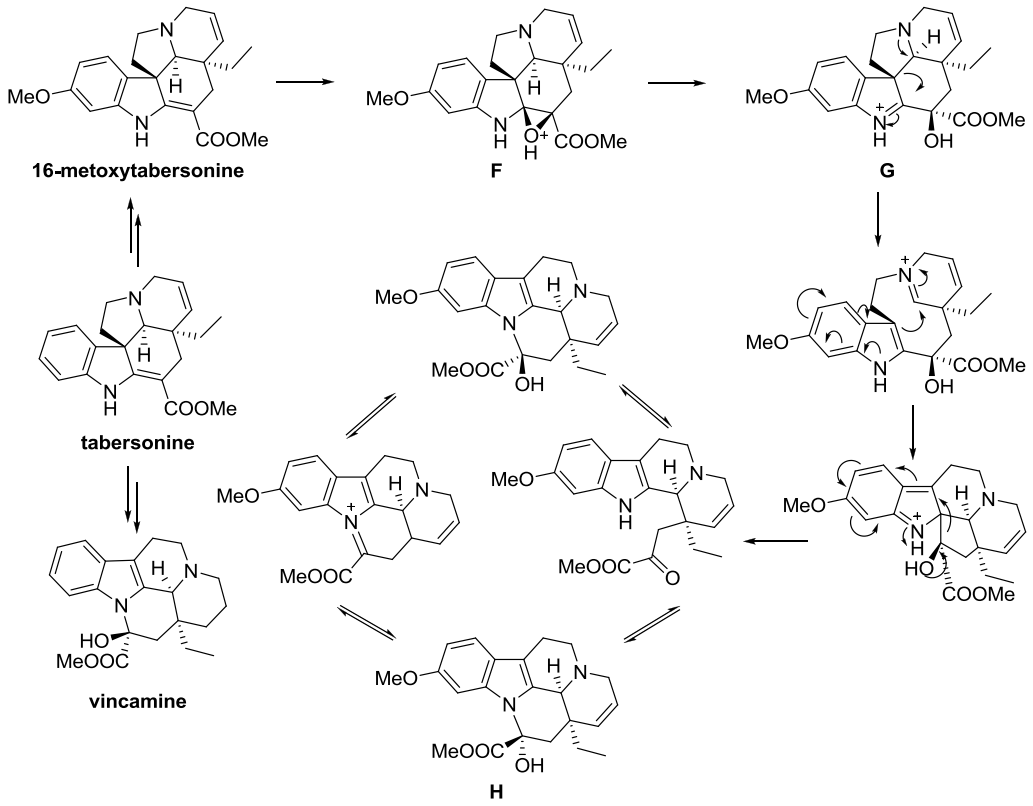

Scheme 2: Rearrangement of epoxide **F** to form vincamine type compounds

[16] Kellner, F.; Geu-Flores, F.; Sherden,N.H.; Brown,S.; Foureau, E.; Courdavault, V.;O'Connor, S.E. *Chem. Commun.* **2015**, *51*, 7626-7628.

2.1.3. Total synthesis of vincamine

Several strategies for the synthesis of (+)-vincamine and analogs have been developed[17] with the aim to find pharmacologically active compounds better characterized and safer to be administered as the natural alkaloids occurring in the plants.

The common aspect in these strategies was to establish first the [ABCD]-type octahydroindolo [2, 3 *a*]-quinolizine ring system (Scheme 3), starting from an indole subunit. The final step of the synthesis lead to the creation of the last ring **E**. As a consequence, strategically, the elaboration of vincamine and related alkaloids reduced to four major strategies for building up the required *gem*-disubstituted tetracyclic skeleton **2**: the Bischler-Napieralski cyclization,[18] the Michael-type alkylation of the so-called "Wenkert's enamine",[19] the Pictet-Spengler cyclization[20] and the annulation reaction of a dihydro-*β*-carboline derivative.[21] Moreover, the intermediate **1** is characterized by the presence of two controlled stereogenic carbon atom, namely the crucial quaternary center at C-20 and the adjacent center at C-21.

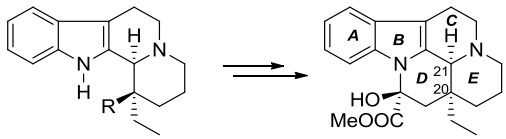

1 vincamine 2

Scheme 3: Common synthetic strategies toward the *vinca* framework

[17] (a) Hugel, G.; Lèvy, J. *Tethraedron* **1984**, *40*, 1067; (b) Hakam, K.; Thielmann, M.; Thielmann, T.; Winterfeldt, E. *Tetrahedron* **1987**, *43*, 2035; (c) Gènin, D.; Andriamialisoa, R.Z.; Langlois, N.; Langlois, Y. *J.Org.Chem.***1987**, *52*, 353; (d) Kaufman, M. D.; Grieco, P.A. *J. Org. Chem.* **1994**, *59*,7197; (e) Wenkert, E.; Hudlicky, T.; Showalter, H.D. *J.Am.Chem. Soc.* **1978**, *100*, 4893; (f) Lavilla, R.; Coll, O.; Bosch, J.; Orozco, M.; Luque, F. J. *Eur. J. Org. Chem.* **2001**, *19*, 3719-3729.

[18] Herrmann, J. L.; Cregge, R. J.; Richman, J. E.; Semmelhack, C. L.; Schlessinger, R. H. *J. Am. Chem. Soc.* **1974**, *96*, 3702-3703.

[19] (a) Rossey, G.; Wick, A.; Wenkert, E. *J. Org. Chem.***1982**, *47*, 4745; (b) Wenkert, E.; Wickberg, B. *J. Am. Chem. Soc.* **1965**, *87*, 1580; (c) Szabo, L.; Sapi, J.; Kalaus, G.; Argay, G.; Kalman, A.; Baitz-Gacs, E.; Tamas, J.; Szantay, C. *Tetrahedron* **1983**, *39*, 3737; (d) Nemes, A.; Czibula, L.; Visky, G.; Farkas, M.; Kreidl, J. *Heterocycles* **1991**, *32*, 2329.

[20] Gmeiner, P.; Feldman, P. L.; Chu- Moyer, M. Y.; Rapoport, H. *J. Org. Chem*. **1990**, *55*, 3068-3074.

[21] (a) Oppolzer, W.; Hauth, H.; Pfäffli, P.; Wenger, R. *Helv. Chim. Acta* **1977**, *60*, 1801-1809; (b) Genin, D.; Andriamialisoa, R. Z.; Langlois, N.; Langlois, Y. *J. Org. Chem.* **1987**, *52*, 353-356.

Wenkert *et al.* reported a five-step procedure for the preparation of alkaloid vincamine (Scheme 4). The key step involved the introduction of a side chain, which then became the functionalized part of the fifth ring of the base, by way of the alkylation of an enamine with methyl bromopyruvate 2,4-dinitrophenylhydrazone **5**. Wenkert's enamine is the key intermediate of the synthetic pathway (Figure 9).

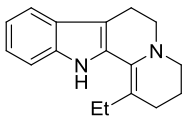

Figure 9: Wenkert's enamine

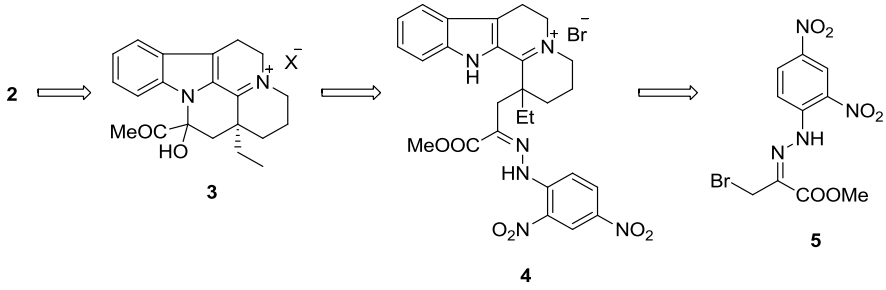

Scheme 4: Synthesis of vincamine proposed by Wenkert *et al.*

(±)-Vincamine were obtained from reduction of the salt **3** with zinc in acetic acid. Aqueous cleavage of the side chain of compound **4** led to salt **3**. Intermediate **4** derived from treatment of hydrazone **5** with Wenkert's enamine and trimethylamine in ethyl acetate solution. 2,4-Dinitrophenylhydrazone **5** was prepared by the interaction of pyruvic acid 2,4-dinitrophenylhydrazone with thionyl chloride in methanol, followed by bromination of the resultant ester.

In 1997, D'Angelo *et al.* described the synthesis of vincamine[22] starting from tryptamine and using as key step the stereocontrolled creation of the quaternary carbon center by using asymmetric Michael reaction involving chiral imine/secondary enamines. The synthetic strategy is outlined in the retrosintetic pathway in Scheme 5.

[22] Alves, J.C. F.; Simas, A. ; Costa, P.; D'Angelo, J. *J. Org. Chem.* **1997**, *62*, 3890-3901.

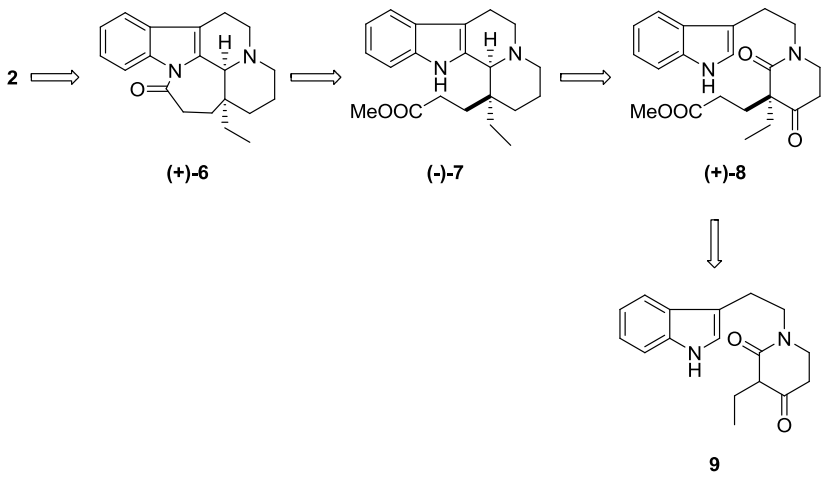

Scheme 5: Asymmetric synthesis of vincamine

Vincamine was obtained from a known precursor **6**, which derived from a base-induced cyclization of **7**. Wolff-Kishner reduction of the additional keto group of **8**, followed by Bischler-Napieralski cyclitazion, led to indoquinolizidine derivate **7**.

Finally, the synthesis of precursor **8**, involved the asymmetric Michael addition of the chiral enaminolactam, obtained from **9** and (*S*)-1-phenylethylamine, to methyl acrylate.

In 1975 Oppolzer and co-workers[21a] illustrated a general methodology for the conversion of apovincamine to vincamine using the aldehyde shows in Figure 10, named Oppolzer's aldehyde. This aldehyde has been the key intermediate in many vincamine syntheses. Since its discovery, Danieli *et al.*,[23] Govindachari and Rajeswari,[24] and Langlois *et al.*[25] reported three other approaches.

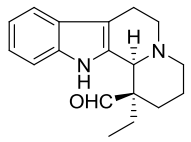

Figure 10: Oppolzer's aldehyde

Tolvanen and Lounasmaa reported the synthesis of vincamine using as key intermediate compound **12** obtained from the Oppolzer's aldehyde **13** (Scheme 6).

[23] Danieli, B.; Lesma, G.; Palmisano, G. *Gazz. Chim. Ital.* **1981**, *111*, 257.

[24] Govindachari, T. R.; Rajeswari, S. *Indian J. Chem., Sect. B* **1983**, *22*, 531.

[25] Langlois, Y.; Pouilhès, A.; Gĕnin, D.; Andriamialisoa, R. Z.; Langlois, N. *Tetrahedron* **1983**, *39*, 3755.

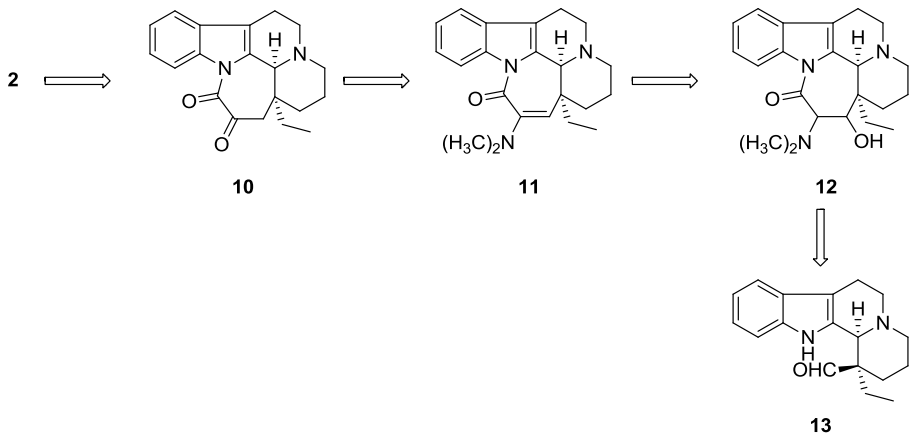

Scheme 6: Retrosynthetic pathway proposed by Tolvanen

Vincamine was obtained from a treatment of oxolactame **10** with a base in methanol. This type of conversion is well documented in literature.[26]

Compound **10** derived from a hydrolysis of the intermediate enamine **11**, which was obtained from a dehydration of lactam **12** using acetic anhydride/DMAP in pyridine at room temperature. Finally, the reaction of aldehyde **13** with the LDA enolate of glycine ester furnished directly the cyclized product **12**.

The synthetic strategy for the synthesis of vincamine proposed by Schultz and co-workers[27] is based on the conversion of apovincamine **14** into vincamine using the reaction conditions reported by Oppolzer. The retrosynthetic pathway is depicted in Scheme 7.

[26] (a) Szantay, C.; Szabo, L.; Kalaus, G. *Tetrahedron***1977**, *33*, 1803; (b) Szabo, L.; Kalaus, G.; Szantay, C. *Arch. Pharm. (Weinheim, Ger.)* **1983**, *316*, 629-638.

[27]Schultz, A.; Malachowski, P.W. *J. Org. Chem.* **1997**, *62*, 1223-1229.

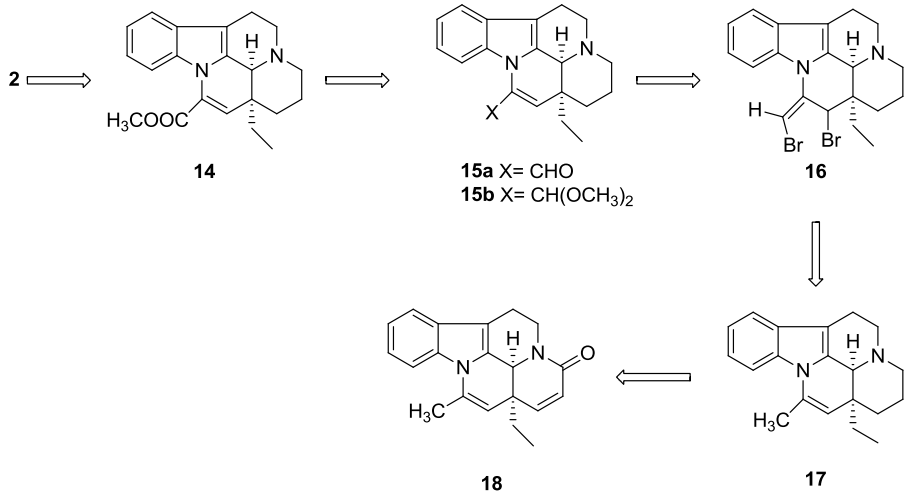

Scheme 7: Retrosynthetic pathway for the preparation of vincamine

Compound **14** was obtained from the conversion of (+)-apovincaminal **15a** to the acetal **15b** followed by a free radical bromination using NBS/AIBN in CCl_4. **15a** derived by the treatment of **16** with $AgBF_4$, DMSO and Et_3N followed by an aqueous work-up procedure. Electrophilic bromination of the double bond in **17** with *N*-bromoacetamide led to dibromide **16**. Reduction of the diene lactam **18** by the method of Shamma[28] *et al.* provided the intermediate **17**. The strategy for production of **18** involved coupling of tryptamine with the chiral enantiomerically pure butyrolactone, followed by acid-catalyzed tricyclization and elimination of MeOH from an amido keto aldehyde intermediate. Butyrolactone resulted from a chiral benzamide by a novel process[29] that affords a practical "asymmetric linkage" between chiral acyclic substrates and aromatic carboxylic acids.

[28] Shamma, M.; Rosenstock, P. O. *J. Org. Chem.***1961**, *26*, 718.

[29] Schultz, A. G.; Hoglen, D. K.; Holoboski, M. A.*Tetrahedron Lett.***1992**, *33*, 6611.

2.1.4. Synthesis of vincamine with tabersonine as starting material

Methods for obtaining vincamine and other indolic alkaloids on an industrial scale can be grouped into three different types of strategies:

a) Extractive method
b) Total synthesis
c) Semi-synthesis

Method of direct extraction from vegetal species have limited applications because vincamine is contained in different species of the genus *Vinca* in a very low amount (0.l-0.2%). Thus, the extraction processes and the purification processes are significantly costly and complicated, and this is the reason of the high disproportion existing between the quantity of starting vegetal product, reagents and solvents necessary, and the amount of substance obtained with suitable purity level.

Total synthesis possesses the advantage to use commercially available chemical compounds as starting material. Nevertheless, these total syntheses involve a large number of steps, due to the complexity of the chemical structure of vincamine and it presents the critical problem of the stereoselctively.

Semi-synthesis is a type of strategy which used compounds isolated from natural sources as starting material. This strategy has the characteristics of low cost, high yield, short time and simple and safe operation and is completely suitable for an industrialized mass production.

In addition this approach has the advantage to overcome problem of stereoselectivity because of the starting material has a specif configuration.

Different processes of semi-synthesis of vincamine or related alkaloids have been proposed, more particularly aiming at simplifying the operative steps and reducing duration thereof. Considering that tabersonine is a biosynthetic precursor of vincamine, it is considered as a suitable starting material for the semi-synthesis of vincamine.

Tabersonine

Tabersonine is an indole alkaloid extracted from *Voacanga africana*. Alkaloids of the *Aspidosperma type*, e.g. tabersonine and vindoline, *and Iboga type*, e.g. catharanthine, derived from the biosynthetic pathway reported in Scheme 8.[30]

The strictosidine derivative preakuammicine is the general precursor for the *strychnos*, *aspidosperma* and *iboga* alkaloids. Even though several mechanisms have been reported in order to elucidate the formation of preakuammicine from geissoschizine,[31] the physiological precursor and mechanism for preakuammicine continues to be unknow.

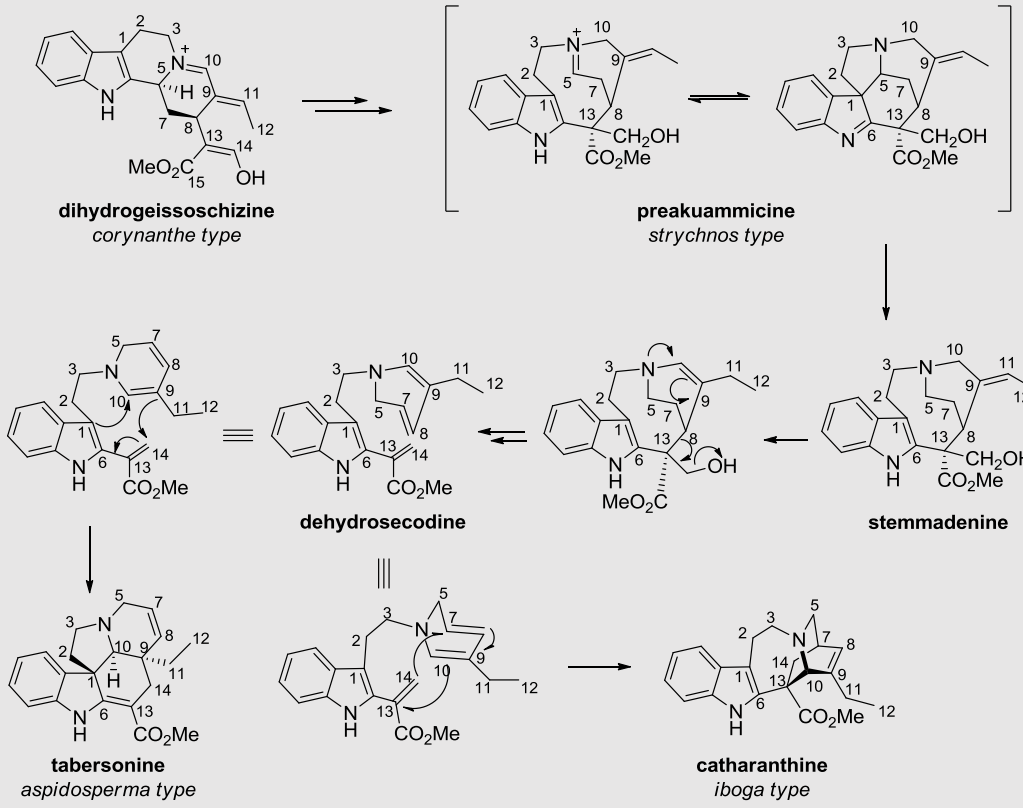

Scheme 8: Biosynthetic pathway of *strychnos*, *iboga* and *aspidosperma* alkaloids.

[30] (a) Battersby, A. R.; Burnett, A. R.; Hall E. S.; Parsons, P. G. *Chem. Commun.*, **1968**, 1582–1583; Scott, A. I.; (b) Cherry,P. C.; Qureshi,. A. A. *J. Am. Chem. Soc.*, **1969**, *91*, 4932–4933; (c) Scott, A. I. *J. Am. Chem. Soc.*, **1972**, ***94***, 8262.

[31] Scott, A. I.; Qureshi, A. A. *J. Am. Chem. Soc.*, **1969**, *91*, 5874–5876; (b) Wenkert, E.; Wickberg, B. *J. Am. Chem. Soc.*, **1965**, *87*, 1580–1589.

Reduction of preakuammicine generates stemmadenine, which rearranges to form the acrylic ester dehydrosecodine. This is a common intermediate for both the *Iboga* and the *Aspidosperma* skeletons. It is possible that the catharanthine and tabersonine are formed from a Diels–Alder reaction of dehydrosecodine, but there is no indication for this reaction in the plant.[32] Tabersonine is used as the biosynthetic precursor to several members of the *Aspidosperma* family, especially vindoline (Scheme 9).[33] In the first step, tabersonine is hydroxylated at the C-16 position by tabersonine-16-hydroxylase (T16H). The hydroxyl group is then methylated by the enzyme 16-hydroxytabersonine-16-*O*-methyltransferase (HTOM) to yield 16-methoxy-tabersonine. Subsequently, hydration of a double bond by an unknown enzyme produces 16-methoxy-2,3-dihydro-3-hydroxytabersonine.

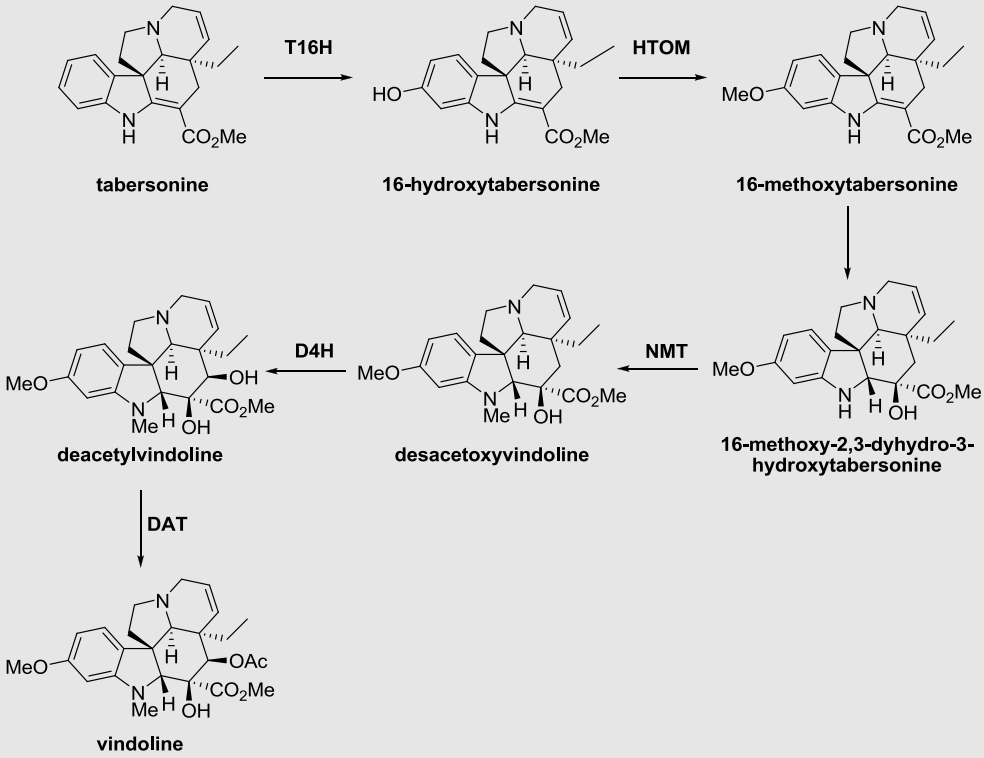

Scheme 9: Vindoline biosynthesis from tabersonine.

[32]S. Laschat, *Angew. Chem., Int. Ed. Engl.*, **1996**, *35*, 289–291.

[33] (a) Danieli, B.; Lesma, G.; Palmisano, G.; Riva, R.*J. Chem. Soc., Chem.Commun.* **1984**, 909-911; (b) Danieli, B.; Lesma, G.; Palmisano, G.; Riva,R. *J. Chem. Soc., Perkin Trans. 1* **1987**, 155-161.

Transfer of a methyl group to the indole nitrogen by an *N*-methyl transferase (NMT) leads to desacetoxyvindoline. The action of the 2-oxoglutarate-dependent dioxygenase desacetoxyvindoline 4-hydroxylase (D4H) produces the intermediate deacetylvindoline which is, finally, acetylated by deacetylvindoline *O*-acetyltransferase (DAT) to give vindoline. Tabersonine is important not only for its biosynthetic relationship to the *Vinca* alkaloids but also because it is the chemical progenitor of these alkaloids. The chemical conversion of tabersonine to various bisindole alkaloids is widely documented.[34]
For these reasons, tabersonine represented an attractive target for synthesis.[35]

In 1978, Paracchini *et al.* reported a new method of partial synthesis of vincamine starting from tabersonine (Scheme 10). [36]

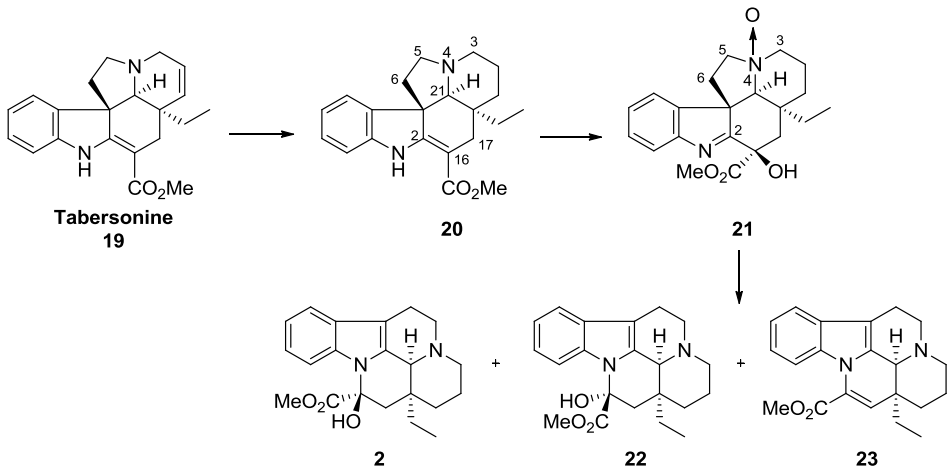

Scheme 10: Synthesis of vincamine **2** starting from tabersonine

First of all tabersonine **19** was catalitically reduced to vincadifformine **20**, which was subsequentelly oxidizetohydroxy-[3H]- indole N(**4**) oxide **21**. Intermediate **21** was reduced

[34] (a) Scott, A. I. *Acc. Chem. Res.***1970**, *3*, 151-157; (b) Basha, A.; Atta-Ur-Rahman, *Biosynthesis of Indole Alkaloids*; Clarendon Press: Oxford, **1983**.
[35] (a) Ziegler, F. E.; Bennett, G. B. *J. Am. Chem. Soc.***1971**, *93*, 5930-5931; (b) Ziegler, F. E.; Bennett, G. B.*J. Am. Chem. Soc*.**1973**, *95*, 7458-7464; (c) Takano, S.; Hatakeyama, S.; Ogasawara, K.*J. Am. Chem. Soc*.**1979**, *101*, 6414-6420; (d) Lèvy, J.; Laronze, J.-Y.; Laronze, J.; Le Men, J.*Tetrahedron Lett.***1978**, 1579-1580.
[36] Paracchini, S.; Pesce, E. *Farmaco*, **1978**, *33*, 573-582.

and after a rearrangement induced by acidic conditions, vincamine **2**, 16-*epi*vincamine **22** and apovincamine **23** were formed (Scheme10).

Scheme 11 illustrates the mechanism of the rearrangement of hydroxy-[3H]- indole N(**4**) oxide **21** to vincamine **2** and *epi*vincamine **22**.

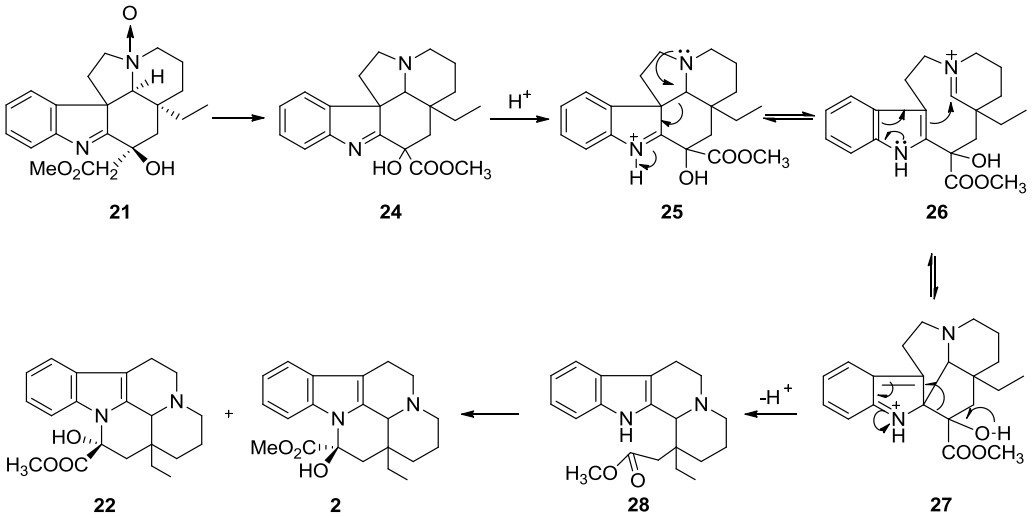

Scheme 11: Rearrangement of **21** to vincamine **2** and *epi*vincamine **22**.

It is important to note that the induction of rearrangement requires the oxidation of vincadifformine **20** to intermediate **21** using peroxy acids (Scheme12).

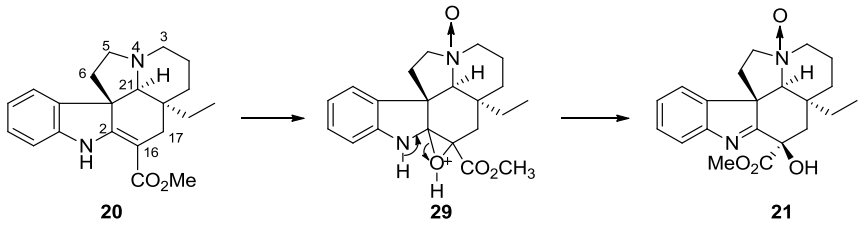

Scheme 12: Conversionof vincadifformine **20** to intermediate **21**.

The semi-synthesis of vincamine starting from tabersonine is a strategy widely used in industry because of it results economic. Therefore, a large number of patent have been published in the last years. [37]

We took into consideration the obtainment of vincamine starting from (-)-tabersonine **19**, an indole alkaloid extracted from *Voacanga Africana* (Scheme 13).

Applying the reaction sequence of Nemes[38] tabersonine is submitted to catalytic hydrogenation in the presence of Ni-Raney to give vincadifformine **20**. The subsequent treatment with 3-chloroperbenzoic acid in toluene generated the intermediate **21**. Treatment of **21** with triphenylphosphine and acetic acid induced formation of a mixture of (+)-vincamine **2** and *epi*vincamine **22**. The use of a base permitted the epimerization at C20 of *epi*vincamine to give (+)-vincamine **2** as main product.

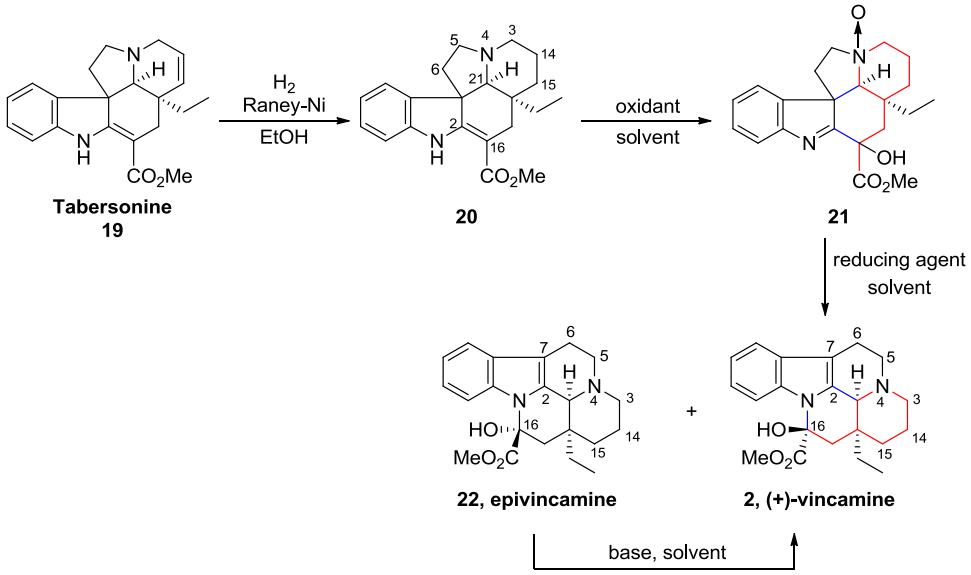

Scheme 13: General procedure for the preparation of vincamine

The complete conversion of tabersonine into (+)-vincamine takes place with a total yield over than 30%.

[37] (a) Xuedong, P.; Xiaobo, W.; Jinshao, Z.; Zhenglian, W. CN 102108082 A 20110629; (b) Wen, S.; Yi, W.; Peng, L.; Jun, L.; Guohui, Y.;Shijiang, L. CN 102276599 A 20111214; (c) Xuedong, P. CN 103232452 A 20130807; (d) Xuedong, P.; Mei, Z.; Jinshao, Z.; Yongyi, Y. CN 104788447 A 20150722.

[38] Nemes, A.; Szàntay, C.; Czibula, L.; Reiner, I. *Heterocycles*, **2007**, *71*, 2347-2362.

The formation of the desired product **2** was evaluated through mass spectroscopy (MS) and nuclear magnetic resonance (NMR) analysis.

Mass spectrum (EI) showed the molecular peak (M) at 354 m/z together with the peaks of characteristic fragments at 339 (M-Me), 325 (M-Et), 307 (M-Et-H_2O), 295 (M-COOMe), 267 (M-COOMe-CO).

^{1}H-NMR analysis of vincamine **2** shows the signal at δ 4.60 ppm related to the OH proton and it does not show correlation with any carbon signal. The signal at δ 3.95 ppm is characeristic of the proton at position 21. COSY spectrum evidences a correlation between the signal of the proton at position 9 at δ 7.50 ppm and the proton at position 21 at δ 3.95 ppm.

Moreover, the signals of the protons at position 17 presents a decreased difference in chemical shift (δ 2.15 e 2.25 ppm, AB system) respect to the corresponding signals of the protons in *epi*vincamine (δ 2.05 and 2.73 ppm, AB system). This is due to the opposite configuration at position 16 and to the effect of COOMe (Figure 10). In addition, the signal of the proton at position 12 presents a highfield shift (δ 7.05-7.15 ppm, multiplet) if compared with the corresponding signal in *epi*vincamine (δ 7.50-7.85 ppm, multiplet).

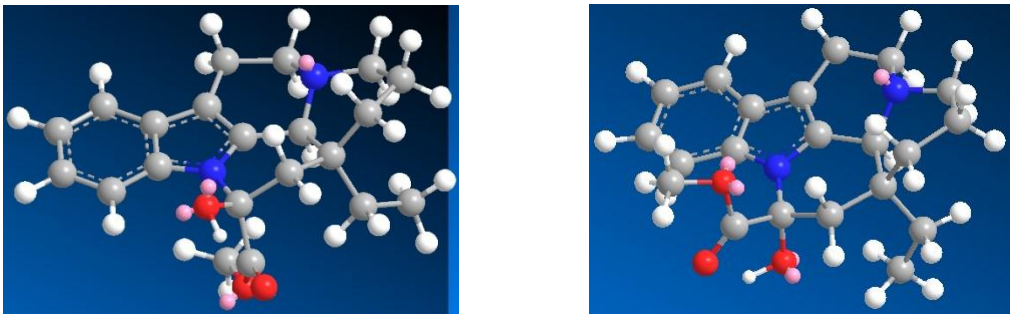

Figure 11: 3D structure of vincamine (on the left) and *epi*vincamine (on the right).

2.1.5. Impurities derived from the synthesis of vincamine

The HPLC analysis of the obtained vincamine shows the presence of crucial impurities (Figure 12), which occur in a range of 0.03-1.89%.

We isolated different byproducts with the aim to identify their chemical structures and to define the reason of their formation.

Name	Retention time (min.)
ImpurityA	0.8
Impurity B (epivincamine)	0.9
Vincamine	9.3
Impurity C (δ-14-vincamine)	1.35
Impurity D (apovincamine)	2.5

Figure 12: Retention time of different impurities

The assignment of the impurities structure was based on the EIMS and NMR analysis (Figure 13).

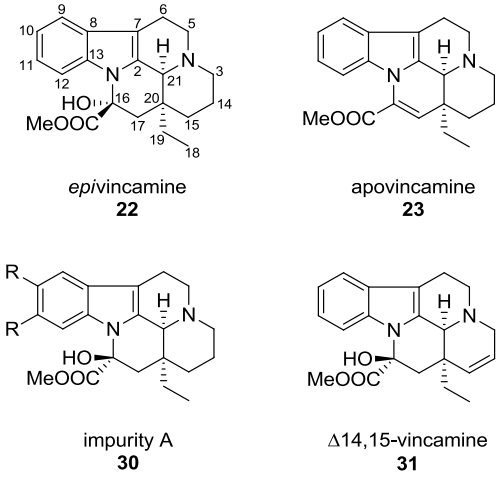

Figure 13: Structure of compounds deriving from industrial synthesis of vincamine

For what regard compound **22**, the mass spectrum (EI) shows the molecular peak at 354 m/z (M) together with the peaks of characteristic fragments at 307 (M-Et-H_2O), 295 (M-COOMe).

^{1}H-NMR spectrum shows the signals of the protons at position 12 and 9 at δ 7.45 and 7.55 ppm, respectively, as doublets together with a multiplet in the region δ 7.0-7.1 ppm due to H-10 and H-11. The signal of H-21 appears at δ 3.90 ppm. The protons at position 17 present an increased difference in chemical shift (δ 2.05 and 2.75 ppm, AB system) if compared with the corresponding signals in vincamine. This is due to the opposite configuration at position 16 and to the effect of COOMe. The proton at position 12 suffers of downfield effect and moves at δ 7.4 ppm (vincamine δ 7.05-7.15 ppm).

Compound **23** presents (EI) a molecular peak (M) at 336 accompanied by other peaks at 307 (M-Et) and 266 that is due to the fragment reported in the Figure 14. The presence of the double bond between the carbons 16 and 17 is confirmed by the signal of the proton at position 17 at δ 6.15 ppm as a singlet and the corresponding signal at 128.2 in the ^{13}C-NMR spectrum.

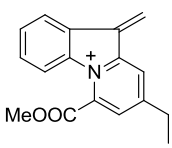

Figure 14: Fragment at 266

The mass spectrum (EI) of compound **30** shows the molecular peak at 384 m/z. The ^{1}H-NMR spectrum shows three signals in the aromatic region for the presence of a substituent on the indole portion. Multiplicity of those signals (d, d and dd) with two different coupling constants (*J*= 2 and 9 Hz) confirms the presence of the substituent at position 10 or 11. COSY spectrum evidences two correlations between the signal at δ 6.93 (*J* = 2 Hz) and the signal at δ 6.72 ppm (*J*= 2 and 9 Hz) with the one at δ 3.91 ppm (H-21). NOESY spectrum shows an interaction between the signal at 6.93 ppm (dd) and the signal at δ 2.5-2.6 ppm (H-6).

Compound **31** presents (EI) the molecular peak at 352 (M) accompanied by other peaks at 323 (M-Et), 319 (M-Me-H_2O), 305 (M-Et-H_2O), 293 (M-COOMe) and the one at 284 due to the fragment reported in the Figure 15.

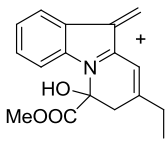

Figure 15: Fragment at 282

In the ^{1}H-NMR spectrum the region of the aliphatic signals results simplified with the disappearance of the signals due to the protons at position 14 and 15. Same trends is detectable in ^{13}C-NMR spectrum. Two signals at δ 5.78 and 5.62 ppm confirm the presence of two vicinal olefinic protons. These signals results coupled to the signals due to the protons at position 3.

2.2. Design of experiment (DOE)

The design of new products or the improvement of existing ones, together with the design and development of manufacturing processes to synthesize them, are critical activities in most industrial organizations.

Statistically designed experiments have a key role for product and process design and development. In the last years, many new developments in experimental design have been made and they have been found broad application in many disciplines. Typical experimental design application areas embrace process and product characterization, control and stability, process optimization, achieving variability reduction, and designing products and processes to accomplish robustness.

Within the theory of optimization, an experiment is a sequence of tests in which the input variables are changed according to a given rule in order to identify the reasons for the changes in the output response. According to Montgomery:[39]

"Experiments are performed in almost any field of enquiry and are used to study the performance of processes and systems. […] The process is a combination of machines, methods, people and other resources that transforms some input into an output that has one or more observable responses. Some of the process variables are controllable, whereas other variables are uncontrollable, although they may be controllable for the purpose of a test. The objectives of the experiment include: determining which variables are most influential on the response, determining where to set the influential controllable variables so that the response is almost always near the desired optimal value, so that the variability in the response is small, so that the effect of uncontrollable variables are minimized."

DOE (Design Of Experiment), or experimental design, is the name given to the techniques used for guiding the choice of the experiments to be performed in an efficient way.

Due to the close link between statistics and DOE, it is quite common to find in literature terms like *statistical experimental design*, or statistical DOE.

[39] Douglas C. Montgomery, Design and Analysis of Experiments, John Wiley & Sons Inc, **2012.**

Statistical experimental design, together with the fundamental ideas underlying DOE, was born in the 1920s from the work of Sir Ronald Aylmer Fisher. He developed the insights that lead to the three basic principles of experimental design: randomization, replication and blocking. In the 1930s, Box and Wilson applied the idea of statistical design to industrial experiments and developed the response surface methodology (RSM), a method that explores the relationships between several explanatory variables and one or more response variables. Finally, the work of Genichi Taguchi in the 1980s had a significant effect on making statistical experimental design popular and stressed the importance it can have in terms of quality improvement.

In order to perform a DOE first it is necessary to identify the problem and choose the variables, which are called *factors* or parameters. A design space, or *region of interest*, have to be defined, that is, a range of variability must be set for each variable. The amount of values the variables can assume in DOE is restricted and usually small. The DOE technique and the number of levels are to be chosen according to the number of experiments that can be afforded. The term *levels* refers to the number of different values a variable can assume according to its discretization. The number of levels usually is the same for all variables, however some DOE techniques allow the differentiation of the number of levels for each variable. In experimental design, the objective function and the set of the experiments to be performed are called *response variable* and *sample space* respectively.

As already said, the three basic principles of experimental design are: **randomization, replication** and **blocking**. Randomization implies that both the allocation of the experimental material and the order in which the scientists runs or trials of the experiments are to be performed are randomly determined. Replication refers to an independent repeat of each factor combination, while blocking is the arranging of experimental units in groups (blocks) that are similar to one another.

Several DOE techniques are available to the experimental designer (Table 1): Randomized Complete Block Design (RCBD), Latin Square, Fractional Factorial, Central Composite, Box-Behnken, Plackett-Burman, Taguchi, Random, Halton - Faure- Sobol, Latin Hypercube, Optimal design and Full Factorial design. The choice of the best experimental design

depends on the problem to be investigated and on the aim of the experimentation. Items to be consider are:

1. the *number of experiments N* which can be given
2. the *number of parameters k* of the experiment
3. the *number of levels L* for each parameter
4. the *aim* of the DOE.

Method	Number of experiment	Suitability
RCBD	$N\ (L_i) = \prod_{i=1}^{k} L_i$	Focusing on a primary factor using blocking techniques
Latin squares	$N\ (L) = L^2$	Focusing on a primary factor economically
Full factorial	$N\ (L, k) = Lk$	Computing the main and the interaction effects, building response surfaces
Fractional factorial	$N\ (L, k, p) = Lk{-}p$	Estimating the main and the interaction effects
Central composite	$N\ (k) = 2k + 2k + 1$	Building response surfaces
Box-Behnken	$N\ (k)$ from tables	Building quadratic response surfaces
Plackett-Burman	$N\ (k) = k + 4 - \mod \frac{k}{4}$	Estimating the main effects
Taguchi	$N\ (kin\ ,\ kout\ ,\ L) = NinNout\ ,\ Nin\ (kin\ ,\ L),\ Nout\ (kout\ ,\ L)$ from tables	Addressing the influence of noise variables
Random	chosen by the experimenter	Building response surfaces
Halton, Faure, Sobol	chosen by the experimenter	Building response surfaces
Latin hypercube	chosen by the experimenter	Building response surfaces
Optimal design	chosen by the experimenter	Building response surfaces

Table 1: DOE methods table

2.2.1. Full factorial design

For our purpose, we used a full factorial design. The most simple form is two-levels full factorial, in which there are *k* factors and $L = 2$ levels per factor. The samples are given by every possible combination of the factors values. Thus, the sample size is $N = 2k$. The two levels are called high ("*h*") and low ("*l*") or, "+1" and "−1". Starting from any sample within the full factorial scheme, the samples in which the factors are changed one at a time are still part of the sample space.

In some full factorial designs also the central point of the design space is added to the samples. The central point is the sample in which all the parameters have a value that is the average between their low and high level and in 2*k* full factorial tables can be individuated with "*m*" (mean value) or "0".

We applied the DOE on the synthesis of vincamine starting from vincadifformine (Scheme 14), in order to evaluate the effect of some parameters (set on two values) on the profile of the impurities and to increase the yield of the reaction.

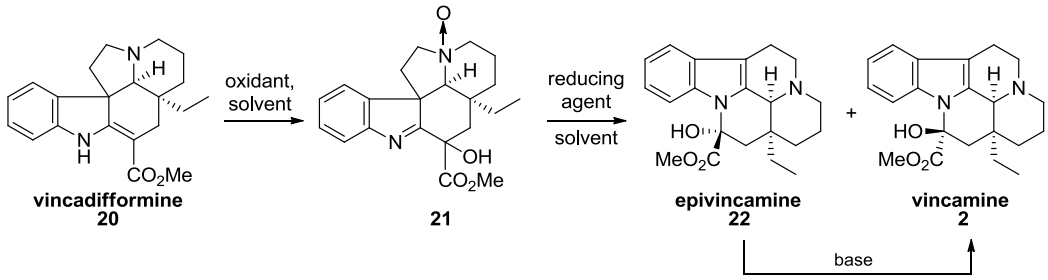

Scheme 14: Synthesis of vincamine from vincadifformine

We considered to change 5 parameters, one parameter each time, for a total of 32 trials:

A. Volume of solvent
B. Temperature
C. Oxidant concentration
D. Reducing agent
E. Reaction time

To these, four experiments have been added as central point "0", in order to estimate the natural variance of the process. (Table 2)

Run	A	B	C	D	E	Run	A	B	C	D	E
1	1	1	1	1	-1	**20**	1	1	1	1	1
2	1	1	1	-1	1	**21**	1	1	1	-1	-1
3	1	1	-1	1	1	**22**	1	1	-1	1	-1
4	1	1	-1	-1	-1	**23**	1	1	-1	-1	1
5	1	-1	1	1	1	**24**	1	-1	1	1	-1
6	1	-1	1	-1	-1	**25**	1	-1	1	-1	1
7	1	-1	-1	1	-1	**26**	1	-1	-1	1	1
8	1	-1	-1	-1	1	**27**	1	-1	-1	-1	-1
9	-1	1	1	1	1	**28**	-1	1	1	1	-1
10	-1	1	1	-1	-1	**29**	-1	1	1	-1	1
11	-1	1	-1	1	-1	**30**	-1	1	-1	1	1
12	-1	1	-1	-1	1	**31**	-1	1	-1	-1	-1
13	-1	-1	1	1	-1	**32**	-1	-1	1	1	1
14	-1	-1	1	-1	1	**33**	-1	-1	1	-1	-1
15	-1	-1	-1	1	1	**34**	-1	-1	-1	1	-1
16	-1	-1	-1	-1	-1	**35**	-1	-1	-1	-1	1
17	0	-1	0	0	0	**36**	0	-1	0	0	0
18	0	-1	0	0	0	**37**	0	-1	0	0	0
19	0	-1	0	0	0						

Table 2: Encoding tests

Graphics and considerations below derived from statistical analysis using the Minitab[40] program and they were made considering a 95% confidence limit ($\alpha = 0.05$). Then it was also taken into account the 90% limit ($\alpha = 0.10$), to check if there was a significant influence of one more factor.

Figure 16 shows the effect of solvent, temperature, oxidant, reducing agent and the reaction time: it is positevely influenced by the increase of the reducing agent, while increasing temperature and concentration of the oxidant we have no effect on the yield. Solvent quantity and time of addition of acid does not show an effect on the yield of the reaction, too.

[40] (a)Meyer, Ruth K.; David D. Krueger (**2004**). *A Minitab Guide to Statistics* (3rd ed.). Upper Saddle River, NJ: Prentice-Hall Publishing; (b) Hardwick, Colin (**2013**). *Practical Design of Experiments: DoE Made Easy!* (1st ed.). United Kingdom: Liberation Books Ltd.

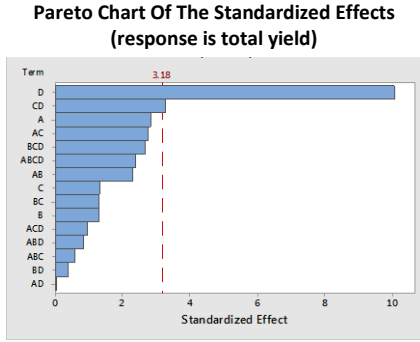

Figure 16: Effect of A (volume), B (temperature), C (oxidant concentration), D (reducing agent), E (time of reaction) on total yield.

As regards the formation of the impurity C (δ-14-vincamine) (Figure 17), the significant parameter is the amount of reducing agent. In fact, the quantity of the impurities decrease with increasing the amount of the reducing agent. The other factors are not significant.

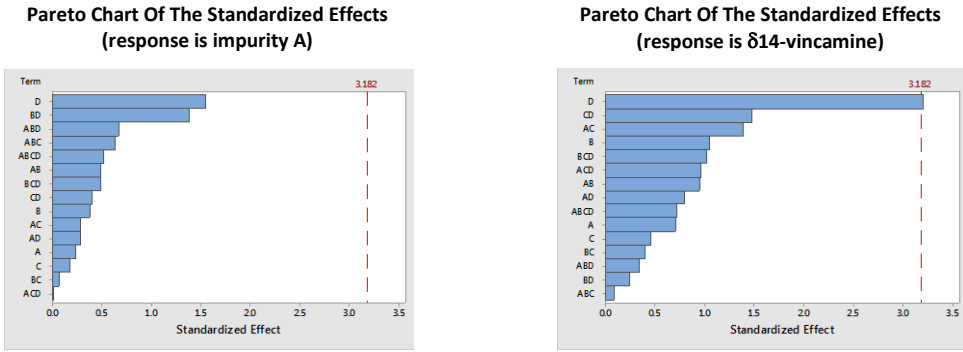

Figure 17: Effect of volume of solvent (A), temperature (B), oxidant concentration (C), reducing agent (D) and time of reaction (E) on some impurities.

In conclusion, the Design of Experiment applied to the synthesis of vincamine from vincadifformine has allowed to obtain some useful information: increasing the stoichiometry of the reducing agent (from "+1" to "-1"), the yield increases. At the same time, the reducing agent leads to the increase of total impurities. Increasing the temperature, the amount of total impurities also increase. The increase in the volume of the reaction affects the formation of dimers, reducing the amount.

We repeated the DOE using an additive in order to evaluate if some impurities could derived from parallel reactions.

We considered to change 4 parameters, one parameter each time, for a total of 20 trials:

A. Volume of solvent
B. Temperature
C. Oxidant concentration
D. Time of reaction

Run	A	B	C	D
1	+1	+1	+1	+1
2	+1	+1	+1	-1
3	+1	+1	-1	+1
4	+1	+1	-1	-1
5	+1	-1	+1	+1
6	+1	-1	+1	-1
7	+1	-1	-1	+1
8	+1	-1	-1	-1
9	-1	+1	+1	+1
10	-1	+1	+1	-1
11	-1	+1	-1	+1
12	-1	+1	-1	-1
13	-1	-1	+1	+1
14	-1	-1	+1	-1
15	-1	-1	-1	+1
16	-1	-1	-1	-1
17	0	-1	0	0
18	0	-1	0	0
19	0	-1	0	0
20	0	-1	0	0

Table 3: Encoding tests

Graphics and considerations below derived from statistical analysis using the Minitab program and they have been made considering a 95% confidence limit ($\alpha = 0.05$).

Figure 18 shows the effect of solvent volume, temperature, oxidant and time of reaction on the molar yield of the reaction: it is positevely influenced by the increase of time reaction, while the other parameters and the combination of them are not statistically significant. In the case of the previous work without the additive (DOE full 5 factors volume, temperature, oxidant and time of addition), it was notice the same effect but the decrease of the yield was even more marked.

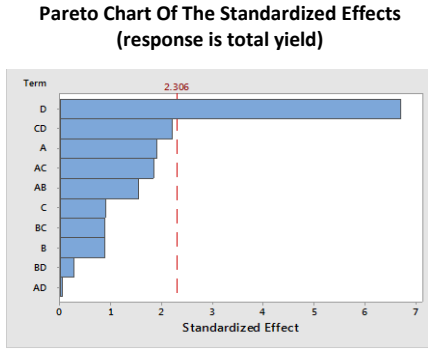

Figure 18: Effect of A (volume), B (temperature), C (oxidant concentration), D (time of reaction) on total yield.

The formation of the impurity A (Figure 19), is no effected by the experimental factors chosen differing from what observed in the DOE without the additive, in which the amount of the impurity decreases with increasing the reducing agent.

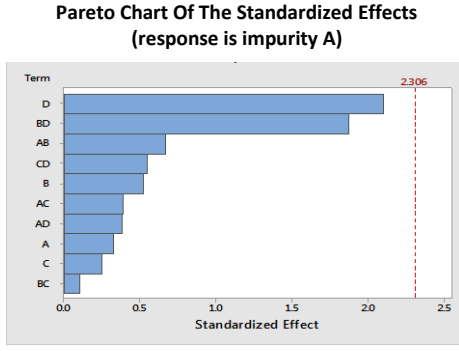

Figure 19: Effect of A (volume), B (temperature), C (oxidant concentration), D (time of reaction) on impurity A.

As regard the formation of impurity C (δ14-vincamine) (Figure 20), the significant parameter is the time of reaction. In the previous DOE without the additive, no factors effected the formation of the impurity.

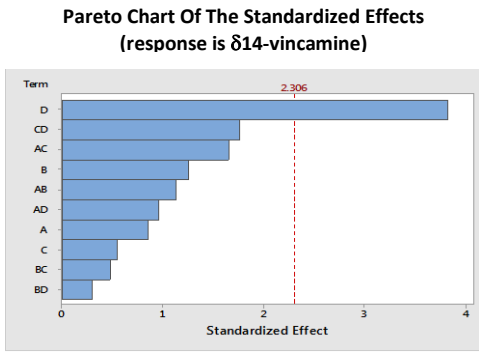

Figure 20: Effect of A (volume), B (temperature), C (oxidant concentration), D (time of addition) on impurity C.

In conclusion, the DOE in the presence of an additive give us some useful information about the formation of the impurities. The volume of solvent showed positive effects on the total impurities, while the temperature had no effect on the impurities formation. The time of addition is an important parameter: increasing the time the total impurities decreases.

2.2.2. Reactivity of 3-oxo-tabersonine and 3-oxo-vincadifformine

In this chapter, the reactivity of both 3-oxo-tabersonine and 3-oxo-vincadifformine is discussed.

3-Oxo-tabersonine and tabersonine are both components of *Voacanga africana*. Since tabersonine is used for the industrial synthesis of vincamine, we decided to synthesize 3-oxo-tabersonine and to apply the same synthetic strategy used to obtain vincamine. The aim of this procedure is to evaluate if impurities formed during the transformation of the tabersonine into vincamine, derive from 3-oxo-tabersonine. Moreover, considering that the preparation of vincamine requires the conversion of tabersonine to vincadifformine, we decided to synthesize 3-oxo-vincadifformine and to submit it to the synthetic condition used to obtain vincamine.

Tabersonine, a terpene indole alkaloid, plays a central role in the biosynthesis of *Aspidosperma* alkaloids. It was first isolated in 1954 by Le Men *et al.*[41] from *Amsonia tabernaemontana.* Shortly after the initial report, the alkaloid was isolated from different other natural sources, demonstrating its relative biological abundance.

In 1978, Aimi and Haginiwa first reported the isolation of 3-oxo-tabersonine from the seeds of *Amsonia elliptica*.[42] Among the alkaloids that they were able to extract and separate from the plant, they were able to obtain a compound with a mass of 350 m/z corresponding to the molecular formula $C_{21}H_{22}O_3N_2$. This data suggested that a methylene group of tabersonine was replaced by a carbonyl group, and an IR absorption band at 1665 cm-1, characteristic of an amide carbonyl group, confirmed this hypothesis. However, from NMR data the signals of AB system were observed at δ 5.94 and δ 6.44 ppm with a coupling constant of 9 Hz, referable to the vicinal olefinic protons on C-14 and C-15, respectively. This information suggested that no proton is present on carbon C-3 and the chemical schift of the olefinic protons suggest a functionalization at C-3. Therefore, this compound was deduced to be 3-oxo-tabersonine. (Figure 21)

[41] Janot, M.-M.; Pourrat, H., Le Men, J. *Bull. Soc. Chim. Fr.***1954**, 707-708.

[42] Aimi, N.; Asada Y.; Sakai, S.I.; Haginiwa J.*Chem.Pharm.Bull.* **1978**, *26*, 1182-1187.

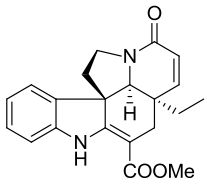

3-oxo-tabersonine
32

Figure 21: Structure of 3-oxo-tabersonine

To confirm the structure, 3-oxo-tabersonine was catalytically reduced with PtO_2 to the dehydro derivative 3-oxo-vincadifformine (Scheme 15).

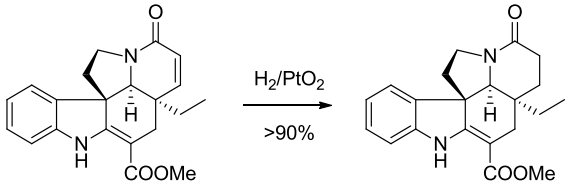

3-oxo-tabersonine
32

3-oxo-vincadifformine
33

Scheme 15: Catalytic reduction of 3-oxo-vincadifformine

Given that Le Men *et al.*[43] reported the synthesis of 3-oxo-vincadifformine, they sent to Prof. Le Men a sample of their product supposed to be 3-oxo-vincadifformine. Le Men confirmed the identity of the sample, proving that Aimi and Haginiwa were able to isolate 3-oxo-tabersonine from the seeds of *Amsonia elliptica*. Then 3-oxo-tabersonine was synthesize by Aimi and Haginiwa on direct oxidation of tabersonine using $KMnO_4$, in order to further support the structure.

Recently, 3-oxo-tabersonine was first isolated also in cultivated *Vinca major* in Kunming botanical garden in China.[44,45] In chapter 4, the isolation and structural characterization of this impurities from the seeds of *Voacanga africana* will be discussed.

In Scheme 16 is reported the synthetic condition for the obtainement of 3-oxo-tabersonine starting from tabersonine.

[43] Laronze, J.Y.; Fontaine, J.L.; Lèvy, J.; Le Men, J. *Tetrahedron Lett*.**1974**, 491.
[44] Cheng, G.G. *et al.Tetrahedron* **2014**, *70*, 8723-8729.
[45] Achenbach, H.; Benirschke, M.; Torrenegra, R. *Phytochemistry* **1997**, *45*, 325-335.

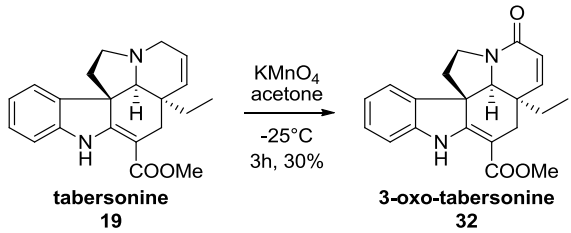

Scheme 16: Synthesis of 3-oxo-tabersonine

Then 3-oxo-tabersonine was submitted to the same sequence to produce vincamine using the same oxidant, solvent, reducing agent and base.

HPLC-MS analysis of the raw material demonstrated that 3-oxo-tabersonine did not react under the reported conditions and the starting material was recovered (Figure 22).

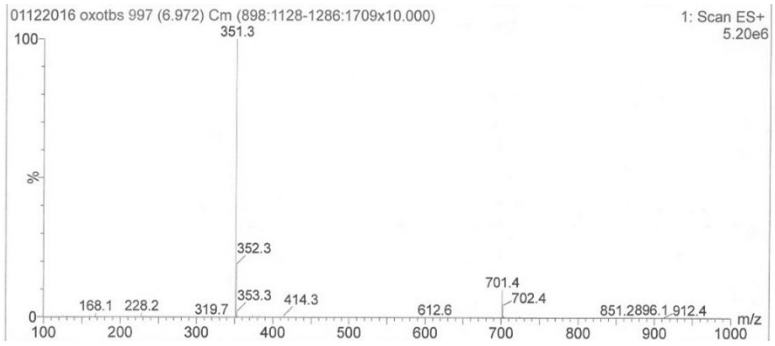

Figure 22: HPLC-MS analysis of the raw material

Le Men *et al.* reported the synthesis of 3-oxo-vincadifformine as an intermediate in their total synthesis of (±) vincadifformine.

3-Oxo-tabersonine has been reduced to 3-oxo-vincadifformine by hydrogenation in the presence of PtO_2 (Scheme 17).

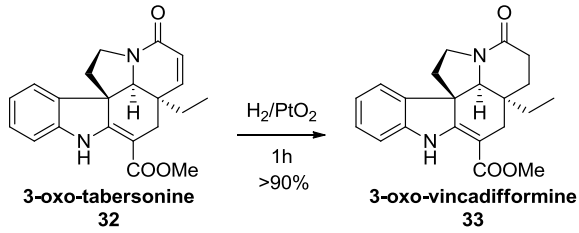

Scheme 17: Synthesis of 3-oxo-vincadifformine

Then 3-oxo-vincadifformine was submitted to the same sequence to produce vincamine using the same reagents.

HPLC-MS analysis of the raw material demonstrated that 3-oxo-vincadifformine did not react under the reported conditions and the starting material was recovered (Figure 23).

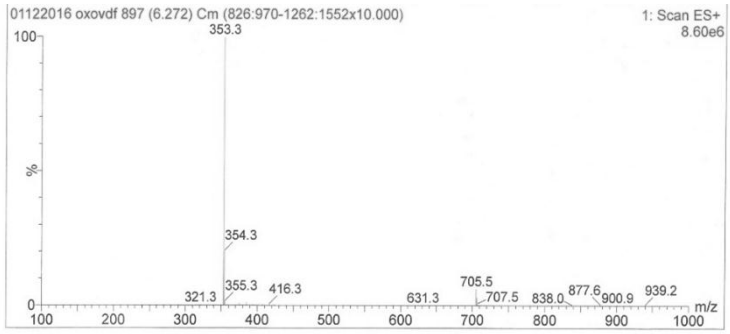

Figure 23: HPLC-MS analysis of the raw material

These analyses revealed that 3-oxo-tabersonine and 3-oxo-vincadifformine did not lead to the formation of crucial impurities.

2.3. Lignans

2.3.1. Introduction

Lignans are naturally occurring plant polyphenols that are derived biosynthetically from phenylpropanoids and they are classified as phytoestrogens due to their structural similarities with mammalian estrogens.[46]

Lignans, which are found in all morphological parts of the plants including roots, leaves, flowers, fruits, and seeds, are secondary metabolites with low molecular weight.

The major dietary sources of lignans are whole vegetables, seeds and legumes, with exceptionally high concentrations of lignans occurring in flaxseed.

Lignans possess numerous pharmacological features including anticancer, antimicrobial, antioxidant, anti-inflammatory and immunomodulating activities, and are largely studied due to their potential usefulness in many hormonal-related conditions such as prostate and breast cancer, cardiovascular disease and conditions associated with the menopause.[47]

Nowadays, their wide use in traditional medicine makes lignans an important family of lead compounds for the development of new therapeutic agents based on structural modifications.[48] Lignans can be classified in five main groups according to their structures: lignans, neolignans, norlignans, hybrid lignans, and oligomeric lignans.

Most lignans are phenylpropanoid dimers, in which the phenylpropane units are linked by the central C-atom, C-8, of their side chains. They differ substantially in substitution pattern, oxidation level, and chemical structure of their basic C-framework.

In addition, lignans are classified in six subgroups based upon the way in which the O-atom is incorporated in the skeleton and cyclization pattern: dibenzylbutyrolactones, dibenzylbutanes, arylnaphthalenes, furofurans, terahydrofurans and dibenzocyclooctadienes (Figure 24).

[46] Dixon, R.A. *Annu Rev Plant Biol.* **2004**, *55*, 225–61.

[47] (a) Knight, D.C.; Eden, J.A. *Obstet Gynecol.* **1996**, *87* ,897–904; (b) Tham, D.M.; Gardner, C.D.; Haskell, W.L. *J. Clin. Endocrinol. Metab.***1998**, *83*, 2223–5.

[48] Gordaliza, M.; Garcia, P. A.; Miguel del Corral, J. M.; Castro, M. A.; Gomez-Zurita, M. A. *Toxicon.***2004**, *44*, 441.

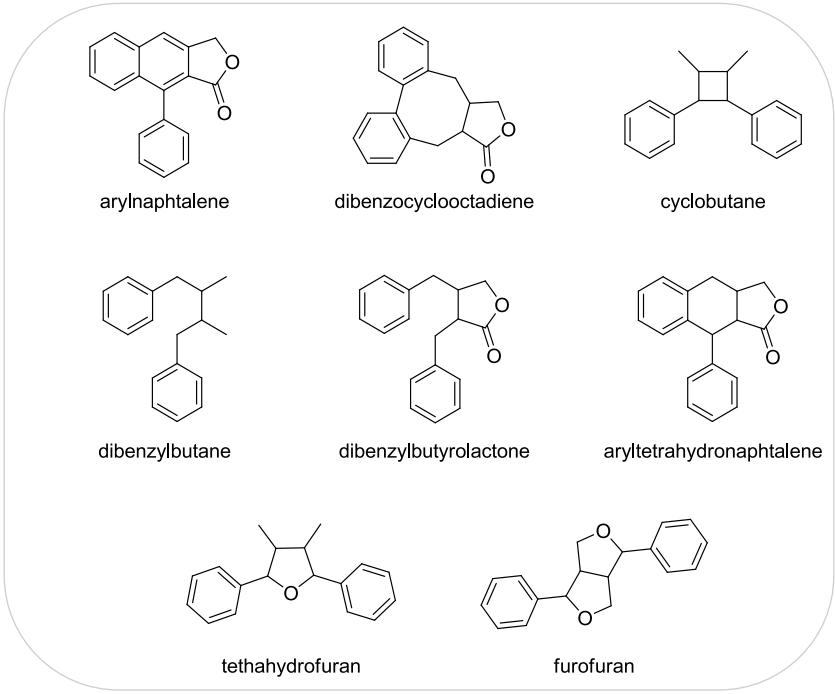

Figure 24: General skeleton of lignans

Among lignans, 7-hydroxymatairesinol (HMR) is the major lignan in Norway spruce (*Picea abies*).

In 1957, Freudenberg and Knof [49] first isolated HMR as a mixture of two isomers in the ratio of ca. 1:3. The two isomers were shown to be diastereomers, since they differ in the relative stereochemistry at position C-7. These isomers were separated, characterized and named by Freudenberg *et al.* as (-)-*allo*-HMR and (-)-HMR, respectively. The stereochemistry of the hydroxymatairesinol isomers has been largely studied by NMR spectroscopy,[50] but only in 2002 Patrik Eklund and Rainer Sjöholm have proved the absolute configurations. They published a paper[51] in which they unambiguously determined that the configurations at C-7 in (-)-*allo*-HMR and (-)-HMR are *R* and *S*, respectively (Figure 25).

[49] Freudenberg, K.; Knof, L.*Chem. Ber.***1957**, *90*, 2857.

[50] (a) Kawamura, F.; Ohashi, H.; Kawai, S.; Teratani, F.; Kai, Y. *Mokuzai Gakkaishi* **1996**, *42*, 301; (b) Mattinen, J. ; Sjöholm, R.; Ekman, R. *ACH Models Chemistry* **1998**, *135* (**4**), 583.

[51] Eklund, P.; Sillanpää, R.; Sjöholm, R.J. *Chem. Soc., Perkin Trans. 1* **2002**, *19*, 1906.

Moreover in 2003[52] they separated the two isomers by chromatography and comparing optical rotation and NMR spectroscopic with previously published data,[13,14] they were able to determine that (-)-*allo*-HMR is the minor while (-)-HMR is the major isomer present in Norway spruce wood.

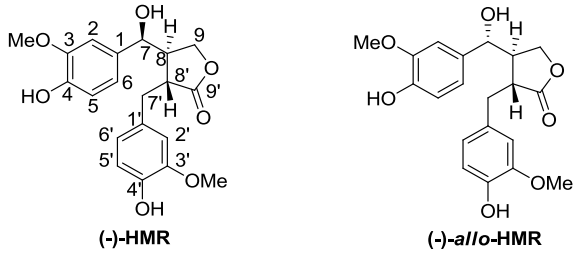

Figure 25: Hydroxymatairesinol isomers

HMR is structurally closely related to the natural plant lignin matairesinol (Figure 26), and it has been shown to metabolise to the known mammalian lignan enterolactone (EL), which possesses antitumourigenic properties for hormone dependent cancer forms.[53] Mammalian lignans bind with low affinity to the estrogen receptors α and β, and are supposed to act as a weak phytoestrogens. However, the mechanism of action for mammalian lignans is not completely understood and other mechanisms than those directly involving estrogen receptors may be involved.

During metabolisation, HMR goes through demethylation and dehydroxylation by intestinal bacteria, forming EL.

Jacobs *et al.*[54] have revealed that enterolactone undergoes further oxidative metabolisation by hepatic microsomes, resulting in hydroxylated compounds by modifications in the aromatic as well as in the aliphatic portions of the molecule.

Conversely, very little is known about the biotransformation of HMR and the biological effects of its metabolites.

[52] Eklund, P. C.; Sjoholm, R. E.*Tetrahedron* **2003**, *59*, 4515-4523.

[53] Saarinen, N. M.; Wärri, A.; Mäkelä, S. I.; Eckerman, C.; Reunanen, M.; Ahotupa, M.; Salmi, S. M.; Franke, A. A.; Kangas, L.; Santti, R. *Nutr. Cancer* **2000**, *36*, 207.

[54] Jacobs, E.; Metzler, M.J. *Agric. Food Chem.***1999**, *47*, 1071.

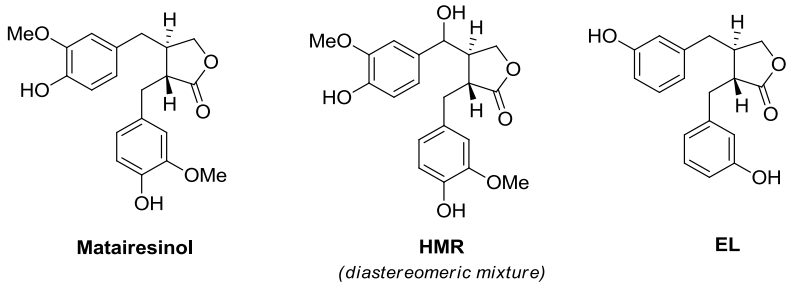

Figure 26: Chemical structures of matairesinol,7-hydroxymatairesinol (HMR) and enterolactone (EL)

HMR is designed for use as a functional food ingredient to decrease the risk of developing certain forms of cancer and the risk of cardiovascular diseases. Moreover, some evidence has been provided that HMR may be a powerful antioxidant.

An important characteristic of HMR is that it could be extracted in large scale from the heartwood of the Norway spruce, *Picea abies*.[55] The spruce knots, that are part of the branches embedded in the stem, contain 6–16% of lignans, and HMR is 65–80% of the total lignan content.[56]

Due to its biological properties and excellent availability, HMR has been proposed as a chemopreventive agent against hormone dependent diseases, cancers and cardiovascular diseases.

[55] Saarinen, N.M.; Warri, A.; Makela, S.I.; Eckerman, C.; Reunanen, M.; Ahotupa, M. *et al. Nutr. Cancer* **2000**, *36*, 207–16.

[56] Hemming, J.; Reunanen, M.; Eckerman, C.; Holmbom, B. *Holtzforschung* **2003**, *57*, 27–36.

The synthesis of oxomatairesinol and (-)-7(*R*)-HMR are reported in the next two sections, **3.4.1** and **3.4.2**. We planned the synthesis of these two lignans in order to have standard reference material for further biological studies. (-)-7(*S*)-HMR is used as starting material, since the potential large-scale isolation from Norway spruce knots makes it readily available (Scheme 18).

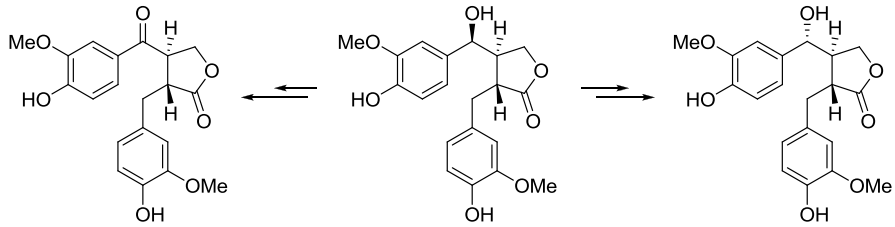

Scheme 18: Transformations of (-)-7(*S*)-HMR

2.4. Lignans derivatives

2.4.1. Synthesis of oxomatairesinol

This chapter is focused on the synthesis of oxomatairesinol starting from (-)-7-(*S*)-HMR **34** via the strategy depicted in Scheme **19**.[57]

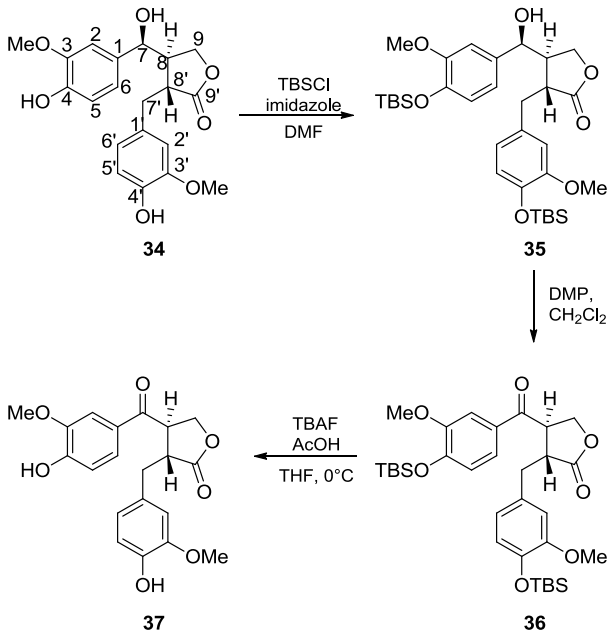

Scheme 19: Transformation of 7(*S*)-HMR in oxomatairesinol

The first reaction was the protection of the hydroxyl groups at position **4** and **4'** of HMR using *tert*-butyldimethylsilyl chloride (TBSCl) and imidazole (Scheme 20).

[57] Fischer, J. A.; Reynolds, J.; Sharp, L. A.; Sherburn, M. S. *Org. Lett.* **2004**, *6*, 1345-1348.

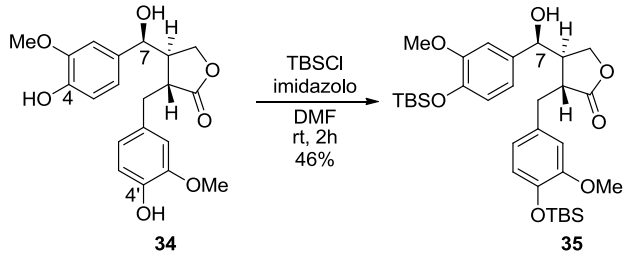

Scheme 20: Synthesis of (-)-bis-TBS-7(*S*)-HMR

The formation of the desired product **35** was evaluated through NMR analysis: it is possible to note the appearance of signals at δ 0.97, 0.95, 0.13, 0.11 ppm related to the *tert*-butyl and methyl protons of the introduced protecting group and the signal at δ 4.58 ppm which refers to the proton at position 7, proving that the protecting groups were introduced only in the desired position 4 and 4'.

The second step (Scheme 21) was the oxidation of the hydroxyl group at position 7 to ketone using Dess-Martin periodinane (DMP) instead of pyridinium chlorochromate (PCC) as reported in literature.

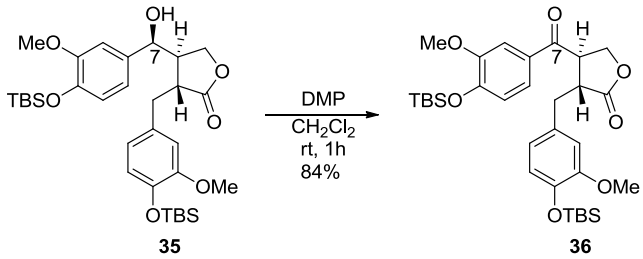

Scheme 21: Synthesis of (+)-bis-TBS-oxomatairesinol **36**

^{1}H-NMR spectrum showed the disappearance of the signal of the proton at position 7 at δ 4.58 ppm, confirming the formation of the desired product **36**.

Finally the deprotection reaction using tetra-*n*-butylammonium fluoride (TBAF), led to the formation of oxomatairesinol in good yield (Scheme 22).

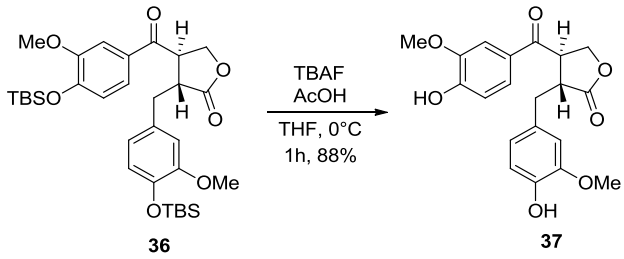

Scheme 22: Synthesis of oxomatairesinol

In literature this reaction was performed at room temperature, but in our case we observed low yield (around 20%). Therefore, we decided to change the reaction conditions decreasing the temperature till 0°C. This trick led us to obtain compound **37** with a very good yield.

NMR analysis of **37** showed the absence of the protecting groups TBS signals. Instead two signals from the hydroxyl group protons appeared at δ 6.15 e 5.47 ppm, respectively. Moreover, spectroscopic data for synthetic oxomatairesinol were compared with those reported in literature, and they were in good agreement with each other.

It is important to note that the configuration at C-8 and C-8' is maintained during the synthethic pathway. ^{1}H-NMR spectrum confirmed that no epimerization occurred, despite the use of mild basic conditions: the proton at position 8' showed a signal at δ 2.90-2.98 ppm as a multiplet in both oxomatairesinol (**37**) and (-)-7-(*S*)-HMR (**34**), while the downfield shift of proton H-8 signal (δ 3.55-3.50 ppm, multiplet) is only due to the presence of a carbonyl group in C-7.

2.4.2. Synthesis of (-)-7(*R*)-HMR

The need to use (-)-7(*R*)-HMR (**39)** as standard reference sample for further biological studies propted us to synthesize this lignan derivative (Scheme 23).

The synthesis involved an inversion of configuration of C-7 using modified Mitsunobu conditions.[58]

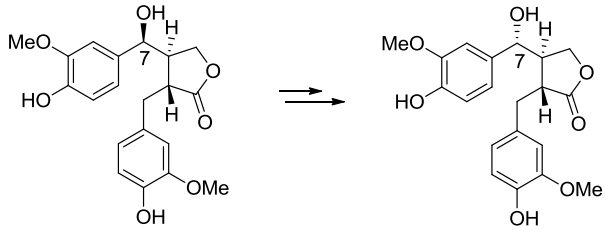

Scheme 23: Conversion of (-)-7(*S*)-HMR in (-)-7(*R*)-HMR

Scheme 24 reported the procedure for the preparation of compound **39**:

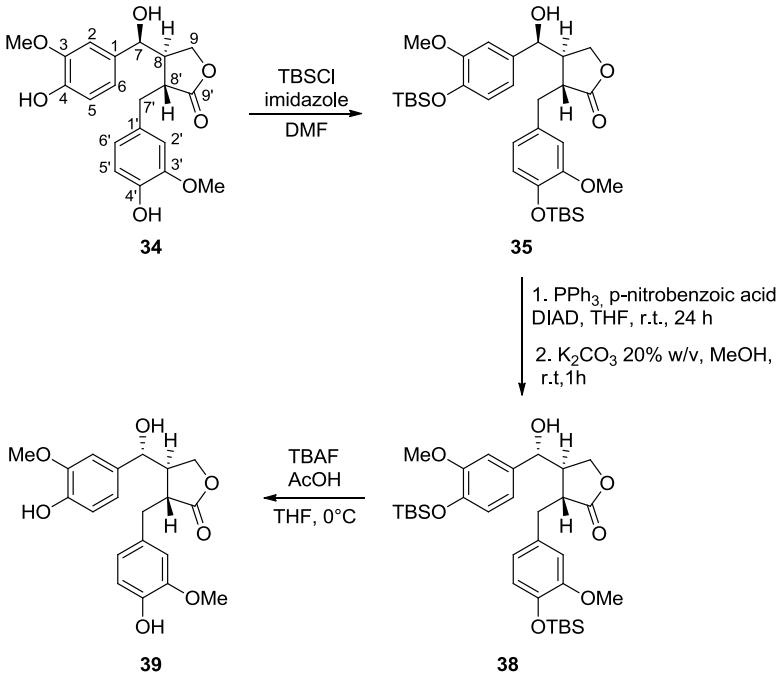

Scheme 24: Synthetic strategy for preparation of (-)-7(*R*)-HMR

[58] Martin, S. F.; Dodge, J. A. *Tetrahedron Lett.***1991**, *32*, 3017-3020.

Starting from (-)-7(*S*)-HMR **34** the first reaction is the protection of the hydroxyl groups at C4 and C4' (Scheme 25).

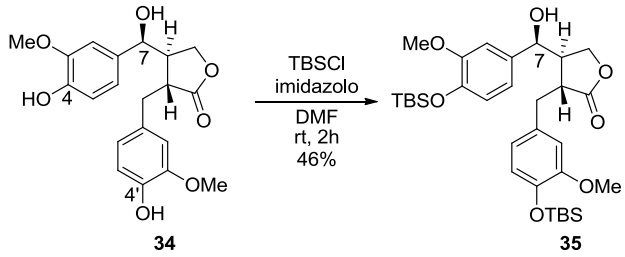

34 **35**

Scheme 25: Synthesis of (-)-bis-TBS-7(*S*)-HMR

The second step involves the inversion of the C-7-hydroxy group of **35** under Mitsunobu conditions (Scheme 26). This reaction was carried out with diisopropyl azodicarboxylate (DIAD) instead of diethyl azodicarboxylate (DEAD) because the former was considered a safer compound and was more readily available.

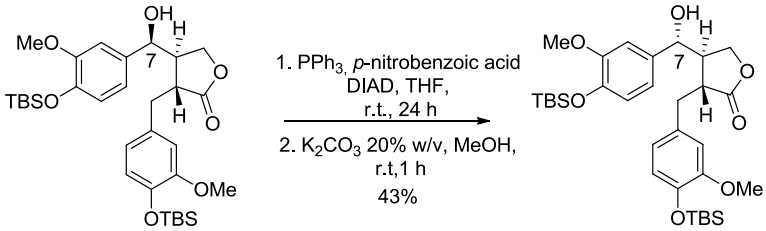

35 **38**

Scheme 26: Synthesis of (+)-bis-TBS-7(*R*)-HMR **38**

The Mitsunobu reaction is one of the most useful reactions in organic synthesis, particularly for the inversion of configuration of secondary alcohols under mild and essentially neutral

reaction conditions.[59,60] In addition, the reaction has proven basically sensitive to the steric environment of the alcohol.[61]

Mitsunobu inversions of encumbered alcohols has proven problematic usually resulting in low yields or recovered starting material. Martin and Dodge reported a simple modification of this reaction that showed an improved yield for the inversion of sterically hindered alcohols. They discovered that simple replacement of benzoic acid with *p*-nitrobenzoic acid[62] occurred in considerably improved yields in the inversion process. The use of *p*-nitrobenzoic acid as the nucleophile in Mitsunobu reaction leads to two other advantages:

1. the *p*-nitrobenzoate esters are readily deprotected through saponification compared to the corresponding benzoates;
2. the *p*-nitrobenzoate esters are frequently crystalline and may be purified without difficulty.

Moreover, the reaction could be performed in anhydrous tetrahydrofuran as an alternative to the commonly used benzene.

Several solvents are suitable for the Mitsunobu reaction. Recently, it was found that the rate of the Mitsunobu esterification reaction is much higher in non-polar solvents.[63] This provides an elucidation as to why the yield in the Mitsunobu reaction, in particular with sterically hindered alcohols, is often higher in non-polar solvents: side reactions, such as acylation of the hydrazine, are much slower in non-polar solvents.[64]

The general mechanism for this reaction is reported in Scheme 27:

[59] (a) Mitsunobu, O. *Synthesis***1981**, 1-28; (b) Kato, K.; Mitsunobu, O. *J.Org. Chem.***1970**, *35*, 4227-4229; (c) Mitsunobu, O.; Yamada, M.*Bull.Chem. Soc. Jpn.***1967**, *40*, 2380.

[60] (a) Jenkins, I. D.; Mitsunobu, O. *In Encyclopedia of Reagents for Organic Synthesis*; Paquette, L. A., Ed.; Wiley: New York, **1995**; Vol. 8, pp 5379 -5390; (b) Hughes, D. L. *Org. React.***1992**, *42*, 335-656.

[61] Bose,A.K.; Lal, B.; Hoffman, W.A.; Manhas, M.S. *Tetrahedron Lett*. **1973**, 1619.

[62] (a)Eaton, P.; Jobe, P.G.; Reingold, I.D. *J.Am.Chem.Soc.***1984**, *106*, 6437; (b)Jarosz, S.; Glodek, J.; Zamojski,A. *Carb. Res.***1987**, *163*, 289.

[63] Camp, D.;Harvey, P.J.; Jenkins I. D. *Tetrahedron* **2015**, *71*, 3932-3938.

[64] Hughes, D. L.; Reamer, R. A. *J. Org. Chem.***1996**, *61*, 2967-2971.

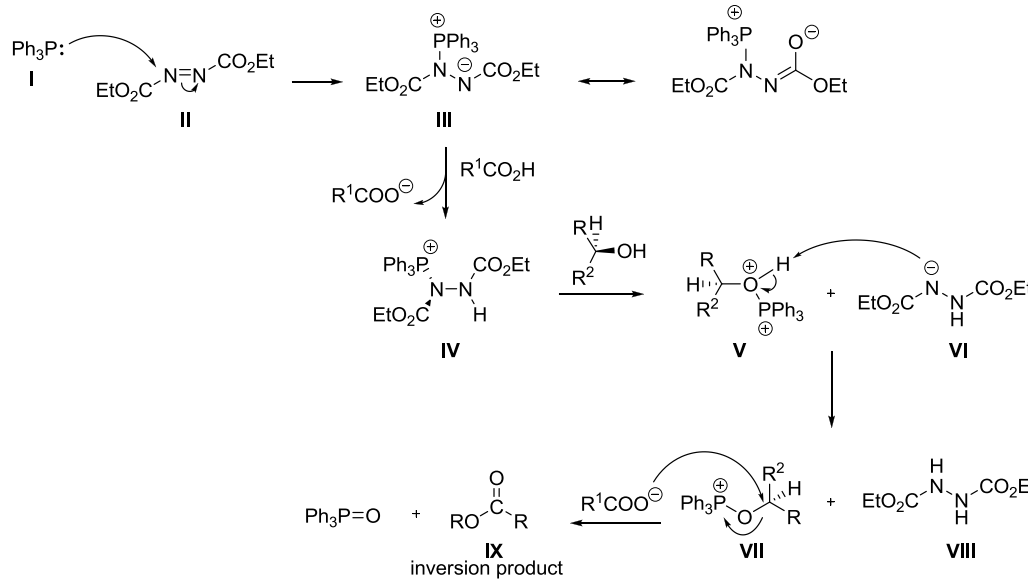

Scheme 27: Mechanism of the Mitsunobu reaction

The first step is the nucleophilic attack of a triphenyl phosphine **I** upon diethyl azodicarboxylate **II** producing a relatively stable betaine intermediate **III**.[65] The anion produced by this first stage is basic enough to remove a proton from the carboxylic acid, generating the nucleophile ready for reaction. Then the positively charged phosphorus is attacked by the alcohol to give compound **V**. The nitrogen anion generated in this step rapidly removes the proton from the alcohol to give intermediate **VII** and a by-product **VIII**, the reduced form of DEAD. Finally, the anion of the nucleophile attacks the phosphorous derivative of the alcohol in a SN_2 reaction at carbon with the posphine oxide as the leaving group.

The formation of intermediate **IX** was evaluated by NMR analysis. The number of ^{1}H-NMR signals indicated that it is a single compound. In particular it was observed a downfield shift of proton H-7 signal (δ 5.82 ppm, doublet) proving the inversion of configuration at C-7.

The hydrolisys of compound **IX** using basic conditions lead to the desired product **38**.

[65] (a) Crich, D.; Dyker, H.; Harris, R. J. *J. Org. Chem.***1989**, *54*, 257-259; (b) Guthrie, R. D.; Jenkins, I. D.Aust. *J. Chem.***1982**, *35*, 767-774; (c) Brunn, E.; Huisgen, R.*Angew. Chem., Int. Ed. Engl.***1969**, *8*, 513-515; *Angew. Chem.***1969**, *81*, 534-536.

Mitsunobu reaction

The mechanism of the Mitsunobu reaction has been the subject of various investigations.[66] A detailed mechanism for this reaction is reported in Scheme 28:

The first step is the nucleophilic attack of a triphenyl phosphine **I** upon diethyl azodicarboxylate **II** producing a relatively stable betaine intermediate **III**.

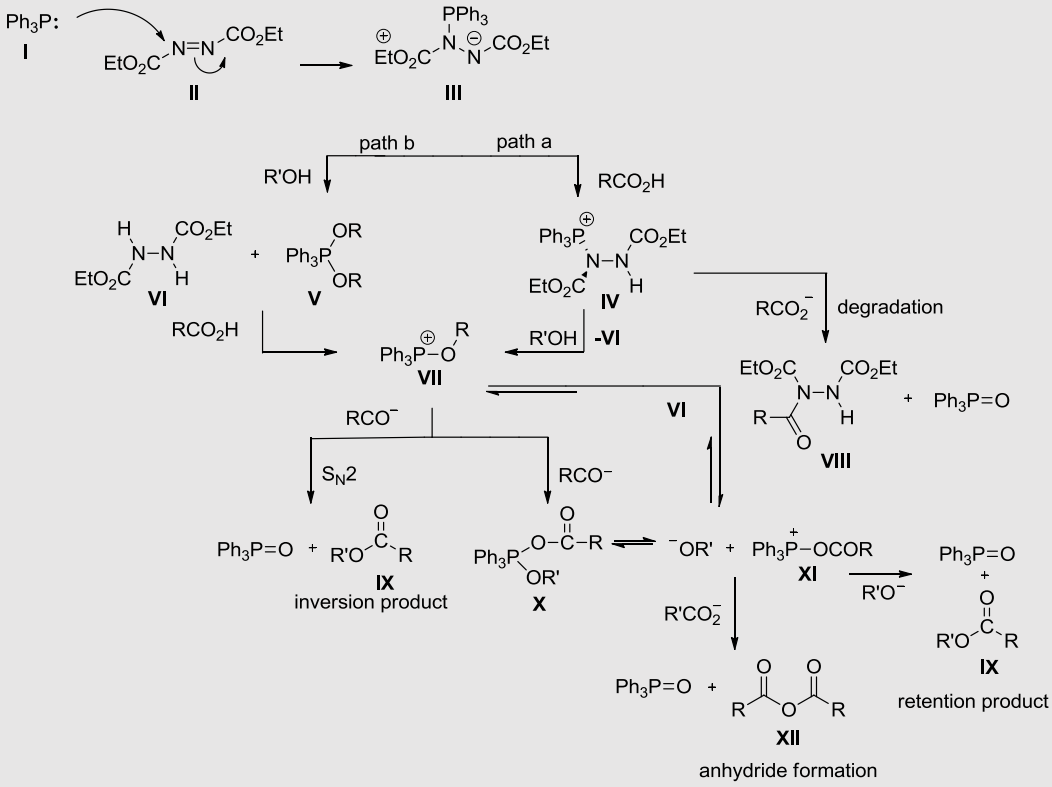

Scheme 28: General mechanism of the Mitsunobu reaction

The second step is not completely clear and many mechanisms were proposed.[67] Betaine **III** can react through two different competing pathways *a* and *b*.[29,68] In path *a* the betaine **III** is

[66] (a)Hughes, D. L.*Org. Prep. Proced. Int.***1996**, *28*,127-164; (b) Dandapani, S.; Curran, D. P. *Chem.Eur. J.***2004**, *10*,3130-3138; (c) Dembrinski, R. *Eur. J. Org. Chem.***2004**, *69*,2763-2772.

[67] (a) Watanabe, T.; Gridnev, I. D.; Imamoto, T. *Chirality* **2000**, *12*, 346-351; (b) Hughes, D. L.; Reamer, R. A.; Bergan, J. J.; Grabowski, E. J. J. *J. Am. Chem. Soc.***1988**, *110*, 6487-6491.

[68] (a) Kumar, N. S.; Kumar, K. P.; Kumar, K. V. P. P.; Kommana, P.; Vittal, J.J.; Swamy, K. C. K. *J. Org. Chem.***2004**, *69*, 1880-1889; (b) Wilson, S. R.; Perez, J.; Pasternak, A. *J. Am. Chem. Soc.***1993**, *115*, 1994-1997

protonated given compound **IV**.[69] After the addition of an equivalent of alcohol, compound **IV** decomposed and a hydrazine **VI** and an alkoxyphosphonium salt **VII** are formed.

In the opposing path *b* the betaine **III** initially reacts with two equivalent of alcohol to produce a dialkoxyphosphorane **V** and a hydrazine **VI**. Subsequently, an acid-induced decomposition of **V** allows the oxyphosphonium salt **VII** under regeneration of one equivalent of alcohol.

In literature there are quite works which shows that the reaction conditions, particularly the order in which the alcohol and acid are added, help to define which pathway is favored.[70] On the contrary, some studies reveal that both pathways are in equilibrium with each other independently of the order of reagent addition.[71]

The nature, in particular the pK_a value, of the carboxylic acid used in the latter step of the Mitsunobu reaction has an important influence on the product yield.[72] This has been identified by a competition between the alcohol and the carboxylate anion for compound **IV**. With acids stronger than acetic acid, for example *p*-nitrobenzoic acid, this degradation side reaction can be avoid. [73]

In addition, also the pK_a of the acid is an important parameter in the reaction pathway. In particular, Jenkins has shown via ^{31}P-NMR that using acids having lower pK_a's than benzoic acid results in equilibria favoring formation of the requisite activated oxyphosphonium intermediate **VII** that undergoes the inversion process.

[69] Varasi, M.; Walker, K. A. M.; Maddox, M. L. *J. Org. Chem.***1987**, *52*, 4235-4238.

[70] (a) Camp, D.; Jenkins, I. D. Aust. *J. Chem.***1992**, *45*,47-55; (b) Von Itzstein, M.; Jenkins, I. D. *J. Chem. Soc., Perkin Trans. 1***1987**, 2057-2060; (c) Von Itzstein, M.; Jenkins, I. D.*J. Chem. Soc., Perkin Trans. 1***1986**, 437-445; (d) Adam, W.; Narita, N.; Nishizawa, Y.*J. Am. Chem. Soc.***1984**, *106*, 6, 1843-1845; (e) Von Itzstein, M.; Jenkins, I. D.Aust. *J. Chem.***1983**, *36*, 557-563. (f) Grochowski, E.; Hilton, B. D.; Kupper, R. J.; Michejda, C. J.*J. Am. Chem. Soc.***1982**, *104*, 6876-6877.

[71] (a) Camp, D.; Jenkins, I. D. *J.Org. Chem*.**1989**,*54*,3045-3049; (b) Camp, D.; Jenkins, I. D. *J. Org. Chem.***1989**,*54*, 3049-3054; (c) Pautard-Cooper, A.; Evans, S. A. Jr.*J. Org. Chem.***1989**, *54*, 2485-2488. (d) Von Itzstein, M.; Jenkins, I. D. Aust. *J. Chem.***1984**, *37*, 2447-2451.

[72] (a) Dodge, J. A.; Trujillo, J. I.; Presnell, M.*J. Org. Chem.***1994**, *59*, 234-236; (b) Caine, D.; Kotian, P. L.*J. Org. Chem.***1992**, *57*, 6587-6593; (c) Saiah, M.; Bessodes,M.; Antonakis, K.*TetrahedronLett.***1992**,*33*, 4317-4320; (d) Martin, S. F.; Dodge, J. A.*Tetrahedron Lett.***1991**, *32*, 3017-3020.

[73] Hughes, D. L.; Reamer, R. A.*J. Org. Chem.***1996**, *61*, 2967-2971.

The last step involves a substitution reaction of the alkoxyphosphonium salt **VII** with a carboxylate ion to produce phosphine oxide and the ester **IX**. To elucidate the second-order kinetics identified for this reaction step in addition to the great excess of inversion product obtained, S_N2 attack by the carboxylate ion on the C-O bond of the activated alcohol has been suggested. At this point if a very weak acid is used and the alcohol is sterically hindered, the Mitsunobu reaction can be diverged into an anhydride channel. The carboxylate anion present in the reaction competes with the alcohol for **VII**, and an acyloxyalkoxyphosphorane **X** is formed.

Moreover, the Mitsunobu procedure can occur with retention of configuration and usually this is due to large mechanistic deviations.

The final step for the synthesis of the desired (-)-7(*R*)-HMR is the deprotection reaction using the same procedure previously described for the synthesis of oxomatairesinol (Scheme 29).

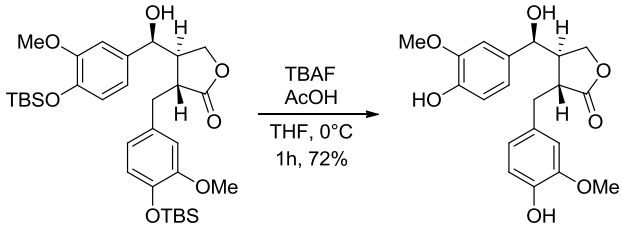

38 **39**

Scheme 29: Synthesis of (-)-7(*R*)-HMR

Spectroscopic data for synthetic (-)-7(*R*)-HMR were in good agreement with those reported in literature. In particular the proton H-7 in (-)-7(*S*)-HMR showed a signal at 4.63 ppm as a doublet (J = 6.5 Hz), while in (-)-7(*R*)-HMR the signal of proton H-7 appears at 4.38 ppm as a doublet (J = 7.8 Hz).

2.5. Experimental part

2.5.1. General information

Thin-layer chromatography (TLC) was performed on Merck precoated 60F254 plates. Reactions were monitored by TLC on silica gel, with detection by Uv light (λ = 254 nm) or by charring with 1% permanganate solution. Flash chromatography was performed using Silica gel (240-400 Mesh, Merck). NMR spectra were recordered with Brucker 300 and 400 MHz spectrometers. Chemical shifts are reported in parts per million (δ) downfield from tetramethylsilane (TMS). EI mass spectra were recorded at an ionizing voltage of 6 kEv on a VG 70-70 EQ. ESI mass spectra were recorded on FT-ICR APEXII. Specific rotations were measured with a P-1030-Jasco polarimeter with 10 cm optical path cells and 1 ml capacity (Na lamp, λ = 589 nm).

Vincamine

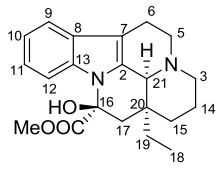

2

[1]H-NMR (400 MHz, $CDCl_3$): δ 7.50 (d, *J* = 6.4 Hz, 1H), 7.19 (dd, *J* = 6.4 and 2.0 Hz,1H), 7.19 (dd, *J* = 6.2 and 2.0 Hz,1H), 7.15 (d, *J* = 6.2 Hz, 1H), 4.60 (bs, 1H), 3.95 (s, 1H), 3.82 (s, 3H), 3.45-3.25 (m, 2H), 3.05-2.97 (m, 1H), 2.85-2.70 (m, 1H), 2.70-2.50 (m, 3H), 2.25 (d, *J* = 14 Hz,1H), 2.15 (d, *J* = 14 Hz,1H), 1.85-1.55 (m, 3H), 1.50-1.40 (m, 2H), 0.95 (t, *J*= 7.2 Hz, 3H) ppm.

[13]C-NMR (100 MHz, $CDCl_3$): δ 175.1, 134.7, 131.9, 129.6, 122.2, 120.9, 119.2, 111.0, 106.6, 82.5, 59.8, 55.0, 51.6, 45.2, 45.0, 35.7, 29.6, 25.7, 21.4, 17.5, 8.3 ppm.

EIMS: *m/z*= 354 (M), 339 (M-Me), 325 (M-Et), 307 (M-Et-H_2O), 295 (M-COOMe), 267 (M-COOMe-CO).

Epivincamine (Impurity B)

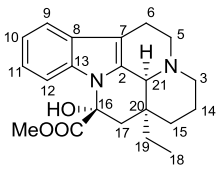

22

^{1}H-NMR (400 MHz, $CDCl_3$): δ 7.07 (d, *J* = 9 Hz, 1H), 6.93 (d, *J* = 2 Hz, 1H), 6.72 (dd, *J* = 9 and 2 Hz, 1H), 4.80 (bs, 1H), 3.91 (s, 1H), 3.83 (s, 3H), 3.77 (s, 3H), 3.40-3.20 (m, 2H), 3.05-2.85 (m, 1H), 2.55-2.45 (m, 3H), 2.30-2.10 (m, 3H), 2.25 (d, *J* = 14 Hz,1H), 2.15 (d, *J* = 14 Hz,1H), 1.88-1.35 (m, 5H), 0.95 (t, *J*= 7 Hz, 3H) ppm.

^{13}C-NMR (100 MHz, $CDCl_3$): δ 173.9, 155.1, 131.7, 130.1, 129.8, 112.0, 11.4, 105.2, 101.0, 82.4, 59.7, 55.5, 53.0, 51.2, 44.7, 44.4, 35.6, 28.6, 25.6, 20.9, 16.9, 7.06 ppm.

EIMS: *m/z*= 354 (M), 307 (M-Et-H_2O), 295 (M-COOMe).

Apovincamine (Impurity D)

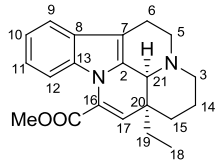

23

^{1}H-NMR (400 MHz, $CDCl_3$): δ 7.44 (d, *J*= 8 Hz, 1H), 7.20-7.02 (m, 3H), 6.15 (s, 1H), 3.90 (bs, 1H), 3.35-3.18 (m, 2H), 3.09-2.95 (m, 1H), 2.65-2.59 (m, 3H), 2.00-1.80 (m, 2H), 1.80-50 (m, 2H), 1.60-1.50 (m, 1H), 1.00-0.90 (m, 1H), 0.05 (t, *J*= 7 Hz, 3H) ppm.

^{13}C-NMR (100 MHz, $CDCl_3$): δ 165.0, 135.0, 130.8, 129.4, 128.9, 128.2, 122.3, 120.6, 118.4, 112.6, 109.0, 55.9, 52.3, 51.5, 45.0, 38.4, 29.2, 27.4, 20.4, 16.4, 8.2 ppm.

EIMS: *m/z*= 336 (M), 307 (M-Et), 266.

Δ14,15-vincamine (Impurity C)

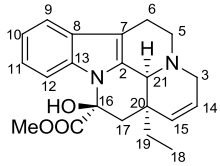

31

^{1}H-NMR (400 MHz, $CDCl_3$): δ 7.50 (d, *J*= 7.5 Hz, 1H), 7.05-7.15 (m, 3H), 5.78 (s, 1H), 5.62 (s, 1H), 4.85 (bs, 1H), 4.13 (s, 1H), 3.90 (s, 3H), 3.50-3.35 (m, 2H), 3.20-3.03 (m, 3H), 2.65-2.55 (m, 1H), 2.43-2.35 (m, 2H), 2.09-1.95 (m, 1H), 1.70-1.60 (m, 1H), 1.05 (t, *J*= 7.5 Hz, 3H) ppm.

^{13}C-NMR (100 MHz, $CDCl_3$): δ 173.1, 134.3, 131.6, 129.2, 128.1, 125.6, 121.7, 120.3, 118.4, 110.5, 106.3, 82.2, 57.5, 54.0, 49.6, 43.8, 43.7, 63.9, 34.9, 16.7, 8.46 ppm.

EIMS: *m/z*= 352 (M), 323 (M-Et), 319 (M-Me-H_2O), 305 (M-Et-H_2O), 293 (M-COOMe), 284.

Synthesis of 3-oxo-tabersonine (32)

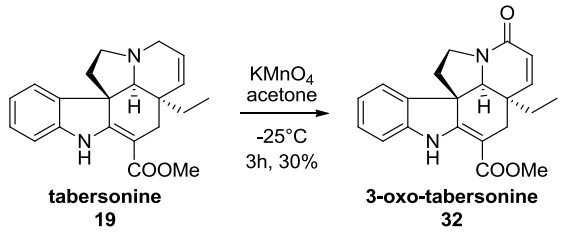

tabersonine
19

3-oxo-tabersonine
32

To a solution of tabersonine (0.200 g, 0.6 mmol) in dry acetone (15 mL), powdered $KMnO_4$ (0.112 g, 0,71 mmol) was added at – 25°C. Within three hours 0.037 g of $KMnO_4$ were added. The reaction mixture was filtered and then was washed with saturated aqueous $NaHSO_3$, alkalized till pH 10 and extracted with CH_2Cl_2. The organic extracts were combined and the solvent was removed in vacuo. The residue was purified by flash chromatography (AcOEt), giving 3-oxo-tabersonine as a colourless oil (0.065 g, 30%).

^{1}H-NMR (400 MHz, $CDCl_3$): δ 9.03 (bs, 1H), 7.32-6.92 (m, 4H), 6.41 (d, *J*= 10.6 Hz, 1H), 5.92 (d, *J*= 10.6 Hz,1H), 4.32-4.27 (m, 1H), 3.76 (s, 3H), 3.52-3.23 (m, 1H), 2.66 (d, *J* = 15 Hz,1H), 2.06 (d, *J* = 15 Hz,1H), 1.98-1.56 (m, 2H), 1.15-0.9 (m, 2H), 0.69 (t, *J*= 7 Hz, 3H) ppm.

^{13}C-NMR (100 MHz, CD_3OD): δ 169.0, 166.7, 163.4, 139.1, 144.8, 136.5, 129.4, 122.8, 122.6, 122.0, 11.3, 90.8, 68.0, 58.3, 51.7, 44.8, 44.6, 41.7, 28.0, 27.5, 7.5 ppm.

ESIMS: *m/z*= 351 $[M+H]^+$

Synthesis of 3-oxo-vincadifformine (33)

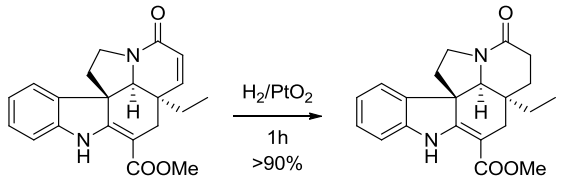

3-oxo-tabersonine
32

3-oxo-vincadifformine
33

3-Oxo-tabersonine (0.05 g, 0.14 mmol) was reduced catalytically in MeOH (4 mL) with PtO_2 (0.005 g) at room temperature. After 1 hour, the reaction mixture was filtered over celite and the solvent was removed in vacuo giving 3-oxo-vincadifformine as white solid (quantitative yield).

^{1}H-NMR (400 MHz, $CDCl_3$): δ 9.01 (bs, 1H), 7.30-6.82 (m, 4H), 4.25 (dd, *J* = 12, 8 Hz,1H), 3.75 (s,3H), 3.50 (bs, 1H), 3.42 (dd, *J* = 12, 6 Hz,1H), 2.66 (dd, *J* = 15.5, 1.5 Hz,1H), 1.98 (d, *J* = 15.5 Hz,1H), 1.82-1.56 (m, 4H), 1.40-1.35 (m, 1H), 1.00 (q, *J*= 6.8 Hz, 2H), 0.71 (t, *J*= 6.8 Hz, 3H) ppm.

^{13}C-NMR (100 MHz, CD_3OD): δ 170.1, 166.5, 163.0, 139.5, 144.5, 129.2, 122.6, 122.0, 11.3, 91.1, 68.0, 58.3, 51.8, 44.8, 44.5, 41.8, 32.5, 28.5, 28.0, 27.5, 8.1 ppm.

ESIMS *m/z*: 353 $[M+H]^+$

S**ynthesis of (-)-bis-TBS-7(*S*)-HMR (35)**

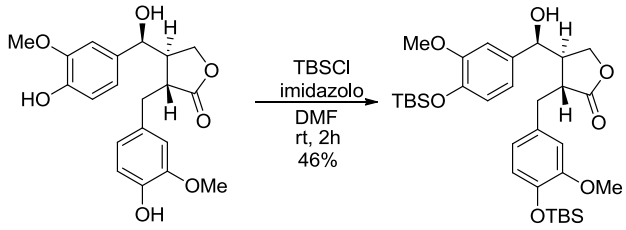

To a solution of (-)-7(*S*)-HMR **34** (0.250 g, 0.66 mmol) in DMF (2.5 mL) at rt was added TBSCl (0.211 g, 1.42 mmol) and imidazole (0.226 g, 3.34 mmol).

The reaction mixture was stirred for 2 hours then washed with saturated aqueous $NaHCO_3$ and brine and dried over anhydrous sodium sulfate. The solvent was removed in vacuo and the crude material was purified by flash chromatography (Hexane/EtOAc 8:2) to give **35** as colourless oil (0.186 g, 46% overall yield).

^{1}H-NMR (400 MHz, $CDCl_3$): δ 6.81 (d, *J* = 8.1 Hz, 1H), 6.78-6.44 (m, 5H), 4.58 (d, *J* = 6.8 Hz, 1H), 3.92-3.83 (m, 2H), 3.78 (s, 3H), 3.75 (s, 3H), 3.13 (dd, *J* = 13.2, 4.9 Hz, 1H), 3.07-2.97 (m,1H), 2.94-2.78 (m,1H), 2.62-2.54 (m, 1H), 0.97 (s, 9H), 0.95 (s, 9H), 0.13 (s, 6H), 0.11 (s, 6H) ppm.

^{13}C-NMR (100 MHz,$CDCl_3$): δ 179.4, 150.9, 150.1, 1454.6, 144.0, 135.1, 131.1, 122.5, 120.9 120.5, 117.5, 113.1, 110.2, 74.9, 68.8, 55.8, 55.0, 45.5, 43.0, 35.0, 26.2, 18.8, -4.5 ppm.

Synthesis of (+)-bis-TBS-Oxomatairesinol (36)

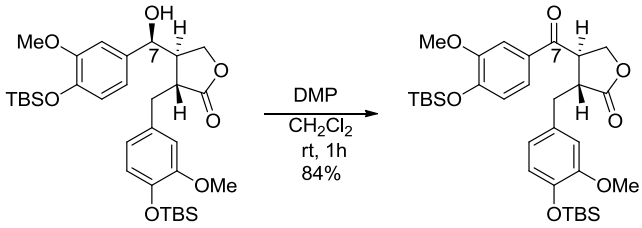

35 **36**

To a solution of the protected HMR **35** (0.186 g, 0.31 mmol) in CH_2Cl_2 (5 mL) was added DMP (0.144 g, 0.99 mmol). The reaction mixture was stirred at rt for 1 hour, then washed with saturated aqueous $NaHCO_3$ and extracted with CH_2Cl_2. The combined organic phases were dried over anhydrous Na_2SO_4, and the solvent was removed in vacuo. The residue was purified by flash chromatography (Hexane/EtOAc 8:2) to give **36** as oil (0.156 g, 84% overall yield).

^{1}H-NMR (400 MHz, $CDCl_3$): δ 7.33 (s, 1H), 7.11 (d, *J* = 8.3 Hz, 1H), 6.79 (d, *J* = 8.1 Hz, 1H), 6.66 (d, *J*= 8.1 Hz, 1H), 6.58 (s, 1H), 6.50 (d, *J* = 8.1 Hz, 1H), 4.40-4.28 (m, 1H), 4.11-3.98 (m, 2H), 3.82 (s, 3H), 3.63 (s, 3H), 3.55-3.48 (m,1H), 3.06-2.94 (m, 2H), 0.98 (s, 9H), 0.95 (m, 9H), 0.17 (s, 6H), 0.05 (s, 6H) ppm.

^{13}C-NMR (100 MHz, $CDCl_3$): δ 195.0, 177.2, 150.9, 151.3, 151.0, 144.0, 130.4, 129.5, 122.6, 121.5, 121.0, 120.2, 112.9, 111.1, 68.3, 55.4, 55.2, 46.8, 44.6, 34.4, 26.0, 25.6, 18.5, 18.4, -4.6, -4.7 ppm.

Synthesis of oxomatairesinol (37)

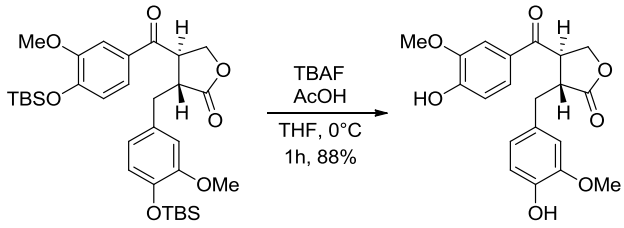

36 **37**

To a solution of the (+)-bis-TBS-oxomatairesinol **36** (0.150 g, 0.25 mmol) in THF (1 mL) and acetic acid (5 µL, 0.99 mmol) was added TBAF (0.2 mL, 1M in THF, 0.99 mmol) at 0°C. The reaction mixture was stirred at 0°C for 2 hours, then washed with saturated aqueous NH_4Cl and extracted with diethyl ether. The organic extracts were combined and the solvent was removed in vacuo. The residue was purified by flash chromatography (Hexane/AcOEt 1:1), giving the oxomatairesinol **37** as a colourless oil (0.082 g, 88% overall yield).

^{1}H-NMR (400 MHz, $CDCl_3$): δ 7.32 (d, *J* = 2.0 Hz, 1H), 7.19 (dd, *J* = 8.3, 2.0 Hz, 1H), 6.89 (d, *J* = 8.3 Hz, 1H), 6.72 (d, *J* = 7.8 Hz, 1H), 6.59 (d, *J* =2.0 Hz, 1H), 6.52 (dd, *J* = 7.8, 2.0 Hz, 1H), 6.16 (s, 1H), 5.48 (s, 1H), 4.39-4.32 (m,1H), 4.15-4.08 (m, 2H), 3.91 (s, 3H), 3.73 (s, 3H), 3.54-3.48 (m, 1H), 2.98-2.90 (m,1H),3.06-2.90 (m, 1H) ppm.

^{13}C-NMR (100 MHz, $CDCl_3$): δ 194.6, 177.0, 151.5, 146.9, 146.5, 144.5, 128.8, 128.6, 123.5, 122.0, 114.3, 113.8, 112.0, 109.9, 68.3, 56.3, 55.7, 46.4, 45.0, 34.3 ppm.

Synthesis of (+)-bis-TBS-7(*R*)-HMR (38)

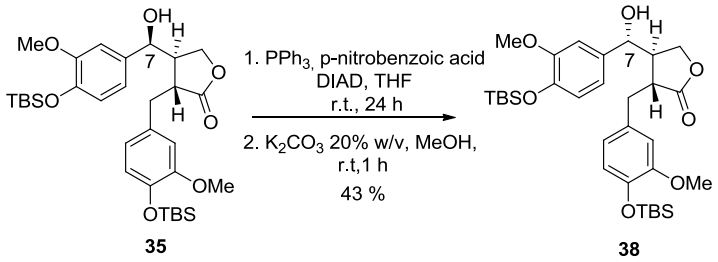

To a solution of the TBS protected HMR **35** (0.180 g, 0.31 mmol), *p*-nitrobenzoic acid (0.150 g, 0.93 mmol) and triphenylphosphine (0.236 g, 0.93mmol) in anhydrous THF (8 mL) at rt was added DIAD (0.2 mL, 0.93 mmol). The mixture was stirred at rt overnight then the solvent was removed in vacuo. The *p*-nitrobenzoate was purified by flash chromatography (Hexane/AcOEt 8:2) then dissolved in methanol (4 mL) and treated with an aqueous solution of K_2CO_3(0.2 mL, 20% w/v). After 1 hour the mixture was diluted with diethyl ether and washed with saturated aqueous NH_4Cl. The organic phase was separated and the aqueous phase was extracted with diethyl ether. The combined organic phases were dried over anhydrous sodium sulfate and the solvent was removed in vacuo. The product was purified by flash chromatography (Hexane/AcOEt 8:2) to give **38** as a colourless oil (0.561g, 43%).

^{1}H-NMR (300 MHz, $CDCl_3$): δ 6.79 (d, *J*= 8.1 Hz, 1H), 6.72 (d, *J*= 7.8 Hz, 1H), 6.65 (d, *J*= 2.0 Hz, 1H), 6.60-6.58 (m, 2H), 6.47 (dd, *J*= 8.1, 2.0 Hz, 1H), 4.39 (dd, *J*= 6.6, 2.2 Hz, 1H), 4.29 (dd, *J*= 9.3, 7.1 Hz, 1H), 3.98 (dd, *J*= 8.1, 8.1Hz, 1H), 3.77 (s, 3H), 3.74 (s, 3H), 2.85-2.67 (m, 3H), 2.58-2.47 (m, 1H), 0.98 (s, 9H), 0.97 (s, 9H), 0.12 (s, 6H), 0.11 (s, 6H) ppm.
^{13}C-NMR (100 MHz, $CDCl_3$): δ 180.0, 151.3, 151.0, 145.1, 143.9, 135.1, 130.9, 121.5, 121.0, 120.7, 118.1, 112.9, 109.5, 74.1, 67.9, 55.4, 46.1, 43.3, 34.7, 25.7, 18.4, -4.7 ppm.

Synthesis of (-)-7(*R*)-HMR (39)

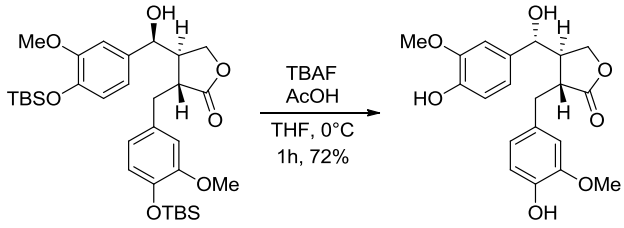

38 **39**

To a solution of the (+)-bis-TBS-7(*R*)-HMR **38** (1.12 g, 1.86 mmol) in THF (50 mL) and acetic acid (0.41 mL, 7.44 mmol) was added TBAF (7.44 mL, 1M in THF, 7.44 mmol) at 0°C. The reaction mixture was stirred at 0°C for 2 hours, then washed with saturated aqueous NH_4Cl and extracted with diethyl ether. The organic extracts were combined and the solvent was removed in vacuo. The residue was purified by flash chromatography (Hexane/AcOEt 1:1), giving 7(*R*)-HMR **39** as a colourless oil (0.500 g, 72%).

^{1}H-NMR (400 MHz, $CDCl_3$): δ 6.82 (d, *J*= 8.0 Hz, 1H), 6.76 (d, *J*= 7.9 Hz, 1H), 6.63 (dd, *J*= 8.1, 1.9 Hz, 1H), 6.54 (d, *J*= 1.9 Hz,1H), 6.47 (dd, *J*= 8.0, 1.9 Hz, 1H), 6.42 (d, *J*= 1.9 Hz, 1H), 4.43 (dd, *J*= 9.5, 5.6 Hz, 1H), 4.38 (d, *J*= 7.8 Hz, 1H), 4.22 (dd, *J*= 9.5, 7.6 Hz,1H), 3.79 (s, 3H), 3.74 (s, 3H), 2.79-2.72 (m, 2H), 2.65-2.59 (m, 1H), 2.54-2.47 (m, 1H) ppm.

$[a]_D^{20}$ = - 3.45 (c 0.10, $CHCl_3$)

^{13}C-NMR (100 MHz, CDCl3): δ 179.4, 146.8, 146.6, 145.5, 144.4, 133.5, 129.3, 122.0, 119.2, 114.0, 113.9, 111.0, 107.9, 74.4, 68.4, 55.7, 45.0, 43.8, 34.9, 29.7 ppm.

3. Isolation and structural characterization of natural products

3.1. Indole alkaloids from *Vocanga africana*

3.1.1. *Voacanga africana*

In the past decades, many investigations were made on plants belonging to the genus *Voacanga* (Apocynaceae) for their biologically active components. In fact, the alkaloids are the principal bioactive compounds responsible for its use as medicinal plants.

Figure 27: *Voacanga africana*

Voacanga africana is a small tropical tree occurring mainly in West Africa. It has white or yellows flowers and its fruits occur mainly in pairs, spherical, green with seeds wrapped in yellow pulp (Figure 27).

In Africa it is traditionally used for the treatment of a wide range of diseases, such as diarrhea, generalized edema, leprosy, convulsions in children and madness. Moreover, bark infusions are used for stomac, hernia, cardiac spams, post partum pain, and kidney affections. In southeastern Nigeria the plant is used in many healing rituals as well to induce hallucinations and trances in religious rituals.

Different compounds were isolated from various organs of *Voacanga* species. The presence of tannins, phenols, flavonoids, terpenes and steroids alkaloids has been reported in the seeds, leaves, stem bark and root.[74] There is a qualitative and quantitative diversity in alkaloid composition and content by plant tissue and species.

The seeds and root bark are the main source of indole alkaloids (the alkaloids content is 5-10%), such as tabersonine, an aspidosperma-type alkaloid. The other alkaloids content was reported as 4-5% in trunk bark, 0.3-0.45% in leaves and 1.5% in seeds.

[74] (a) Tona, L.; Kambu, K.; Ngimbi, N.; Cimanga, K.; Vlietinck, A.J. *J. Ethnopharmacol* **1998,** *61*, 57-65; (b) Gangoue-Pieboji, J.; Pegnyemb, D.E.; Niyitegeka, D.; Nsangou, A.; Eze, N.; Minyem, C.; Mbing, J.N.; Ngassam, P.; Tih, R.G.; Sodengam, B.L.; Bodo, B. *Ann. Trop. Med. Parasit.* **2006**, *100*, 237-243; (c) Agbor, G.A.; Kuate, D.; Oben, J.E. *Pak. J. Biol. Sci.* **2007,** *10*, 537-544.

Alkaloids found in *Voacanga*, such as voacamine and voacangine, have also been found in other species of the family Apocynaceae (for example *Peschiera fuschiaefolia*). In table 4 are reported some compounds isolated from different sources of Voacanga.[75,76]

Alkaloid	*Organ Distribution*	*Species/Sources*
Amataine	Root Bark	*V. Chalotina*
(-)-Tabersonine	Cell Culture	*V. africana*
Folicangine	Leaves	*V. africana*
Vincamol	Seed	*V. africana*
Voacafrine	Bark	*V. africana*
Voacangine	Trunk Bark	*V. africana*
Vincamone	Seed	*V. africana*
Vacorine	Tree Bark	*V. africana*
Voacristine	Bark	*V. africana And V. Thousarsii*
Voacryptine	Bark and Root Bark	*V. africana*
Voacamidine	Bark and Root Bark	*V. africana*
Voafolidine	Leaf	*V. africana*
Voafoline	Leaf	*V. africana*
Tabernanthin	Root bark	*V. africana*
Δ14-Vincanol	Seed	*V. africana*
Cuanzine	Root bark	*V. Chalotiana*
Campesterol	Seed	*V. africana*
Voafrine A And B	Cell Culture	*V. africana*
Vobtusamine	Leaves	*V. Chalotiana*
Voafolidine	Leaves	*V. Thouarsii*
Lupeol	Leaves	*V. Globosa*
Vobasinol	Bark	*V. schweinfurthii*

Table 4: Some alkaloids isolated from different sources of Voacanga

[75] Hussain, H.; Hussain, J.; Al-Harrasi, A.; R. Green, I.; *Pharm. Biol* .**2012**, *50*,1183–1193.

[76]Koroch, A. R.; Juliani, H. R.; Kulakowski, D.; Arthur, H.; Asante-Dartey, J.; Simon, J. E. *ACS Symposium Serie s***2009**, *1021*, 363-380.

3.1.2. Isolation and structure elucidation of *Voacanga* alkaloids

The isolation of interesting products, mainly indole alkaloids, from plants of the *Voacanga* genus prompted us to isolate and to determine the alkaloids structure from *V. africana* (Apocynaceae) seeds.

The idea of the extraction is to separate the soluble plant secondary metabolites, leaving behind the residual plant material (marc). The crude extracts includes complex mixture of many plant metabolites, for example alkaloids, glycosides, lignans, flavonoids and terpenoids. However, some of the initially obtained extracts may be directly use as medicinal agents in the form of fluid extracts and tinctures but some need additional processing.

Different methods[77] can be employed to extract active compoundsfrom the plant material:

- Maceration
- Infusion
- Digestion
- Decoction
- Percolation
- Hot continuos extraction (Soxhlet extraction)
- Fermentation
- Counter-current extraction
- Sonication
- Supercritical fluid extraction
- Phytonic extraction (with hydrofluorocarbon solvents)

We evaluated the alkaloids composition in the extracts of *V. africana* seeds employing two different methods: extraction at room temperature and Soxhlet extraction.

[77] Handa SS, Khanuja SPS, Longo G, Rakesh DD (**2008**) Extraction Technologies for Medicinal and Aromatic Plants, (1stedn), no. 66. Italy: United Nations Industrial Development Organization and the International Centre for Science and High Technology.

In Soxhlet method the sample, which is reduced to fine particles, is positioned in a porous bag or "thimble" composed by a strong filter paper or cellulose, which is placed in thimble chamber of the Soxhlet apparatus (Figure 28). The extracting solvent is heated in a bottom flaskand it vaporizes into the sample thimble. The vapor condenses in the condenser and drip back, extracting the crude drug by contact. When the liquid content arrives at the siphon arm, the liquid contents let out into the bottom flask again and the process begins again. The advantage of this extraction technique is that large amounts of drug can be extracted with a much smaller quantity of solvent.

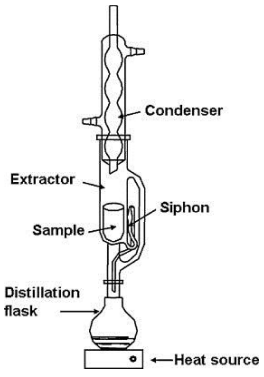

Figure 28: Soxhlet apparatous

The main steps of the alkaloids extraction are indicated in the Scheme 30. A 100 g batch of *Voacanga* seeds yielded 4g of alkaloids mixture by both extraction at room temperature and Soxhlet extraction. The total alkaloids extract was separated by column chromatography.

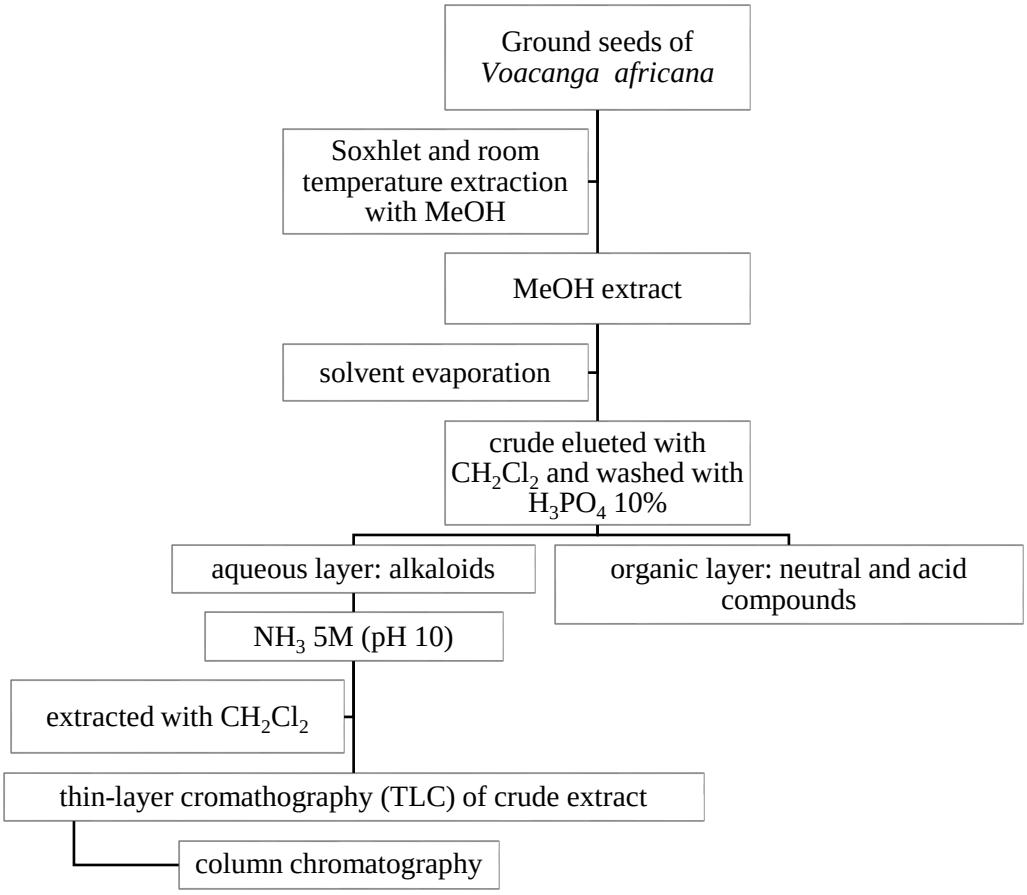

Scheme 30: Isolation of plant natural products

Ten known indole alkaloids **40-47** (Figure 29) were isolated from the seeds of *Voacanga africana* (Apocynaceae) and their chemical structures were determined by spectroscopicand mass analysis.

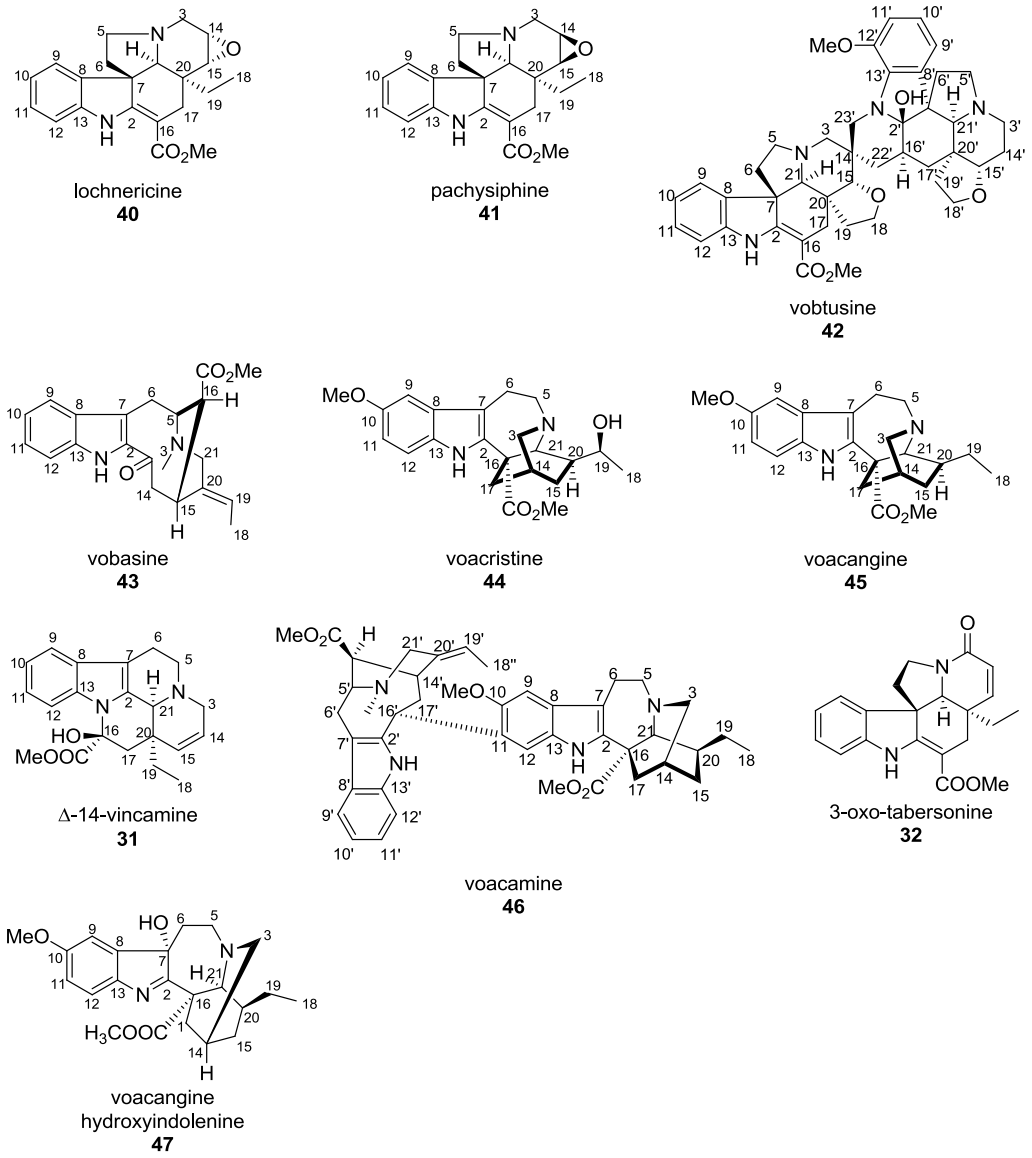

Figure 29: Structures of voacanga alkaloids.

The mass spectrum (ESI) of lochnericine **40** showed the peak $[M+H]^+$at m/z 353. The ^{1}H-NMR spectrum showed the signals of the protons at position 14 and 15 at δ 3.51-3.45 (m, 2H) and δ 3.14 (1H, d, *J*= 4 Hz) respectively.The orientation of the C-14, C-15 epoxide in lochnericine was confirmed by the correlation peaks observed between H-3a**,** H-17a, H-14 and H-15 in the NOESYspectrum of **40**.

Moreover the spetctroscopic data of lochnericine were compared with those reported in literature, and they were in good agreement.[78]

For what regard alkaloid **41**, the presence of an epoxide ring in the structure of **41** was confirmed by two signals at 3.59-3.51 (m, 1H) and 3.25 ppm (lH, dd, *J*= 5.3 and 3.9 Hz) respectively in its ^{1}H-NMR spectrum, that appears in vicinal positions as confirmed by ^{1}H-^{1}H COSY experiment. The orientation of the C-14, C-15 epoxide in pachysiphine was determined by comparison with the ^{13}C data for lochnericine.

Alkaloid **42**, named vobtusine, presented a molecular peak ([M+H]$^{+}$) at m/z 719, accompanied by the other peaks at 701 (M-H_2O) and 691 (M-28), 365 and 304. Comparison of the ^{13}C-NMR spectral data of **42** with already known *Voacanga* alkaloids suggested a spirocyclic bisindole skeleton having two units of an *Aspidosperma* substructure characteristic for a vobtusine congener.

^{1}H-NMR spectral data revealed signals assignable to one N-H at δ 8.92 ppm as a singlet, seven aromatic protons in a range of δ 7.4-6.5 ppm, two methoxy groups at δ 3.77 (s, OCH_3) and at δ 3.67 (s, COOCH_3) ppm. Vobtusine was identified based on comparison of its spectral data with the one reported in literature.

Vobasine **43**, showed a molecular peak (ESI) at m/z 353 ([M+H]$^{+}$). The ^{1}H-NMR spectrum showed 4 signals in the aromatic region. Mutiplicity (d, d, t, t) confirmed the presence of an indole moiety. The signal of the protons at position 4 appeared at δ 2.63 ppm as singlet, while the presence of the OMe group was revealed by the presence of a signal at δ 2.61 ppm as a singlet. ^{13}C-NMR data confirmed the presence of two carbonyl groups at δ 189.6 and δ 171.3 ppm respectively. In addition it was observed the presence of a single olefinic signal at δ 119.4 ppm (C-19). These data were compared with those reported in literature and they were in agreement with each other.[79]

For what regard compound **44**, the mass (ESI) revealed a molecular peak at m/z 385 ([M+H]$^{+}$).

[78] Eles,J.; Kalaus, G.; Greiner, I.; Kajtàr-Peredy, M.; Szabò, P.; Keserû, G.M.; Szabò, L.; Szàntay, C. *J. Org. Chem.* **2002**, *67*, 7255-7260.

[79] Pereira, P.S.; Franca, S.; Anderson de Oliveira, P.V.; Pereira, S. I. *Quim.Nova* **2008**, *31*, 20-24.

The ^{1}H-NMR spectrum showed 3 signals in the aromatic region due to the presence of a substituent on the indole portion. Mutiplicity of those signals (d, d, dd) with two different coupling constants (*J*= 8.9 and *J*= 3Hz) confirmed the presence of the substituent at position 10 or 11. Moreover, the proton of the OMe group showed a signal at δ 3.97 ppm as a singlet, while the signal of the protons of the COOMe group apperead at δ 3.67 ppm as a singlet. The signal of the proton at position 18 at δ 1.03 ppm as a doublet confirmed the presence of an OH group on H-19, whose signal appeared at δ 4.32-3.89 as a multiplet. These data were compared with those reported in literature and they were in agreement with each other.

Voacangine **45** showed the peak $[M+H]^+$ (ESI) at 369 accompanied by a peak at 391 $[M+Na]^+$. This value showed a decrease of 16 units if compared with the mass of voacristine, suggesting the absence of the OH group on C-19. The ^{1}H-NMR spectrum showed 3 signals in the aromatic region due to the presence of a substituent on the indole portion. Mutiplicity of those signals (d, d, dd) with two different coupling constants (*J*= 8.9 and *J*= 3Hz) confirmed the presence of the substituent at position 10 or 11. In addition the ^{13}C-NMR data revealed a highfield shift of the signal at C-19 (δ 26.7 ppm) if compared with the corresponding signal in voacristine (δ 71.2 ppm).

For compounds **31** and **32** see section **3.1.5** and **3.2.2** respectively, where there is a discussion of their structures.

Voacamine **46** presented (ESI) the peak $[M+H]^+$ at 705 accompanied by a peak at 727 (M+23) and a peak at 353. This data suggested a bis-indole structure with the peak at 353 corresponding to the monomeric moiety.

The junction of the two moieties by a bond between C-11 and C-16^{1} was suggested by the presence of two singlet signals of the protons at positions 9 (δ 6.92 ppm) and at position 12 (δ 6.74 ppm). A crosspeak is detectable between the signal at δ 5.15 ppm (H-16^{1}) and a singlet at δ 9.13 ppm (N-H) and between the signal at δ 3.78 ppm (H-14^{1}) and a singlet at δ 1.98 ppm (H-17^{1}).

The configuration of the double bond at C-19^{1} and C-20^{1} was deduced by a NOE observed between H-18^{1} (δ 1.65 ppm) and H-14^{1} (δ 3.78 ppm). These data were similar

to those reported in literature. Thus the structure of compound **46** was characterized as voacamine, and absolute configuration was postulated on the basis of the $[\alpha]_D^{20}$value -53.11 (*c* 1.1 $CHCl_3$) in accordance with the value reported in literature.[80]

The mass spectrum (ESI) of alkaloid **47** showed the peak $[M+H]^+$ at 385.

The ^{1}H-NMR spectrum showed 3 signals in the aromatic region due to the presence of a substituent on the indole portion. Mutiplicity of those signals (d, d, dd) with two different coupling constants (*J*= 8.2 and *J*= 2.5 Hz) confirmed the presence of the substituent at position 10 or 11. Moreover the spectrum showed the signal of the proton of the methoxy group at δ 3.81 ppm as a singlet and the signal of the protons of the carbomethoxy group at δ 3.60 ppm as a singlet. Other characteristic signals appeared at δ 1.41 and δ 0.86 ppm due to the presence of an ethyl side chain.

Even though the absolute configuration of iboga alkaloids is known,[81] the absolute stereochemistry at C-7 in the hydroxyindolenines derivatives is still unknown.

A long range coupling was observed between H-15 and H-17 toghether with a NOE between H-3 and H-15. The spetctroscopic data of compound **47** were compared with those reported in literature, and they were in good agreement with each other.

[80] Medeiros, W.L.; Vieira, I.J.C.; Mathias, L.; Braz- Filho, R.; Leal, K.Z.; Rodrigues-Filho, E.; Schripsema, J. *Magn. Reson. Chem.* **1999**, *37*, 676-681.

[81] Blahà,K.; Koblicovà, Z; Trojanek, *Tetrahedron Lett.***1972**, *27*, 2763-2766.

3.2. (-)-Cytisine: natural sources

3.2.1. Introduction

Cytisine (Figure 30) is a member of the lupine alkaloids family, first isolated in 1865 by Hussemann and Marmè[82] from different plants belonging to the *Leguminosae* (Fabaceae) family and principally from the seeds of the common deciduous tree *Laburnum anagyroides* (*Cytisus Laburnum*, Golden rain acacia) (Figure 31). From a chemical point of view, (-)-cytisine is a quinolizidine alkaloid with a tricyclic skeleton, containing thebispidine framework (B- and C-rings) fused to a 2-pyridonemoiety (A-ring). It bears two stereogenic centers, which were established to be 7*R*, 9*S*.

Figure 31: *Laburnum anagyroides*

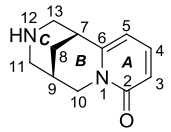

Figure 30: Structure of (-)-cytisine

Thousands of years ago, Indians in America started to consume *Laburnum* seeds for their purgative and emetic effects.[83] In Europe, (−)-cytisine was used as a diuretic, a respiratory analeptic or an insecticide. Furthermore, during the Second World War, the leaves of *Laburnum anagyroides* were used as tobacco substitute. In addition (-)-cytisine have shown analgesic, antioxidant, antispasmotic and insecticidal activities.

In 1890, the correct molecular formula of cytisine ($C_{11}H_{14}N_2O$) has been assigned.[84] Although it was first isolated in the mid-19th century, only in 1932 [85] the structure of

[82] Husemann, A.; Marmé ,W.Z. *Chem.***1865**, *1*, 161.

[83] (a) Tzankova, V.; Danchev, N.*Biotechnol. Equip.***2007**, *21*,151; (b) Tutka, P.; Zatoński, W. *Pharmacol. Rep.***2006**, *58*, 777.

[84] Partheil, A. Ber. *Dtsch. Chem. Ges.***1890**, *23*, 3201.

[85] H. R. Ing, *J. Chem. Soc.*, **1932**, 2778.

this alkaloid was clarified, after approximately 40 years of many efforts[86] focused largely on analysis of the products (isolated as salts) derived from electrophilic substitutions and degradations/reductions of both cytisine and its methyl or acetyl derivatives. Moreover, its absolute configuration was established almost thirty years later [87] by chemical transformations by Okuda *et al.*

Finally, in the mid-1980s it was totally characterized by spectroscopic analyses.

(−)-Cytisine has been marketed in Eastern and Central Europe in tablet form under the trade name Tabex and used for over 40 years to help people with smoking cessation. In fact, its molecular structure has some similarity to that of nicotine and it has also similar pharmacological effect: it was demonstrated that it has a high affinity at nicotinic acetylcholine receptors (nAChRs) (Figure 32) with high α4β2 subtype selectivity. [88]

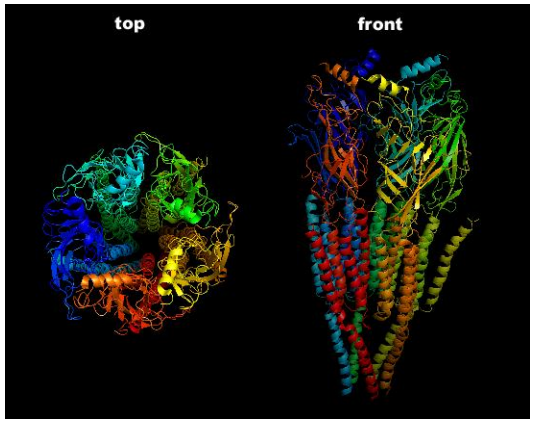

Figure 32: Top and front view to the 3D structure of the pentameric nicotinic acetylcholine receptor

[86] Leonard, N. J. Lupin *Alkaloids. In The Alkaloids*; Manske, R. H. F., Holmes, H. L., Eds.; Academic Press: New York, **1953**; *Vol. 3*, pp 119−199.

[87] S. Okuda, K. Tsuda and H. Kataoka, *Chem. Ind.* (London), **1961**, 1751.

[88] (a) Hall, M.; Zerbe, L.; Leonard, S.; Freedman, R.*Brain Res*. **1993**, *600*, 127;(b) Papke, R. L.; Heinemann, S. F.*Mol. Pharmacol*. **1994**, *45*, 142; (c) Anderson, D. J.; Arneric, S. P.*Eur. J. Pharmacol.* **1994**, *253*, 261.

nAChRs are widely expressed in the vertebrate nervous system, where they act as postsynaptic receptors exciting neurons or as presynaptic receptors modulating the release of many neurotransmitters. [89]

nAChRs are known to be involved in various central nervous system (CNS) disorders including degenerative ones such as Tourette's syndrome, Parkinson and Alzheimer diseases, schizophrenia and some forms of epilepsy[90]. Moreover, they have also been associated with some lung tumors and autoimmune diseases.[91] The possibility to use nicotinic ligands in the treatment of neurodegenerative disorders has been recognized[92] and encouraged the synthesis of a large number of structural analogues of nicotine, a very potent natural nAChRs agonist that is unfortunately characterized by many undesirable side effects not easily removed.

Cytisine possesses high affinity for numerous nAChR subtypes and has also the capability to discriminate among some of them. Moreover, it has not received much attention as a lead compound for the design of structural analogues able to interact, allosterically or directly, with one or more receptor subtypes. In fact, one of its disadvantages is its low lipophilicity, which could complicate the crossing of the blood brain barrier.[93]

The previous considerations stimulated many research groups to carry out a systematic structural modification of cytisine, in order to synthesize compounds of potential therapeutic interest either at central or peripheral level, with a particular attention for new nAChR subtype selective ligands.

Furthermore, the structural modifications of cytisine should favour the passage through the blood brain barrier and decrease the affinity for ganglionic receptors.

---

[89] Jones, S.; Sudweeks, S.; Yakel, J.L. *Trends Neurosci*. **1999**, *22*, 555-561.

[90] F. Clementi, D. Fornasari, C. Gotti (Eds.), Neuronal Nicotinic Receptors, Handbook of experimental pharmacology, vol. 144, Springer Verlag, Berlin **2000**, pp. 751-778.

[91] Vernino, S.; Adamaski, J.; Kryzer, T.; Fealey, R. V. *Neurology* **1998**, *50*, 1806- 1813.

[92] (a)Williams, M.; Sullivan, J. P.; Arneric, S. P.*Drug News Perspect.* **1994**, *7*, 205; (b) Gualtieri, F. *Chem.Med.Chem.* **2007**, *2*, 746; (c) Jensen, A. A.; Frølund, B.; Liljefors, T.; Krogsgaard-Larsen, P.*J. Med. Chem.***2 005**, *48*, 4705; (d) Gualtieri, F.*Chem.Med.Chem.* **2007**, *2*, 746. (e) Jensen, A. A.; Frølund, B.; Liljefors, T.; Krogsgaard-Larsen, P.*J. Med. Chem*. **2005**, *48*, 4705.

[93] Reavill, C.; Walther, B.; Stolerman, J.P.; Testa, B. *Neuropharmacology* **1990**, *29*, 619- 624.

The chemical modifications usually made on cytisine involved the secondary amino group and the pyridone ring (for example additions to the conjugated double bonds or electrophilic substitutions). In addition, in order to preserve the central nicotinic activity, it is generally claimed[94] that the cationic character of the molecule should be ensured, leaving unchanged the typical distance between the carbonyl dipole and the basic nitrogen, which should be involved in a hydrogen bond with a donating group of the receptor.

(−)-Cytisine looked as a lead candidate to develop novel molecules able to interact more selectively with the nAChRs of the central nervous system showing insignificant side effects.

[94] Barlow, R.B.; Mc Leod,L.J. *J. Pharmacol.* **1969**, *35,* 161-174.

3.2.2. Biosynthesis

In the 1960s the first studies on the biosynthesis of (−)-cytisine were described.[95] They were later proved by extensive research on the biosynthesis of different quinolizidine alkaloids of the lupines family, in particular of that of sparteine. [96]

The lupine alkaloids are synthesized in the green parts of the plants and then they are translocated to other organs. In the intact plants, they are accumulated as salts such as malates in the epidermal tissues, petioles, leaves, and stems.

Lupine alkaloids biosynthesis (Scheme 31) starts with the production of cadaverine by decarboxylation of lysine[97], catalyzed by lysine decarboxylase, an enzyme located in chloroplast stroma.

Subsequently a diamine oxidase catalyzes the oxidative deamination of cadaverine in favor of the synthesis of δ-amino pentanal. An intramolecular imine cyclization of δ-amino pentanal leads to the formation of Δ^1-Piperideine, a key intermediate for the formation of the quinolizidine ring system.

After four minor reactions (Aldol-type reaction, hydrolysis of imine to aldehyde/amine, oxidative reaction and again Schiff base formation), the pathway is divided into two directions.

The subway leads to the synthesis of (-)-lupinine by two reductive steps, while the main synthesis stream goes through the Schiff base formation and coupling to the compound substrate, from which again the synthetic pathway splits to form (+) lupanine synthesis and (-)-sparteine synthesis. From (-)-sparteine, the route by conversion to (+)-cytisine synthesis is open.

[95] (a) Schütte, Von H. R.; Lehfeldt, J. *J. Prakt. Chem.* **1964**, *24*, 143; (b) Schütte, H. R.; Lehfeldt, J. Z. *Naturforsch.***1964**, *19b*, 1085.

[96] Ohmiya, S.; Saito, K.; Murakoshi, I. *Lupine Alkaloids. In The Alkaloids*; Cordell, G. A., Ed.; Academic Press: New York, **1995**; *47*, 2−114; (b) Saito, K.; Murakoshi, I. *In Studies in Natural ProductsChemistry. Structure and Chemistry (Part C)*; Atta-ur-Rahman, Ed.; Elsevier: Oxford, **1995**, *15*, 519−549.

[97] Nowacki, E. K.; Walter, G. R. *Phytochemistry* **1975**, *14*, 165.

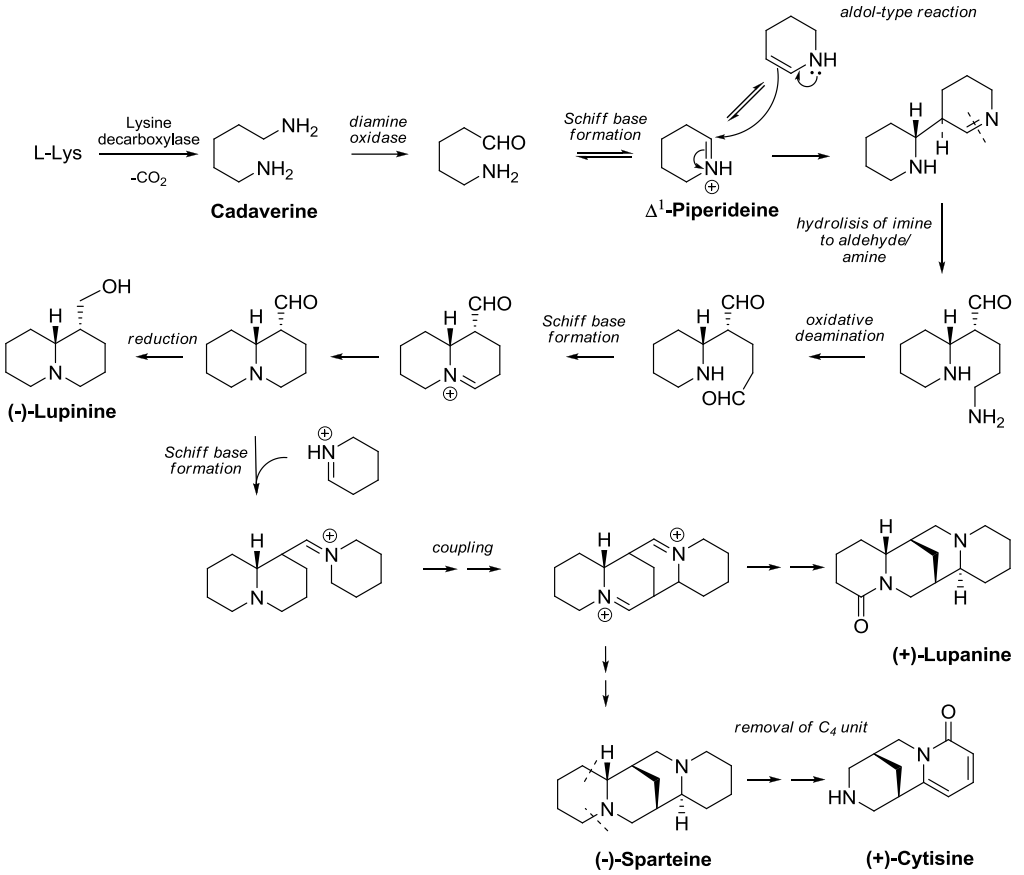

Scheme 31: Biosynthesis ofcytisine starting from L-lysine

3.2.3. Total synthesis of the lupin alkaloid cytisine

The first total synthesis of (±)-cytisine was reported by van Tamelen in 1955[98] and this was closely followed by Bohlmann's[99] and Govindachari's[100] syntheses in the late 1950s. In 2000 two new routes to (-)-cytisine were described by O'Neill[101] and Coe[102] at Pfizer. Then, Gallagher[103] and O'Brien[104] also completed the syntheses of (-)-cytisine. Whereas the first asymmetric synthesis of (-)-cytisine was reported by Danieli[105] in 2004 and was closely followed by the syntheses of (+)-cytisine proposed by Honda[106] and Gallagher[107]. All of these different routes are summarized in Figure 33.

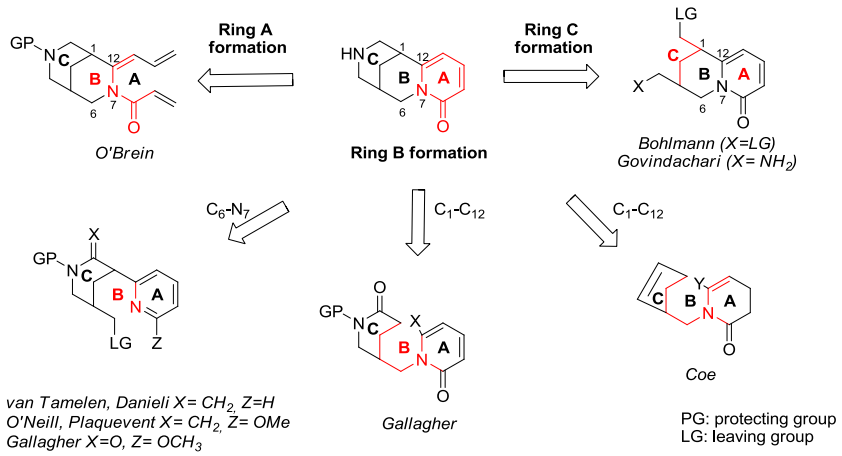

Figure 33: Different routes to the tricyclic core of cytisine

[98] (a) Van Tamelen, E. E.; Baren, J. S. *J. Am. Chem. Soc.***1955**, *77*,4944; (b) van Tamelen, E. E.; Baran, J. S. *J. Am. Chem. Soc.* **1958**, *80*,4659.

[99] Bohlmann, F.; Englisch, A.; Ottawa, N.; Sander, H.; Weise, W. *Chem. Ber.* **1956**, *89*, 792.

[100] Govindachari, T. R.; Rajadurai, S.; Subramanian, M.; Thyagarajan, B. S. *J. Chem. Soc.***1957**, 3839.

[101] O'Neill, B. T.; Yohannes, D.; Bundesmann, M. W.; Arnold, E. P. *Org. Lett.***2000**, *2*, 4201.

[102] Coe, J. W. *Org. Lett.***2000**, *2*, 4205.

[103] Botuha, C.; Galley, C. M. S.; Gallagher, T. *Org. Biomol. Chem.***2004**, *2*, 1825.

[104] Stead, D.; O'Brien, P.; Sanderson, A. *J. Org. Lett.***2005**, *7*, 4459.

[105] Danieli, B.; Lesma, G.; Passarella, D.; Sacchetti, A.; Silvani, A.; Virdis, A. *Org. Lett.***2004**, *6*, 493.

[106] Honda, T.; Takahashi, R.; Namiki, H. *J. Org. Chem.***2005**, *70*, 499.

[107] Gray, D.; Gallagher, T. *Angew. Chem., Int. Ed.***2006**, *45*, 2419.

In four of the synthetic pathways to cytisine, a pyridine derivative was involved as a precursor of the pyridone A-ring of cytisine (Scheme 32).

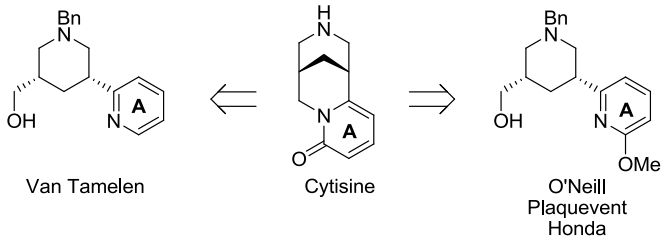

Scheme 32: Synthesis using a pyridine-derived A-ring

A key difference between van Tamelen and O'Neill's route is that the first one used a monosubstituted pyridine, whilst the second approach employed a methoxy-substituted pyridine, thus avoiding the require for an oxidation step to create the pyridone ring. In each of these synthetic stratgies, a *cis*-3,5-disubstituted piperidine needs to be assembled. In the synthetic pathways of cytisine reported by Coe and Gallagher (Scheme 33), a different pyridone disconnection was planned in which the B-ring of cytisine would be produced by a palladium(0)-mediated intramolecular process. In fact, in Gallagher's second-generation approach (X=H), addition of the enolate directly to the pyridone was applied to close the ring. Gallagher's approach also facilitated the pyridone A-ring of cytisine to be intact during the synthesis. Another advantage in the use of these strategies for the synthesis of cytisine is that they remove the need for a *cis*-3,5- disubstituted piperidine.

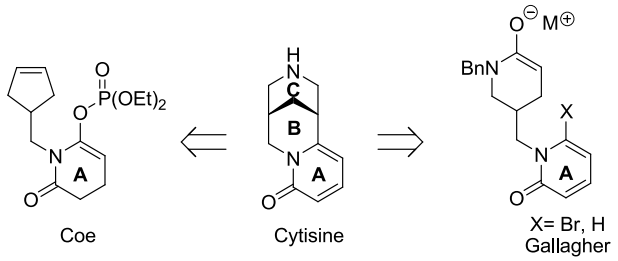

Scheme 33: Synthesis using a glutarimide- or pyridone-derived A-ring

Bohlmann and Govindachari explored the use of a substituted pyridine as a precursor to the B-ring of cytisine (Scheme 34). In each synthetic route, hydrogenation of a 3,5-

disubstituted pyridine (after production of the pyridone A-ring) was performed in order to establish the *cis* stereochemistry essential for the preparation of the bispidine.

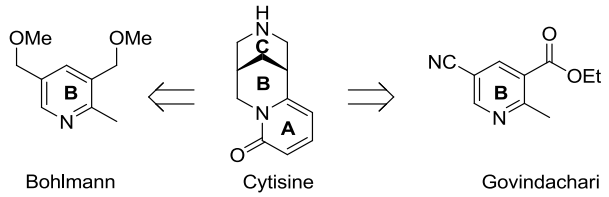

Scheme 34: Synthesis using a pyridine-derived B-ring

In 2004, Danieli reported the first synthetic approach to cytisine that has involved the construction of the C-ring from a piperidine. This route, besides being enantioselective, is the only one route that started with the C-ring, using a piperidine derivative as a starting material to complete the entire synthesis (Scheme 35).

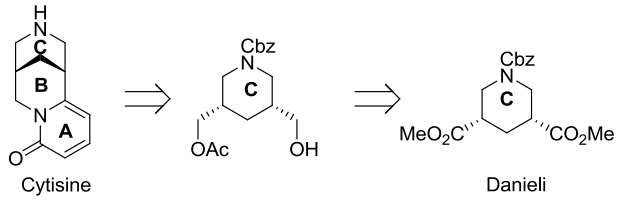

Scheme 35: Synthesis using a piperidine-derived C-ring

These routes are the best way of preparing (-)-cytisine and its analogues for biological evaluation. Actually, the O'Neill approach has been used specifically for that purpose, even though the synthesis of each analogue of cytisine required a separate total synthesis. As a result, there is still a need to elaborate an approach to cytisine that produces a late-stage intermediate that is characterized by an appropriate functionality for analogue preparation. Moreover, an efficient asymmetric synthesis of cytisine is still necessary, since each of the three asymmetric routes to (-)- or (+)-cytisine has limits.

3.2.4. (-)-Cytisine derivatives: synthesis of *N*-formyl and *N*-methyl derivatives

(-)-Cytisine and its analogues are of interest as pharmacological tools and as potential drugs for the treatment of a wide range of conditions, from alcohol and nicotine dependence, eating disorders, to schizophrenia, depression and neurodegenerative diseases.

(-)-Cytisine is now an expensive chemical even if it is commercially available from general suppliers. Nevertheless, recently, a variation of known described methods permitted its efficient extraction from the seeds of *Laburnum anagyroides* easily available at low cost from seed producers.[108] The availability of (−)-cytisine permitted its used for the synthesis of a large number of substituted derivatives[109] and of more complex structures including natural products, such as *N*-methyl cytisine and *N*-formyl cytisine.

Up to now many *N*-substituted (-)-cytisine derivatives synthesized so far were prepared by Sparatore's group since 1999[110] and also few analogues were synthesized by modifying the pyridone ring.

We taken into account the possibility to synthesize *N*-methyl (caulophylline) and *N*-formyl cytisine because they are less toxic than cytisine.

Like cytisine, *N*-methylcytisine is selective for $\alpha4\beta2^*$ nAChR over the other major CNS subtype ($\alpha7$), but its functional potency and affinity are lower.

In literature two different procedures have been reported for the synthesis of *N*-methylcytisine starting from cytisine.[111,112] In our case the desired *N*-methyl derivative has been prepared as described in Scheme 36:

[108] (a) Marrière, E.; Rouden, J.; Tadino, V.; Lasne, M.-C. *Org. Lett.***2000**, *2*, 1121; (b) Dixon, A. J.; McGrath, M. J.; O'Brien, P.*Org. Synth.***2006**, *83*, 141.

[109] Rouden,J.; Lasne,M.C.; Blanchet,J.; Baudoux, J. *Chem. Rev.* **2014**, *114*, 712−778.

[110] Canu Boido, C.; Tasso, B.; Boido,V.; Sparatore, F. *Il Farmaco***2003,** *58*, 265-277.

[111] Przybył, A.K.; Kubicki, M. *J.Mol. Struct.***2011**, *985*, 157–166.

[112] Frigerio, F.; Haseler, A.C.; Gallagher, T.*Synlett.* **2010**, 729-730.

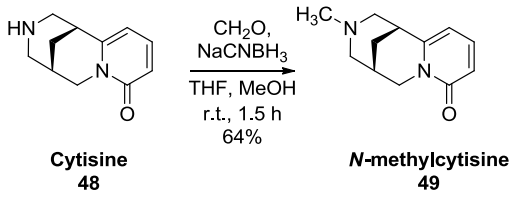

Scheme 36: Synthesis of *N*-methylcytisine

In NMR analysis of *N*-methylcytisine it was observed the absence of N*H* signal at δ 2.31 ppm as a broad signal and the presence of a signal at δ 2.20 as a singlet, corresponding to the methyl group. Moreover, spectroscopic data for synthetic *N*-methyl cytisine were compared with those reported in literature for this compound, and it was observed that they were in good agreement with each other.

In addition crystallization of the crude material from hexane/CH_2Cl_2 mixture, leads to some colourless prisms that were analyzed by single-crystal X-ray diffraction (Figure 34).

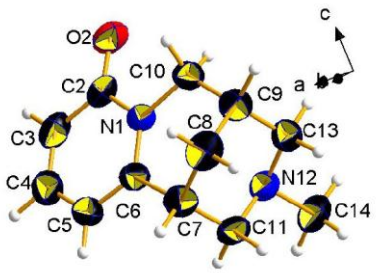

Figure 34: Asymmetric unit of *N*-methylcytisine, with the atom-numbering Scheme. Thermal ellipsoids of non-H atoms at RT were drawn at the 50 % probability level. The usual colour code was employed for atoms (black: C; white: H; blue: N; red: O).

The absolute configuration cannot be reliably assessed with the employed X-ray wavelength in the absence of anomalous scatterers. However, the configurational descriptors of the stereogenic centres are either C7 (*R*) and C9 (*S*) or C7 (*S*) and C9 (*R*). This analysis demonstrated that the compound crystallizes in an acentric space group with one molecule per asymmetric unit. Figures 35 shows the relative configuration of the chiral centres.

According to literature data[113] and on the base of the $[\alpha]_D^{20}$ value (-129.4 in $CHCl_3$), we were able to confirm the *N*-methylcytisine absolute configurationas depicted in Figure 35.

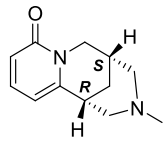

Figure 35: Molecular structure of *N*-Methylcytisine, with the CIP descriptors highlighted according to the asymmetric unit in Figure 8.

Nguyen and co-workerks[114] reported a novel general method of transamidation of carboxamides with amines using catalytic amounts of readily available, environmentally friendly and nontoxic boric acid under solvent-free conditions.

Transamidation is an attractive tool in synthetic organic chemistry. Numerous efforts were made in order to develop more convenient protocols that allow the reactions to take place at relatively lower temperatures by utilizing catalysts or activating reagents.[115]

These procedures posses some disadvantages, because of they involved either energetically favorable systems or the use of expensive activation reagents and/or moisture-sensitive. In addition, the scope of these methods is limited to primary amines and amides. Nguyen and co-workerks were able to develop a methodology whose scope was demonstrated with (i) aliphatic, aromatic, cyclic, acyclic, primary, and secondary amines and (ii) primary, secondary, tertiary amides and phthalimide.

Moreover they proposed a mechanism for the transamidation reaction using $B(OH)_3$ as catalyst. (Scheme 37)

[113] Freer, A. F.; Robins, D. J.; Sheldrake, G. N. *Acta Crystallogr*. **1987**, *C43*, 1119-1122.

[114] Nguyen, T.B.; Sorres,J.; Quan Tran, M.; Ermolenko, L.; Al-Mourabit A. *Org.Lett.***2012**, *14*, 3202-3205.

[115] (a) Starkov, P.; Sheppard, T.D. *Org. Biomol. Chem.***2011**, *9*, 1320; (b) Dineen, T. A.; Zajac, M. A.; Myers, A. G. *J. Am. Chem. Soc.***2006**, *128*, 16406; (c) C-alimsiz, S.; Lipton, M.A. *J. Org. Chem.* **2005**, *70*, 6218.

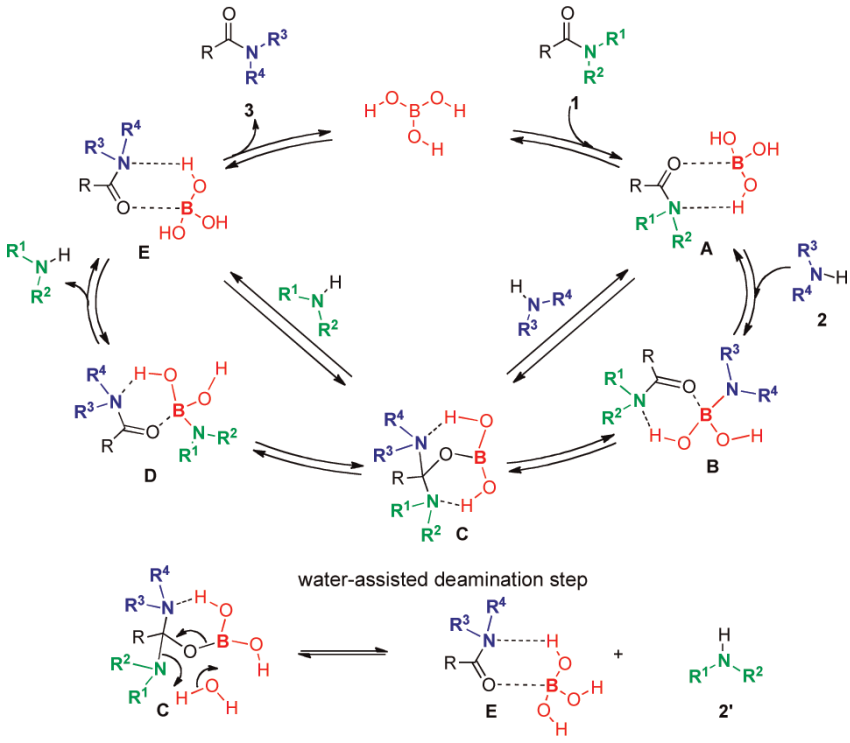

Scheme 37: Proposed activation mode of boric acid

The catalytic cycle could starts with the reaction of amide with boric acid catalyst forming adduct **A**, which could take place via concerted proton transfer and B-O bond formation. Subsequently an addition of amine **2** to the adduct **A** could occur directly at the carbonyl (CO) bond leading to the intermediate **C**. Another option leading to **C** which could be predicted is the attack of amine **2** on the boron atom followed by intramolecular rearrangement of the amino group from **B** to **C**. Elimination of amine **2'** from tetrahedral intermediate **C** can occur in the same manner. The deamination step from **C** to **E** could be supported by water as described in the Scheme 37. The catalytic cycle finishes with the dissociation of amide **3** from boric acid.

The function of water in improving the rate of transamidation can also be explained by its capacity to enhance the solubility of boric acid and avoid the formation of boric acid aggregates, which are less catalytically active than the boric acid.

We applied the same reaction condition reported by Nguyen for the synthesis of *N*-formylcytisine, as depicted in Scheme 38.

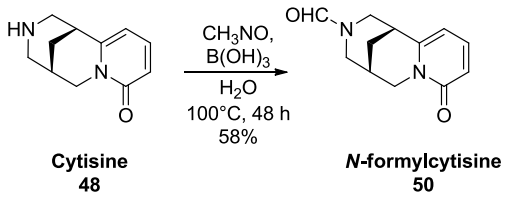

Cytisine
48

***N*-formylcytisine**
50

Scheme 38: Synthesis of *N*-formylcytisine

It is important to note that ring **A** in cytisine has a planar conformation, while ring **B** is in a sofa conformation with the bridging C-8 atom pointed out of plane. Moreover ring **C** adopts a chair conformation and the nitrogen atom has a free electron pair in the axial position.

N-Formylcytisine may occur in solution as a mixture of two conformers, in a ca. 1:1 ratio, which differ for ring **C** conformation (Figure 36).

The presence of these conformers in solution was revealed by NMR analysis because of the presence of a double set of signals in both ^{1}H and ^{13}C NMR. The spectrum was recorded heating from 50°C up to 100 °C, but it was impossible to observe coalescence of the signals. This is due to the fact that the energy barrier is too high.

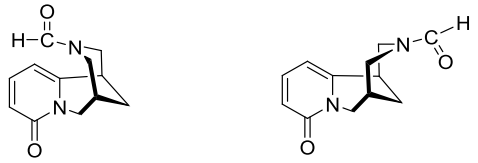

chair (trans) boat (cis)

Figure 36: The two possible isomers of *N*-formylcytisine

3.3. Experimental part

3.3.1. General information

Thin-layer chromatography (TLC) was performed on Merck precoated 60F254 plates. Reactions were monitored by TLC on silica gel, with detection by Uv light (λ = 254 nm) or by charring with 1% permanganate solution. Flash chromatography was performed using Silica gel (240-400 Mesh, Merck). NMR spectra were recordered with Brucker 300 and 400 MHz spectrometers. Chemical shifts are reported in parts per million (δ) downfield from tetramethylsilane (TMS). EI mass spectra were recorded at an ionizing voltage of 6 kEv on a VG 70-70 EQ. ESI mass spectra were recorded on FT-ICR APEXII. Specific rotations were measured with a P-1030-Jasco polarimeter with 10 cm optical path cells and 1 ml capacity (Na lamp, λ = 589 nm).

Lochnericine

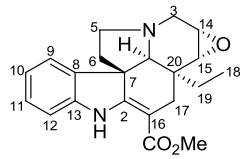

40

[1]H-NMR (400 MHz, $CDCl_3$): δ 8.96 (bs, 1H), 7.29-7.14 (m, 2H), 6.90 (d, *J*= 7.5 Hz,1H), 6.82 (t, *J*= 7.8 Hz,1H), 3.81(s, 3H), 3.51-3.45 (m, 2H), 3.14 (d, *J*= 4 Hz,1H), 3.01-2.89 (m, 2H), 2.71-2.42 (m, 4H), 2.12-1.89 (m, 1H), 1.82-1.71 (m, 1H), 1.21-1.11 (m, 1H), 1.04-0.91 (m, 1H), 0.77 (t, *J* =7.5 Hz, 3H) ppm.

[13]C-NMR (100 MHz, $CDCl_3$): 168.7, 167.8, 142.9, 137.6, 127.8, 121.4, 120.7, 109.5, 90.7, 67.6, 57.1, 54.9, 53.8, 51.08, 50.7, 50.1, 44.6, 41.0, 24.4, 23.3, 7.2 ppm.

ESIMS: *m/z*= 353 $[M+H]^+$

$[\alpha]_D^{20}$= -348 (*c* 0.7 $CHCl_3$).

Pachysiphine

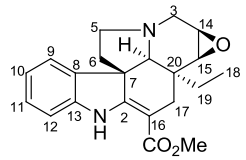

41

^{1}H-NMR (400 MHz, $CDCl_3$): δ 8.97 (bs, 1H), 7.15 (d, *J*= 6.6 Hz, 1H), 7.12 (t, *J*= 7.5 Hz, 1H), 6.87 (d, *J*= 7.3 Hz,1H), 6.80 (t, *J*= 7.7 Hz,1H), 3.76 (s, 3H), 3.59-3.51 (m, 1H), 3.25 (dd, *J*= 5.3 and 3.9 Hz,1H), 3.05 (d, *J* =3 .8 Hz,1H), 2.96 (bs,1H), 2.90-2.86 (m, 1H), 2.74-2.61 (m, 2H), 2.70-2.45 (m, 2H), 2.12-2.05 (m, 1H), 1.71 (dd, *J*= 11.2 and 5 Hz, 1H), 1.14-0.91 (m, 2H), 0.74 (t, *J* =8 Hz, 3H) ppm.

^{13}C-NMR (100 MHz, $CDCl_3$): 168.9, 159.8, 143.1, 137.7, 127.9, 122.4, 121.5, 108.9, 91.2, 71.1, 56.3, 54.7, 52.1, 51.2, 51.0, 49.6, 44.0, 37.1, 26.6, 23.6, 7.2 ppm.

ESIMS: *m/z*= 353 $[M+H]^+$

$[\alpha]_D^{20}$= -247 (*c* 1.1 EtOH).

Vobtusine

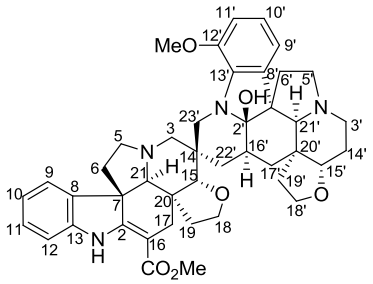

42

^{1}H-NMR (400 MHz, $CDCl_3$): δ 8.92 (bs, 1H), 7.20-7.10 (m, 2H), 6.92-6.75 (m, 2H), 6.72-6.68 (m,1H), 6.62-6.60 (m, 2H), 3.77 (s, 3H), 3.67 (s, 3H) ppm.

^{13}C-NMR (100 MHz, $CDCl_3$): 168.5, 167.1, 144.3, 142.8, 137.5,137.0, 134.1,127.2, 121.1, 120.5, 118.5, 114.9, 110.9, 109.0, 94.5, 93.7, 87.5, 80.5, 69.0, 65.3, 64.2, 63.6, 55.7, 55.0, 54.8, 53.8, 52.0, 51.0, 50.9, 48.5, 47.6, 46.2, 45.0, 44.5, 39.6, 37.0, 34.1, 34.5, 32.4, 31.5, 31.0, 25.4, 27.2 ppm.

ESIMS: *m/z*= 719 $[M+H]^+$, 701 $[M-H_2O]$, 691 [M-28], 365, 304

Vobasine

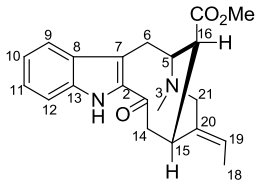

43

[1]H-NMR (400 MHz, $CDCl_3$): δ 10.4 (bs, 1H), 7.81 (d, *J*= 9.0 Hz, 1H), 7.50 (d, *J*= 3.5 Hz, 1H), 7.29 (t, *J*= 9.0 Hz,1H), 7.13 (t, *J*= 3.5 Hz,1H), 5.42 (q, *J*= 6.0 Hz, 1H), 4.01-3.82 (m, 2H), 3.72-3.53 (m, 2H), 3.51-3.43 (m, 2H), 3.01-2.98 (m, 1H), 2.88-2.73 (m, 1H), 2.63 (s,3H), 2.61 (s,3H), 2.51-2.48 (m, 1H), 1.72 (dd, *J*= 7 and 1.8 Hz, 3H) ppm.

[13]C-NMR (100 MHz, $CDCl_3$): 189.6, 171.3, 138.2, 137.7, 134.1, 129.3, 126.4, 121.5, 120.3, 120.0, 119.4, 11.3, 58.0, 54.9, 50.1, 47.5, 43.8, 42.3, 31.2, 20.3, 12.0 ppm.

ESIMS: *m/z*= 353 $[M+H]^+$

$[\alpha]_D^{20}$= -100.1 (*c* 0.3 $CHCl_3$).

Voacristine

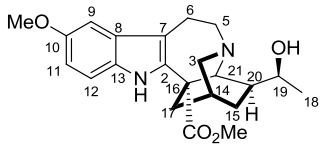

44

^{1}H-NMR (400 MHz, $CDCl_3$): δ 9.34 (bs, 1H), 7.19 (d, *J*= 8.9 Hz, 1H), 6.96 (d, *J*= 3.0 Hz, 1H), 6.70 (dd, *J*= 8.9 and 3.0 Hz,1H), 4.32-3.89 (m,1H), 3.97 (s,3H), 3.67 (s,3H), 3.51-3.36 (m, 2H), 3.21-2.66 (m, 7H), 2.20-1.67 (m, 2H), 1.62-1.48 (m, 2H), 1.03 (d,*J*= 6.5 Hz, 3H) ppm.

^{13}C-NMR (100 MHz, $CDCl_3$): 175.6, 155.0, 137.5, 131.0, 128.7, 112.1, 111.5, 108.9, 100.6, 72.3, 59.6, 55.9, 54.0, 52.7, 52.3, 51.4, 39.1, 36.5, 26.1, 23.0, 21.4, 20.3 ppm.

ESIMS: *m/z*= 385 $[M+H]^+$

$[\alpha]_D^{20}$= -22.7 (*c* 0.2 $CHCl_3$).

Voacangine

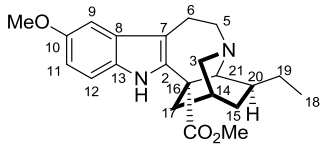

45

^{1}H-NMR (400 MHz, CD_3COCD_3): δ 8.12 (bs, 1H), 7.13 (d, *J*= 8.5 Hz, 1H), 6.93 (d, *J*= 2.8 Hz, 1H), 6.80 (dd, *J*= 8.9 and 3.0 Hz,1H), 3.83 (s, 3H), 3.72 (s, 3H), 3.45-3.35 (m, 2H), 3.23-2.63 (m, 7H), 2.20-1.28 (m, 6H), 0.98 (t, *J*= 7 Hz, 3H) ppm.

^{13}C-NMR (100 MHz, CD_3COCD_3): 175.8, 153.9,137.2, 130.5, 128.7, 111.8, 111.0, 110.1, 100.8, 57.2, 56.2, 55.2, 52.8, 52.1, 51.8, 38.9, 36.5, 31.5, 26.7, 26.1, 22.8, 11.2 ppm.

ESIMS: *m/z*= 369 $[M+H]^+$, 391 $[M+Na]^+$

$[\alpha]_D^{20}$= -32.9 (*c* 0.3 $CHCl_3$).

Voacamine

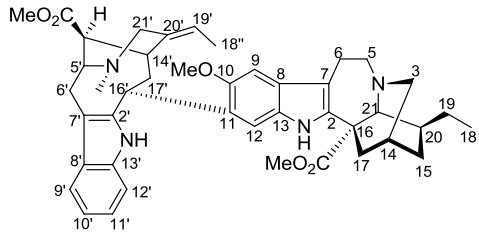

46

^{1}H-NMR (400 MHz, CD_3COCD_3): δ 9.31 (s, 1H), 9.13 (s, 1H), 7. 76-7.49 (m, 1H), 7.15-7.08 (m, 1H), 7.02-6.92 (m, 3H), 6.73-6.42 (m, 1H), 5.27 (q, *J*= 7 Hz, 1H), 5.20 (brd, 1H), 4.07-3.98 (m, 4H), 3.78-3.48 (m, 8H), 3.23-2.97 (m, 7H), 2.72-2.48 (m, 6H), 2.44 (s, 3H), 1.98-1.70 (m, 6H), 1.64 (d, *J*= 7.3 Hz, 3H), 1.27-1.07 (m, 2H), 0.84 (t, *J*= 6.8 Hz, 3H) ppm.

^{13}C-NMR (100 MHz, CD_3COCD_3): 174.8, 171.1, 151.6, 138.7, 138.5, 137.1, 136.0, 130.6, 129.9, 129.6, 127.8, 121.4, 118.7, 118.3, 117.5, 111.2, 109.9, 109.8 (d), 99.5, 60.3, 57.6, 56.1, 54.2, 53.7, 52.8, 52.5, 50.4, 49.9, 43.8, 40.8, 38.6, 37.5, 36.8, 36.4, 34.0, 32.0, 27.6, 26.5, 22.7, 19.5, 12.5, 10.1 ppm.

ESIMS: *m/z*= 705 $[M+H]^+$, 727 [M+23]

$[\alpha]_D^{20}$= -53.11 (*c* 1.1 $CHCl_3$).

Voacangine hydroxyindolenine

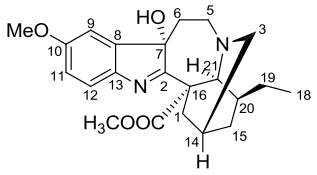

47

^{1}H-NMR (400 MHz, $CDCl_3$): δ 7.24 (d, *J*= 8.2 Hz, 1H), 6.88 (d, *J*= 2.5 Hz, 1H), 6.81 (dd, *J*= 8.4 and 2.5 Hz,1H), 3.81 (s, 3H), 3.60 (s, 3H), 3.48 (ddd,*J*= 12.5, 12 and 4.5 Hz,1H), 2.95 (dd, *J*= 14.5 Hz,1H), 2.73 (s, 2H), 2.72-2.68 (m, 1H), 2.12-2.02 (m, 1H), 1.94-1.71 (m, 5H), 1.61-1.20 (m, 3H), 0.86 (t, *J*= 7 Hz, 3H) ppm.

^{13}C-NMR (100 MHz, $CDCl_3$): 185.2, 172.8, 159.2, 144.7, 144.0, 121.3, 113.2, 108.2, 88.2, 58.5, 58.2, 55.1, 53.5, 49.0, 48.4, 37.2, 34.5, 34.1, 32.2, 27.0, 26.8, 11.2 ppm.

ESIMS: *m/z*= 385 $[M+H]^+$

Synthesis of *N*-methylcytisine

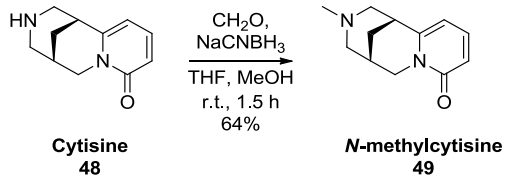

Cytisine
48

***N*-methylcytisine**
49

To a solution of (-)-cytisine (0.500 g, 2.60 mmol) in MeOH (15 mL) and THF (15 mL) wasadded formaldehyde (37% aq solution, 1.1 mL, 15.6 mmol) followed by $NaCNBH_3$ (0.571 g, 9.10 mmol). The reaction mixture was stirred at r.t. for 1.5 h. The solvent was removedin vacuo and the reaction mixture was eluited with CH_2Cl_2 and washed with saturated aqueous NH_4Cl solution. The organic extracts were combined and the solvent was removed in vacuo giving *N*-methylcytisine as a colourless oil (0.342 g, 64%).

^{1}H-NMR ($CDCl_3$, 300 MHz): δ 7.25 (m, 1H), 6.41 (d, *J*= 8,8 Hz, 1H), 5.96 (d, *J*= 6,5 Hz, 1H), 4.02 (d, *J*= 15,3 Hz, 1H), 3.87 (dd, *J*= 15,3 Hz; 6,5 Hz, 1H), 2.91-2.80 (m, 4H), 2.49-2.41 (m, 1H), 2.32-2.20 (m, 1H), 2.29 (s, 3H), 1.88 (d, *J*=11 Hz; 1H), 1.77 (d, *J*=12 Hz; 1H) ppm.

^{13}C-NMR (100 MHz, $CDCl_3$): 163.7, 151.3, 138.7, 116.7, 104.8, 62.4, 62.0, 46.1, 35.4, 29.7, 27.9, 25.3 ppm.

Synthesis of *N*-formyl cytisine

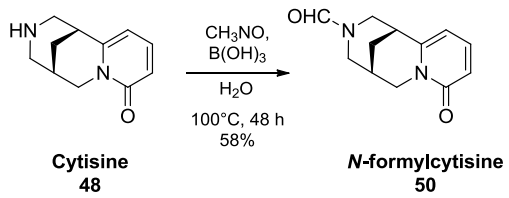

Cytisine
48

***N*-formylcytisine**
50

A mixture of cytisine (0.500g, 2.6 mmol), formammide (0.117g, 2.6 mmol), water (0.93 g, 5.2 mmol) and boric acid (0.016 g, 0.26 mmol) was stirred at 100°C.
After 48 hours the mixture was diluted with H_2O and the aqueous phase was extracted with diethyl ether. Then the mixture was washed with saturated aqueous NH_4Cl and the organic extracts were dried over anhydrous sodium sulfate. The solvent was removed in vacuo giving the *N*-formylcytsineas a colourless oil (0.330 g, 58% overall yield).

Major rotamer:

^{1}H-NMR ($CDCl_3$, 500MHz):δ 7.88 (s, 1H), 7.22 (dd, *J* = 1.0, 6.9 Hz, 1H),6.52 (d, *J* = 6.6 Hz, 1H), 6.02 (dd, *J* = 6.9, 1.0 Hz, 1H), 4.52-4.43 (m, 1H), 4.12 (d, *J* = 6.0 Hz, 1H), 3.90-3.95 (m, 1H), 3.64-3.69 (m,1H), 3.46-3.40 (m, 1H), 3.16 (br. s, 1H), 2.95-2.90 (m, 1H), 2.55 (br. s, 1H), 2.07-2.11 (m, 2H) ppm.

^{13}C-NMR ($CDCl_3$, 125 MHz): 163.0, 159.9, 147.1, 139.0, 117.5, 106.1, 52.2, 48.4, 46.9, 34.2, 27.4, 26.9 ppm.

Minor rotamer:

^{1}H-NMR ($CDCl_3$, 500MHz): δ 7.65 (s, 1H), 7.25 (dd, *J* = 6.9, 1.0 Hz, 1H,),6.44 (d, *J* = 6.9 Hz,1H), 6.02 (dd,*J* = 6.9, 1.0 Hz, 1H,), 4.52-4.43 (m, 1H),4.12 (d, *J* = 6.0 Hz, 1H), 3.90-3.95 (m, 1H), 3.53-3.57 (m,1H), 3.46-3.40 (m, 1H), 3.11 (br. s, 1H), 2.93-2.89 (m, 1H), 2.55 (br. s, 1H), 2.15-2.19 (m,2H) ppm.

^{13}C-NMR ($CDCl_3$, 120MHz): 163.1, 161.0, 148.0, 138.6, 118.1, 105.5, 53.0, 48.8, 46.1, 34.2, 26.7, 26.0 ppm.

4. Natural products as lead compounds

4.1. Synthesis of an analogue of the natural product doliculide

4.1.1. Introduction

This project was performed under the umbrella of COST Action CM1407 (Challenging Organic Synthesis Inspired By Nature: From Natural Product Chemistry To Drug Discovery). It was developed in the laboratory of Prof. Karl-Heinz Altmann (Zurich, Switzerland) in order to continue the collaboration between Prof. Karl-Heinz Altmann and Prof. Daniele Passarella and to combine our experience in the synthesis of natural products.

Doliculide (Figure 37), a 16-membered depsipeptide, has been isolated in 1994 from the Japanese sea hare *Dolabella auricularia*.[116] The great deal of attention in the synthesis of this natural product is due to its cytotoxic properties[1]: it exhibited extraordinarily potent cytotoxic activity against $HeLaS_3$ cells with an IC value of 0.001 μg/mL.[117]

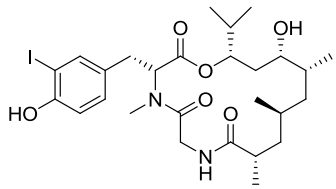

Figure 37: Doliculide structure

Furthermore, doliculide is a very potent actin binder. Actin, a globular multi-functional protein,[118] is one of the targets in cancer research. It can be present as either a free monomer called G-actin (globular) or as part of a linear polymer microfilament called F-actin (filamentous), both of which are essential for such important cellular functions as the mobility and contraction of cells during cell division.

The actin cytoskeleton is therefore a target for toxins and the actin equilibrium can be disturbed or overridden. The effect of doliculide is essentially the same as of the natural products jasplakinolide and phalloidin: it promotes assembly of pure G-actin into F-

[116] Ruoli B. *et al.J. Biol. Chem.* **2002**, *277*, 32165.
[117] Ishiwata, H.; Nemoto, T.; Ojika, M.; Yamada, K. *J. Org. Chem.***1994**, *59*, 4710.
[118] R. Dominguez and K. C. Holmes, *Annu.Rev. Biophys.* **2011**, *40*, 169.

actin. Doliculide causes over-polymerisation into F-actin by binding to the actin cytoskeleton at a similar as phalloidin (Figure 38).[119]

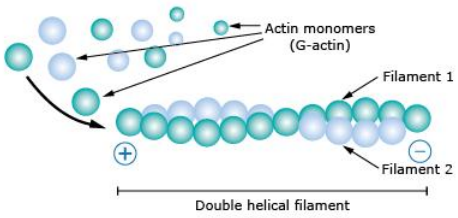

Figure 38: Assembly dynamics

Only a few total syntheses of doliculide have been reported to date. The Altmann group, has recently reported a new total synthesis of doliculide[114] which features a longest linear sequence of 11 steps and a highly atom efficient strategy.

In addition, several analogues of doliculide have been synthesised in the Altmann group in order to determine which features of the doliculide structure are essential for binding to the actin cytoskeleton and causing cytotoxic effects.

[119] Foerster, F.; Braig, S.; Altmann, K-H.; Chen, T.; Vollmar, A. M.; *Bioorg.Med. Chem.* **2014,** *22*, 5117.

4.1.2. Aim of the project and retrosynthetic plan

As part of these SAR investigations conformational studies were also conducted by solution NMR (with free doliculide), which indicated an anti-periplanar conformation about the C4-C5 bond. Based on these findings and in order to investigate if restricting the conformation about the C4-C5 bond in the preferred conformation deduced from the solution NMR studies, the group designed 5-desmethyl analog **51** (Figure 39), which incorporates a trans double bond between C4 and C5. Preliminary work towards the synthesis of this analog has already been performed in the Altmann group, but the synthesis has not been completed.

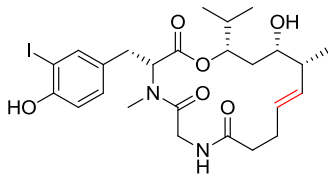

51

Figure 39: Structure of doliculide analogue

The aim of this project was to complete the synthesis of the new doliculide analogue **51**. Scheme 39 shows the retrosynthetic analysis for the target structure.

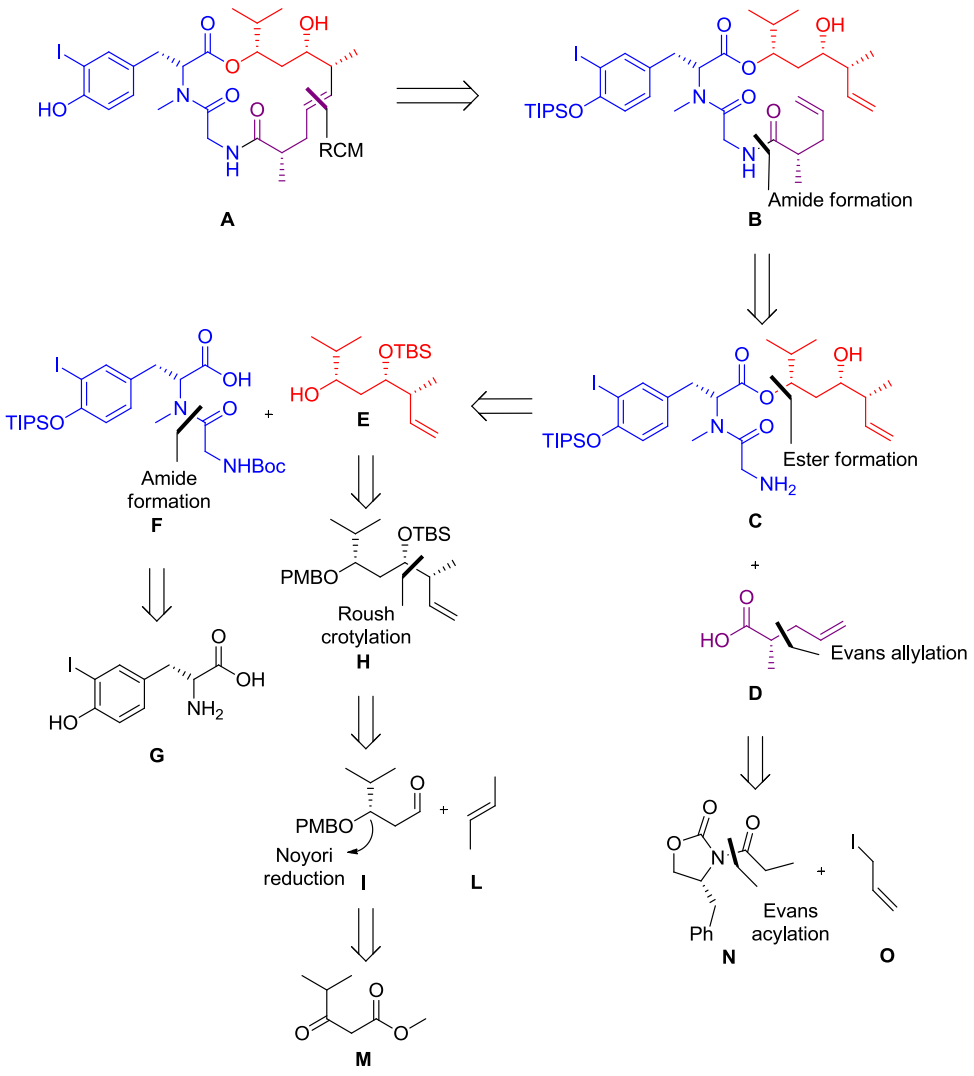

Scheme 39: Retrosynthesis of the target doliculide analogue.

4.2. Result and discussion

4.2.1. Synthesis of dipeptide

Protected dipeptide 5**6** was prepared from commercially available 3-iodo-D-tyrosine (Scheme 40). Ghosh *et al.* proposed this route[120] in the total synthesis of doliculide.

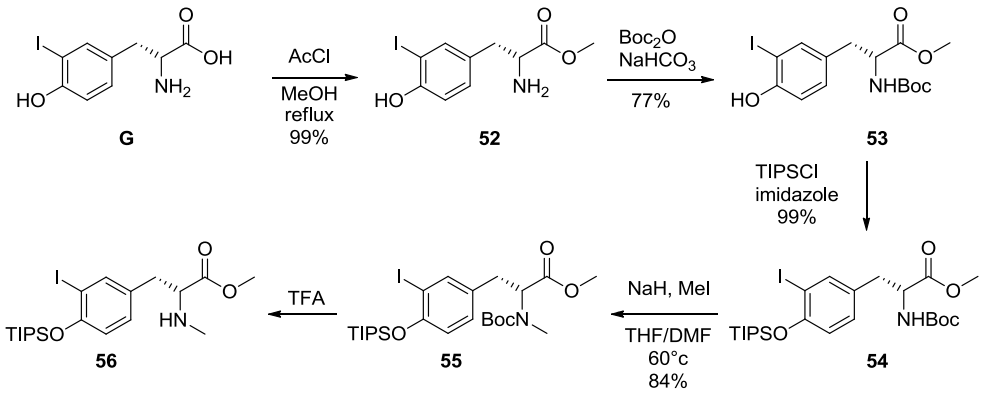

Scheme 40: Synthesis of *N*-methylated peptide 5**6**

Commercially available 3-iodo-D-tyrosine was converted into the corresponding ester derivative 5**2**, which was transformed into the corresponding *N*-Boc-protected derivative **53**. Protection of the phenolic group as a TIPS ether followed by *N*-methylation with sodium hydride and methyl iodide in a mixture (10:1) of THF and DMF furnished the *N*-methylated tyrosine derivative **56**.

After cleavage of the *N*-Boc protecting group, the resulting intermediate **56** was condensed with *N*-Boc-glycine with EDC/HOBt (Scheme 41). Unfortunately a cleavage of the TIPS protecting group occur. To avoid this problem, the amide coupling step was previously tried by Altmann group using PyBroP as the coupling agent. PyBroP successfully coupled the amine and carboxylic acid with no cleavage of the TIPS protecting group.

[120] Ghosh A. K. and Liu C.*Org. Lett.* **2001**, *4*, 635.

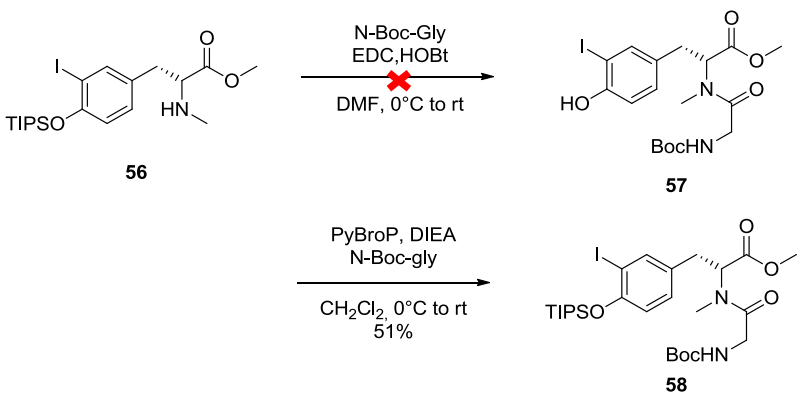

Scheme 41: Formation of the dipeptide unit

Selective cleavage of the ester group could be accomplished with LiOH at 0°C (Scheme 42). The resulting dipeptide acid **F** was directly used in the following step without further purification.

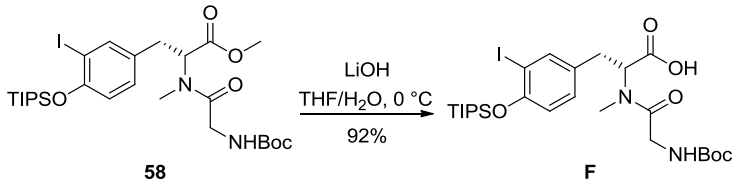

Scheme 42: Preparation of acid **F**

4.2.2. Synthesis of secondary alcohol fragment

The synthesis of secondary alcohol fragment **E** starts with crotylation of aldehyde **I**. The crotylation step first required the synthesis of the reagent **61** (Scheme 43), which can be prepared from trans-2-butene, Schlosser's base (generated *in situ*), triisopropyl borate, and (−)-DIPT.[121]

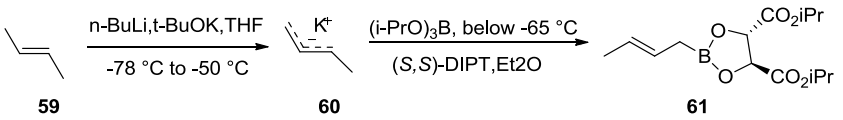

Scheme 43: Generation of crotylation reagent **61**

This reaction proceeded in a low yield of only 19% with the crude spectrum showing a 2:1 mixture of DIPT and **61**. However, it has been reported in literature that the crude reagent with excess DIPT (≤ 0.4 eq.) is routinely used in crotylation reactions without purification as the purity seems to have no apparent effect on stereoselectivity. The aldehyde **I** was therefore crotylated using the impure reagent **61** to yield free alcohol **62**, as is shown in Scheme 44. **62** was in a *de* of 50 % as shown in Figure 40 and Figure 41.[122]

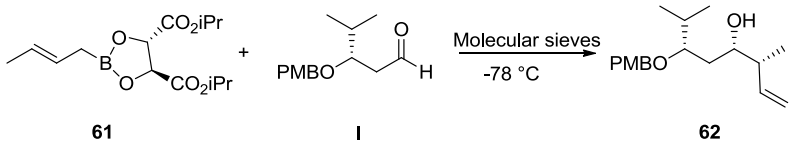

Scheme 44: Crotylation of aldehyde **62**

[121] Roush W. R. *et al., J.Am. Chem.Soc.* **1990**, *112*, 6339.
[122] Roush, W. R.; Walts, A. E.; Hoong, L. K. *J. Am. Chem. Soc.* **1985,** *107*, 8186.

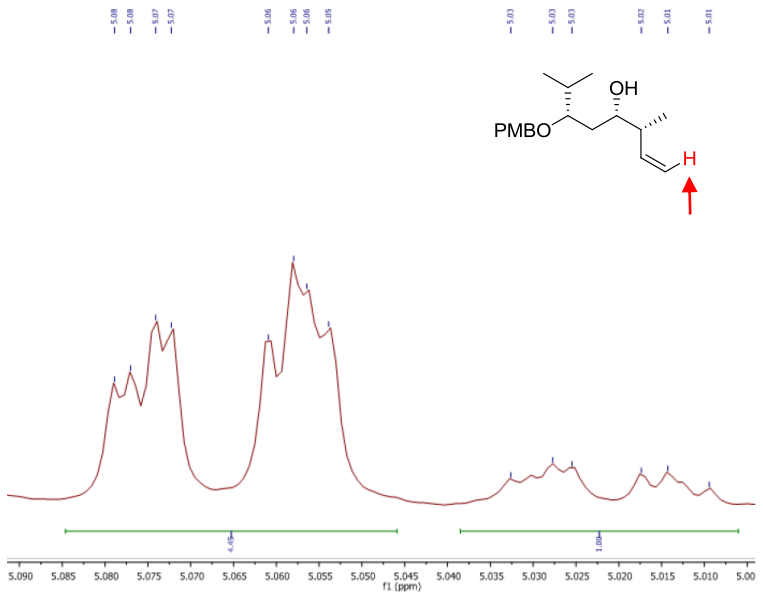

Figure 40: Diastereomericcalculation by ^{1}H-NMR

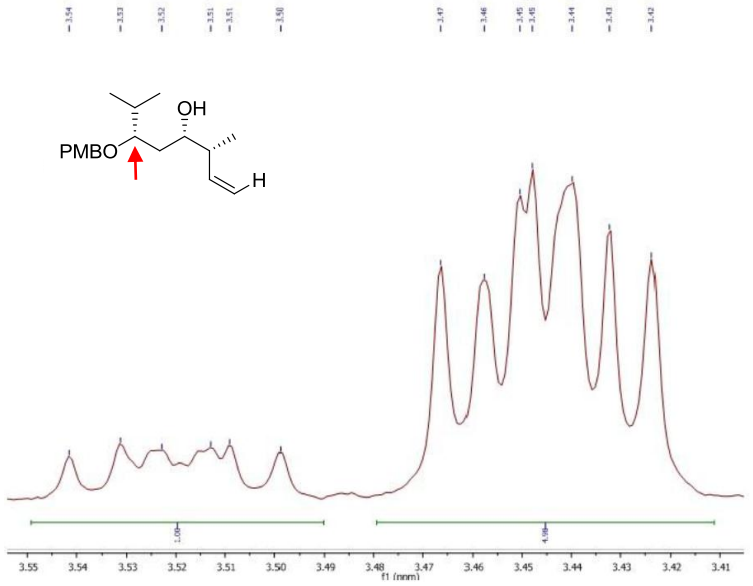

Figure 41: Diastereomeric calculation by ^{1}H-NMR

The predicted Zimmerman-Traxler 6-membered chair-like transition state for this crotylation is depicted in Figure 42. This transition state accounts for the stereoselectivity of the crotylation.

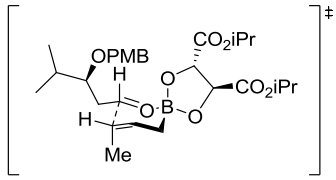

Figure 42: Intermediate formed in the crotylation reaction

To yield the secondary alcohol fragment **E**, **H,** which was already available in the laboratory, was submitted to a selective cleavage of the PMB (4-Methoxybenzyl ether) protecting group in the presence of DDQ (2,3-Dichloro-5,6-dicyano-1,4-benzoquinone) (Scheme 45). The resulting secondary alcohol **E** was directly used in the following step without further purification.

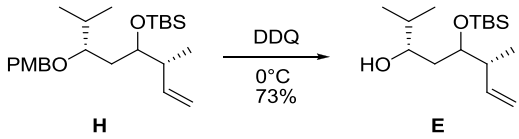

Scheme 45: Deprotection reaction of **H**

4.2.3. Fragment coupling and completation of the synthesis

The secondary alcohol **F** was coupled to the dipeptide unit **E** to form an ester **63** (Scheme 46).

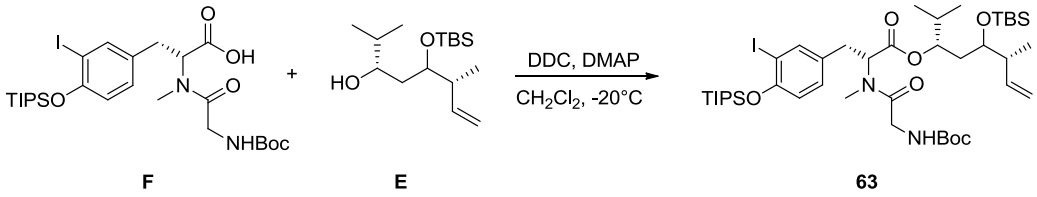

F **E** **63**

Scheme 46: Coupling of **F** and **E**

Unfortunately, the product decomposed during the reaction, and this step could not be repeated because the time was limited.

For completion of the analogue, **H** should be again resynthesized. Next step will be again PMB cleavage using DDQ/ H_2O to yield a secondary alcohol. This secondary alcohol can then be coupled to the dipeptide unit to form an ester. After coupled to the dipeptide unit to form an ester. This ester will then be Boc cleaved to allow coupling of **D** via an amide formation. The depsipeptide could then be cyclised by a ring closing metathesis. Cleavage of the silyl protecting groups would then give the doliculide analogue **51** (Scheme 47).

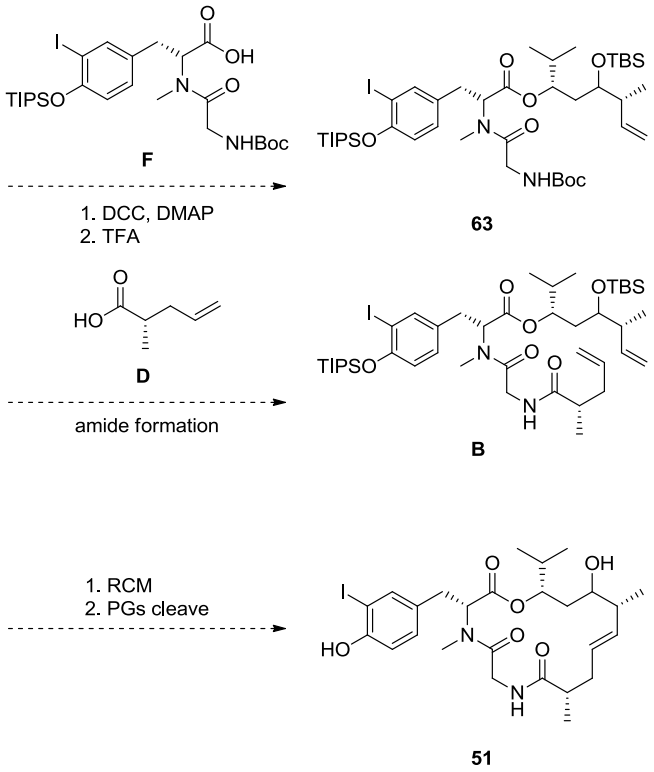

Scheme 47: Plan for the completion of the target doliculide analogue **51**.

This compound will be assessed for its effects on actin polymerization and cancer cell proliferation in collaboration with the group of Prof. Angelika Vollmar at the Ludwig-Maximilians-Universtity in Munich.

4.3. Pironetin-dumetorine hybrid compounds

4.3.1. Introduction

Microtubules, major structural components in eukaryotic cells, are the target of a large and various group of natural product anticancer drugs.

They are dynamic polymers with a fundamental role in many cellular processes, most particularly cell division process, as they are key constituents of the mitotic spindle.[123]

Microtubules are composed of tubulin heterodimers, each consisting of two tightly bound tubulin subunits called α- and β-tubulin. Tubulin subunits self-assemble in longitudinal rows called protofilaments, which organized themselves in parallel structures of 13 units forming cylindrical microtubules with a hollow core (Figure 43).

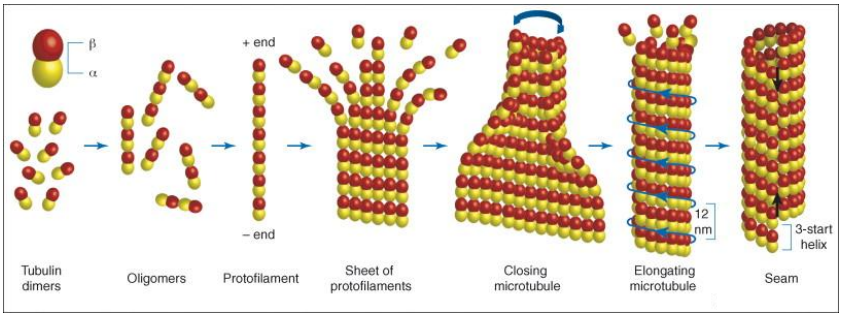

Figure 43: Polymerization of microtubule

Microtubules characteristics properties are dynamic instability and polarity.

In fact, the assembly of tubulin heterodimers creates a polarity on the microtubule that significantly influences the polymerization rates of the two ends of the microtubule. The faster growing end, with β-tubulin facing the solvent, is called the plus (+) end whereas the slower growingend, with α-tubulin facing the solvent, is named the minus (-) end.

The biological functions of microtubules in cells are determined and regulated in large part by their polymerization dynamics. Microtubules are in a constant state of formation

[123] The Role of Microtubules in Cell Biology, in: T. Fojo (Ed.), *Neurobiology and Oncology, Humana Press, Totowa, New Jersey*, **2008**.

and disruption, called dynamic instability.[124] It is charachterized by four main parameters: a) the rate of shortening; b) the rate of microtubules growth; c) the frequency of transition from shortening to growth (named "rescue frequency"); and d) the frequency of transition from the growth or paused state to shortening (named "catastrophe frequency"). Different factors regutale the dynamic of microtubule formation, however the most important is the rate of GTP (guanosine triphosphate) hydrolisis.There are two GTP-binding stes on tubulin, a hydrolysable site on the β-subunit and a non-hydrolyzable site on the α-subunit.

Both α- and β-tubulin bind GTP in a reversible way at a site in the β-subunit and the GTP hydrolyzed guanosine diphosphate (GDP) and orthophosphate (P_i) during polymerization.

This GTP hydrolysis decreases the binding affinity of tubulin for closest molecules, thereby favouring depolymerization and resulting in the dynamic behaviour of microtubules (Figure 44).

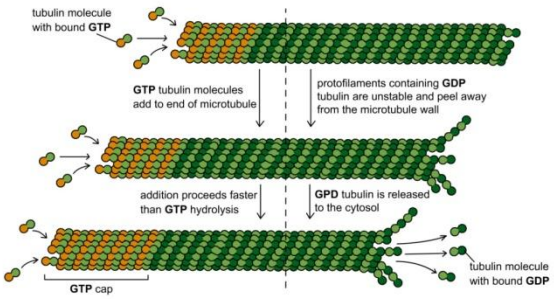

Figure 44: Microtubule dynamics

Microtubule dynamics are crucial to the process of mitosis: when cells enter mitosis during the cell cycle, microtubule reorganized into the mitotic spindle. The processes of depolymerizing the interphase microtubule structure and forming the mitotic spindle involve highly coordinated microtubule dynamics. Thus, any molecules able to interact

[124] Mitchison, T.; Kirschner, M. *Nature* **1984**, *312*, 237-242.

with microtubules dynamics, will have the ability to influence cell cycle division process by inhibition or promotion of microtubule assembly.

Drugs that inhibit microtubule dynamics are classified as microtubule stabilizer or destabilizer, respectively. Both microtubules stabilizing and destabilizing agents have been successfully applied in the treatment of several types of cancer.[125]

Microtubules stabilizing agents arrest microtubules depolymerisation targeting two different sites on β-tubulin, the taxoid or the laulimalide/peloruside binding site, while microtubules destabilizing agents block microtubules assembly and/or induce depolymerisation by binding to the vinca or the colchicine binding site. Either sites are localized at the interface between α- and β- subunits, whose reciprocal orientation is modified upon ligand binding.

Recently, microtubules targeting agents have also been shown to be neuroprotective in neurodegenerative diseases, such as Parkinson's and Alzheimer's diseases.[126][127]

Most of tubulin-binding molecules interact with β-tubulin, producing either disruption or stabilization of microtubules. A well-known representative of this kind of molecules is paclitaxel, the first described tubulin interacting drug that was found to stabilize microtubules. [128]

On the contrary, only few compounds have been identified to bind α-tubulin. One of them is the 5,6-dihydro-α-pyrone pironetin (Figure 45), a natural potent inhibitor of tubulin assembly that has been found to arrest cell cycle progression at G2/M phase. Thus, it constitutes a pharmacologically interesting compound.

[125] Dumontet, C.; Jordan, M.A. *Nat. Rev. Drug Discov.* **2010**, *9*, 790-803.

[126] (a) Brunden, K.R.; Trojanowski, J.Q.; Smith, A.B. *et al. Bioorg. Med. Chem*. **2014**, *22*, 5040-5049; (b) Ballatore, C.; Brunden, K.R.; Huryn, D.M. *et al. J. Med. Chem*. **2012,** *55*, 8979-8996.

[127] Cappelletti,G.; Cartelli, D.; Christodoulou, M.S.; Passarella, D. *Curr. Pharm.Des*. **2016**, *22*.

[128] Fu, Y.; Li, S.; Zu, Y.; Yang, G.; Yang, Z.; Luo, M.; Jiang, S.; Wink, M.; Efferth, T. *Curr. Med. Chem*. **2009,** *16*, 3966-3985.

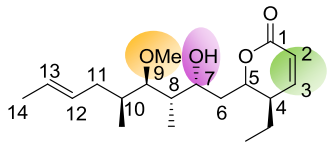

Pironetin

Figure 45: Pironetin and its groups essential for the biological activity

Some structure-activity relationships studies[129] on natural pironetin (Figure 46) displayed that the presence of the conjugated C2-C3 double bond and of the hydroxyl group at C-9 together with the hydroxyl group at C-7, either free or methylated, are essential for its biological activity. There are no data available about the importance of the remaining structural features.

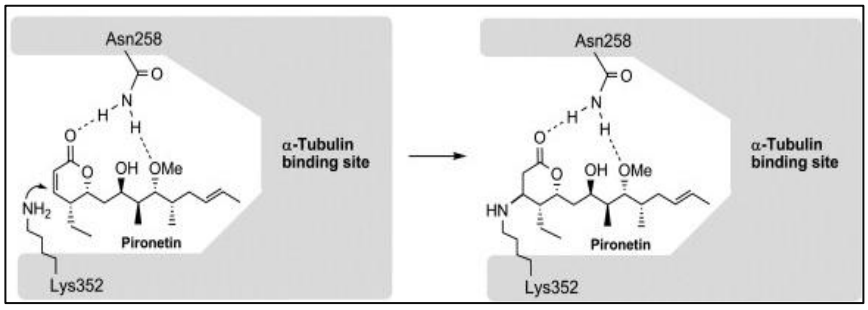

Figure 46: Schematic model of the covalent union of pironetin to its binding site at the α-tubulin surface

It has been proposed that the Lys-352 residue of the α-tubulin chain adds in a Michael fashion to the conjugated double bond of pironetin therefore forming a covalent bond with C-3 of the dihydropyrone ring. In addition, Asn-258 residue of α-tubulin holds the pironetin molecule through two hydrogen bonds to the pyrone carbonyl C-1 and the methoxy oxygen atoms C-9.

[129] (a) Kondoh, M.; Usui, T.; Kobayashi, S.; Tsuchiya, K.; Nishikawa, K.; Nishikiori, T.; Mayumi, T.; Osada, H. *Cancer Lett*. **1998,** *126* , 29-32; (b) Kondoh, M.; Usui, T.;Nishikiori, T.;Mayumi, T.; Osada, H. *Biochem. J.* **1999,** *340*, 411-416; (c) Watanabe, H.; Watanabe, H.; Usui, T.; Kondoh, M.; Osada, H.; Kitahara, T. *J. Antibiot.***2000,** *53*, 540-545; (d) Usui, T.; Watanabe, H.; Nakayama, H.; Tada, Y.; Kanoh, N.; Kondoh, M.; Asao, T.; Takio, K.; Watanabe, H.; Nishikawa, K.; Kitahara, T.; Osada, H. *Chem. Biol.***2004,** *11*, 799-806.

4.3.2. Docking studies of pironetin

Docking studies have been performed in order to evaluate the interactions modes of pironetin with α-tubulin. Figure 47 shows the formation of hydrogen bonds between the conjugated pyrone ring of pironetin and Lys-352, Cys-315 residues of the α-tubulin chain. The hydroxyl group of pironetin interacts with Met-313 and Thr-257 residues according its orientation.

There are also non-polar interactions between the alkylic chain of pironetin and the Leu-254, Val 260 and Pro-261 residues.

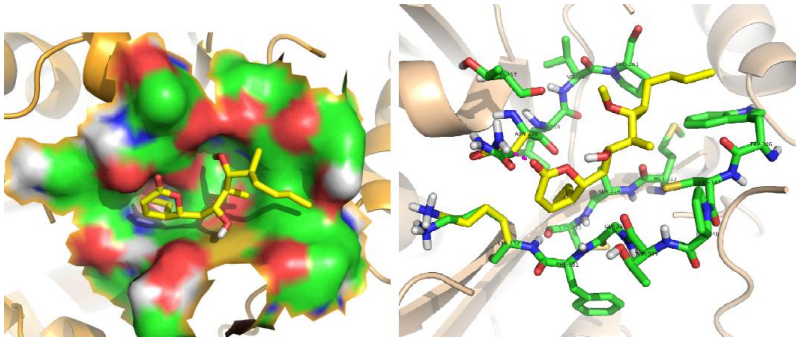

Figure 47: Binding pocket of pironetin (on the left) and interactions of pironetin with α-tubulin (on the right)

4.3.3. Aim of the project and retrosynthetic plan

In this context, we were fascinated by the pironetin and dumetorine structures and we planned the synthesis of hybrid compounds (Figure 48), as new tubulin binders, bearing a piperidine ring instead of oxygen in position 9 (OMe), that has been recognised as a previleged structure in medicinal chemistry.[130]

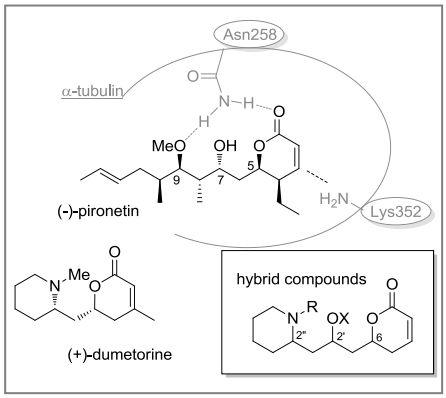

Figure 48: Design of hybrid compounds

Moreover, these hybrid compounds should contain a conjugated double bond C8-C9 and a hydroxyl group at C2', either free or methylated, according to structure activity studies on natural pironetin that showed those groups are essential for biological activity.

These compounds are characterized by the presence of three stereogenic centers so we were able to prepare eight stereoisomers with the aim of evaluating their influence on tubulin–microtubule polymerization processes.

The key steps for the synthesis of the desired compounds are the allylation mediated by enantiopure DIP-Cl (diisopinocampheyl chloroborane) and the ring closing metathesis according to the synthetic plan previously described for the preparation of dumetorine.[131]

Scheme 48 reports the retrosynthetic plan for the preparation of the eight pure stereoisomers with the aim to study the direct interaction with tubulin. In this way, we aimed to find new scaffolds in order to investigate the chemical space of the tubulin

[130] Watson, P.S.; Jiang, B.; Scott, B. *Org. Lett.* **2000**, *2*, 3679–3681.

[131] (a) Riva, E.; Rencurosi, A.; Gagliardini, S.; Passarella, D.; Martinelli, M. *Chem. Eur.J.* **2011**, *17*, 6221-6226; (b) Passarella, D.; Riva, S.; Grieco, G.; Cavallo, F.; Checa, B.; Arioli, F.; Riva, E.; Comi, D.; Danieli, B. *Tetrahedron: Asymmetry* **2009**, *20*, 192-197.

binders[132] and to develop new drugs active against cancer, Parkinson's[133] and Alzheimer's diseases.[134]

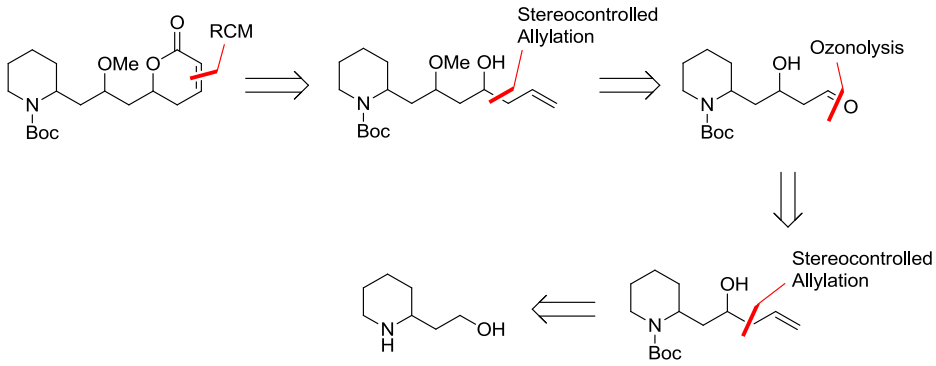

Scheme 48: Retrosynthetic plan for all hybrid compounds

[132] Canela, M.; Perez-Perez, M.; Noppen, S.; Saez-Calvo, G.; Diaz, J.; Camarasa, M.; Liekens, S.; Priego, E. *J. Med.Chem.***2014**, *57*, 3924-3938.

[133] Cartelli, D.; Casagrande, F.; Busceti, C. L.; Bucci, D.; Molinaro, G.; Traficante, A.; Passarella, D.; Giavini, E.; Pezzoli, G.; Battaglia, G.; Cappelletti, G. *Sci. Rep.* **2013**, *3*, 1837-1846.

[134] Zhang, B.; Carroll, J.; Trojanowski, J. Q.; Yao, Y.; Iba, M.; Potuzak, J. S.; Hogan, A.M.L.; Xie, S. X.; Ballatore, C.; Smith, A. B.; Lee, V. M. Y.; Brunden, K. R. *J.Neurosci.* **2012**, *32*, 3601-3611.

4.3.4. Hybrid compounds docking

For these compounds, only a rigid docking has been performed thanks to the collaboration with Prof. M. Sironi and Dr. S. Pieraccini of Dipartimento di Chimica at Università degli studi di Milano. These studies demonstrate that the binding modes and the orientation of hybrids are similar to those observed in the rigid docking of natural pironetin (Figure 49).

The pyrone ring is directed towards the entrance of the pocket while the piperidine ring occupies the position of the alkyl chain of pironetin.

It is important to note that these compounds are able to form more hydrogen bonds with α-tubulin compared to pironetin, with a consequent increase of the interaction with tubulin.

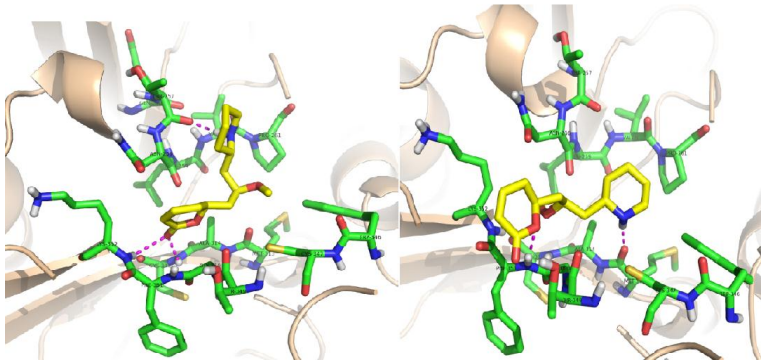

Figure 49: Some interactions modes of hybrids compound and α-tubulin. Hydrogen bonds between the pyrn ring andresidues Lys-352, Phe-351, Cys-315.

4.4. Result and discussion

4.4.1. Synthesis of hybrid compounds

Commercially available racemic 2-(piperidin-2-yl) ethanol **64** was converted into the corresponding N-Boc-protected derivative **65** (Scheme 49). Oxidation of alcohol **65** under Swern condition provided aldehyde **66**.

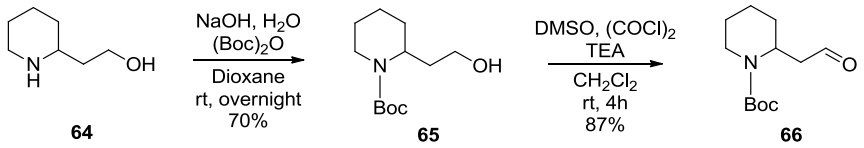

Scheme 49: Synthesis of aldehyde **66**

Subsequent reaction is based on the reactivity and versatility of aldehyde **66** (Scheme 50), previously used in both racemic and enantiopure forms.[135]

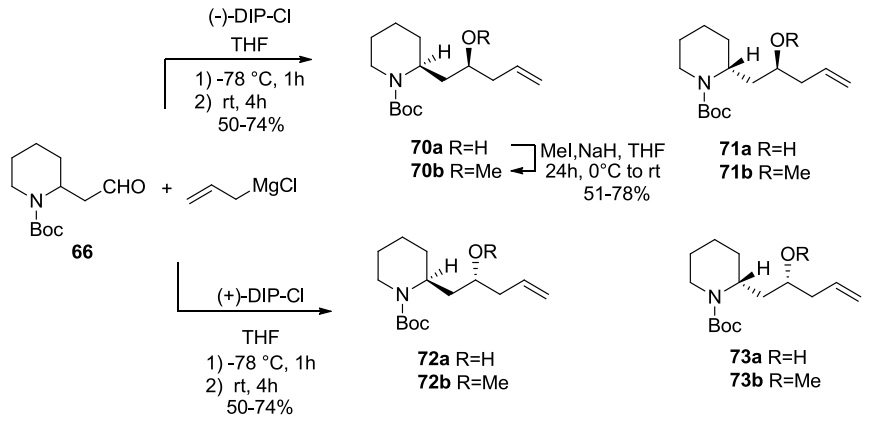

Scheme 50: Stereoselective allylation of aldehyde **66**

[135] Perdicchia, D.; Christodoulou, M. S.; Fumagalli, G.; Calogero, F.; Marucci, C.; Passarella, D. *Int. J. Mol. Sci.***2016**, *17*, 17.

Brown's asymmetric allylation with the B-allyl diisopinocampheylborane,[136] allowed formation of allylic alchols **70a–73a** with total stereocontrol at C2′ (numbering system of the target compound) thus providing two enantiopure diastereoisomers (on the basis of HPLC traces).[137]

Using (–)-DIP-Cl (Scheme 50) we were able to obtain **70a** and **71a** characterized by the *S* configuration at position 2′ whereas the use of (+)-DIP-Cl (Scheme 50) lead to compounds **72a** and **73a**. On the basis of previously reported spectroscopic data [138,139] and by performing the same reaction on small scale using, as substrates, the pure enantiomers of aldehyde **66**, we were able to confirm the assignment of the structures. In particular, the reaction of (*S*)-**66** with (–)-DIP-Cl furnished **70a** as a single product revealing that the configuration of the newly formed stereogenic center is dictated by the chirality of DIP-Cl. In the same manner, reaction of (*R*)-**66** with (–)-DIP-Cl gave **71a** whereas the use of (+)-DIP-Cl with (*S*)-**66** and (*R*)-**66** provided **72a** and **73a** respectively. Enantiomerically pure compounds **70a–73a** were submitted to methylation reaction (Scheme 50) and subsequent ozonolysis oxidation provided corresponding aldehydes **74-77** in 40–50 % yield. (Scheme 51)

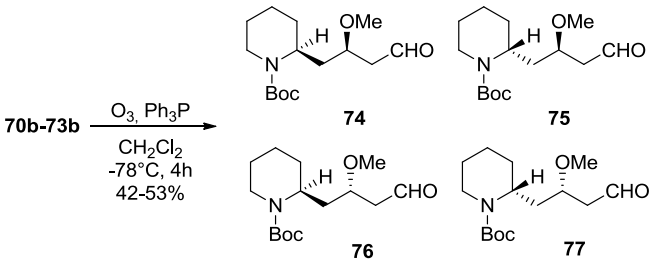

Scheme 51: Synthesis of aldehydes **74-77**

[136] Ramachandran, P. V.;Chen, G. M.; Brown, H. C. *Tetrahedron Lett.***1997**, *38*, 2417–2420.

[137] Angoli, M.; Barilli, A.; Lesma, G.; Passarella, D.; Riva, S.; Silvani, A.; Danieli, B. *J. Org. Chem.***2003**, *68*, 9525–9527.

[138] Passarella, D.; Barilli, A.; Belinghieri, F.; Fassi, P.; Riva, S.; Sacchetti, A.;Silvani, A.; Danieli,B. *Tetrahedron: Asymmetry*, **2005**, *16*, 2225–2229.

[139] Passarella, D.; Angoli, M.; Giardini, A.; Lesma, G.; Silvani, A.; Danieli, B. *Org. Lett.***2002**, *4*, 2925-2928.

One more Brown's asymmetric allylation reaction afforded compounds **78a**–**85a** as pure single stereoisomers (Scheme 52).

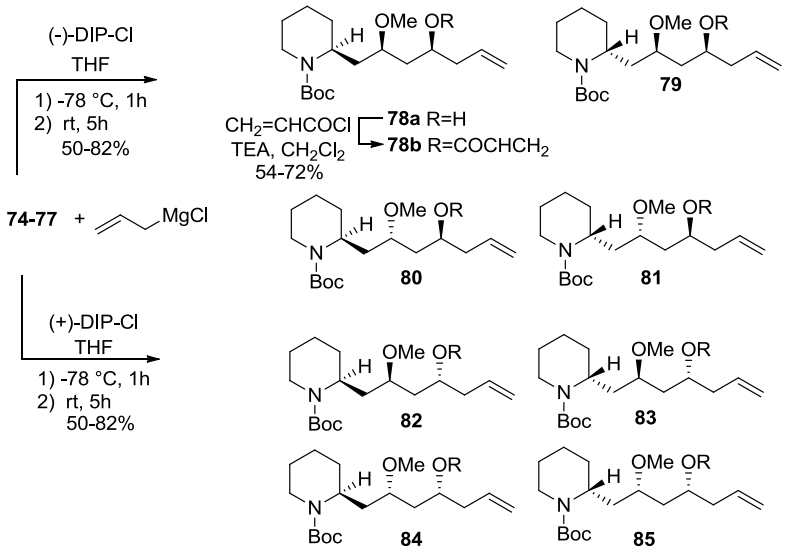

Scheme 52: Stereoselctive allylation of aldehydes and acylation reaction

Acylation of compounds **78a-85a** with acryloyl chloride led to the formation of **78b-85b**. Subsequent ring closing metathesis in the presence of Hoveyda–Grubbs-II catalyst (Scheme 53) gave compounds **86a**–**93a** with 70–80 % yield and then they were submitted to Boc cleavage with TFA in CH_2Cl_2 (via *b* in Scheme 53).

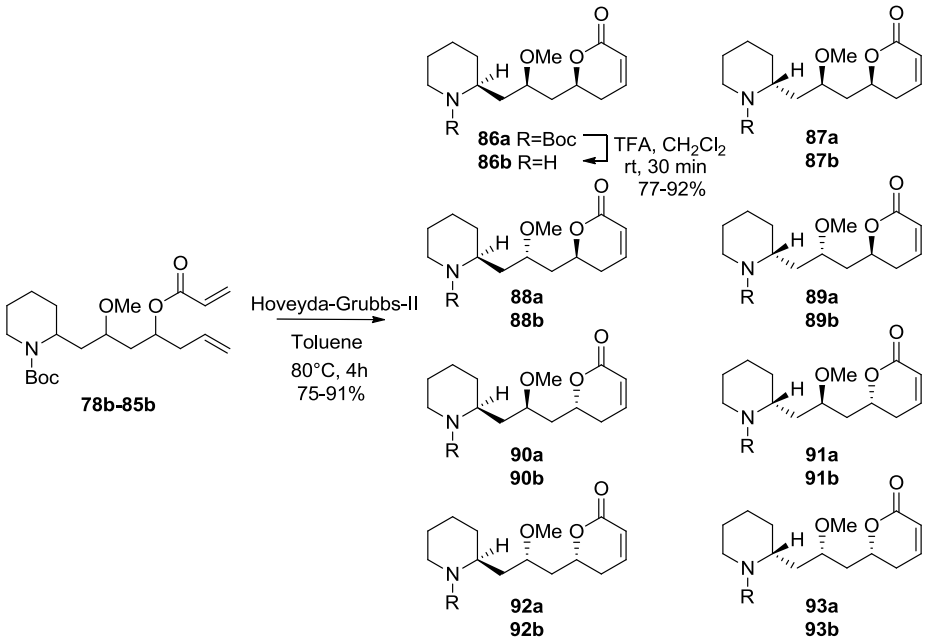

Scheme 53: Synthesis of target compounds **86b-93b**

Finally, target compounds **86b–93b** were obtained as ammonium trifluoroacetate salts and they were submitted to biological evaluations with the aim of illustrating theirinfluence on the tubulins-microtubules polymerization.

4.4.2. Biological evaluation

The ability of compounds **86b–93b** to influence tubulin polymerization was evaluated by sedimentation assays (Figure 50) thanks to the collaboration with Prof. G.Cappelletti of the Dipartimento di Biologia at Università degli studi di Milano.

Thiocolchicine (10 μM) was used as a reference compound that, as expected, acts by inhibiting the aggregation of tubulin. We also compared the activities of **86–93** against that of previously reported pironetin analog **94**.[140]

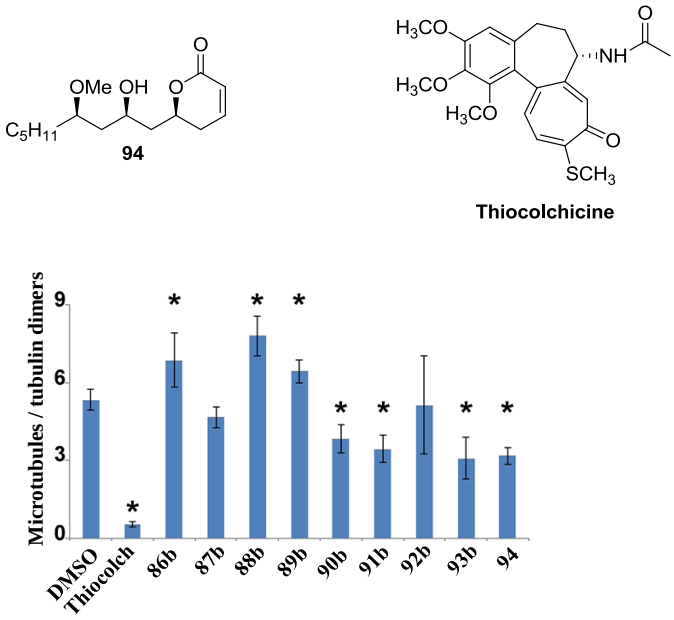

Figure 50: Biological results

From this analysis we observed that the new compounds appear to moderately impact microtubule formation.

In particular **86b**, **88b** and **89b** significantly increase the ratio between microtubules and tubulin dimers, whereas agents **90b**, **91b** and **93b** inhibit microtubule assembly in a fashion similar to that previously reported for **94**.

[140] Alberto Marco, J.; Garcia-Pla, J.; Carda, M.; Murga, J.; Falomir, E.; Trigili, C.; Notararigo, S.; Fernando Diaz, J.; Barasoain, I. *Eur. J. Med. Chem.***2011**, *46*, 1630–1637.

4.5. Bivalent compounds toward α,β-tubulin interaction

4.5.1. Introduction

In the last years, our research group explored the possibilities offered by the concept of multivalency[141] for the design of new antitubulin agents.[142] The theory of multivalency is based on the consideration that in Nature the activity and selectivity of several lead compounds are improved through the creation of their homo- or heterodimers.[143] As a result, the concept of multivalency can be applied as a successful approach for designing bivalent compounds.

In particular microtubule-targeting bivalent hybrids represent an emerging class of molecules that may be a valuable tool to increase the activity and selectivity of monomeric drugs. Thus, bifunctional drugs, characterized by two components able to bind to different sites inducing a multiple effect and increasing their pharmacological activity, represent a specif class of microtubules targeting agents.

According to Meunier[144] hybrid molecules can be divided into three categories (Figure 51):

a) Both parts of the hybrids act on the same target (not necessarily on the same site)
b) Each parts acts on a different target: the hybrids are like dual prodrugs if the linker is cleaved in the biologycal system.
c) The parts of the hybrid molecule may act at the same time on two connected and closely related binding sites of the same target.

[141] Synthetic Multivalent Molecules; Choi, Seok-Ki, Ed.; Wiley Interscience: USA, **2004**.
[142] Passarella, D.; Giardini, A.; Peretto, B.; Fontana, G.; Sacchetti, A.; Silvani, Al.; Ronchi, C.; Cappelletti, G.; Cartelli, D.; Borlak, J.; Danieli, B. *Bioorg. Med. Chem.***2008**, *16*, 6269–6285.
[143] Berube, G. *Curr. Med. Chem*. **2006**, *13*, 131.
[144] Meunier, B. *Acc. Chem. Res.* **2007**,*41*, 69.

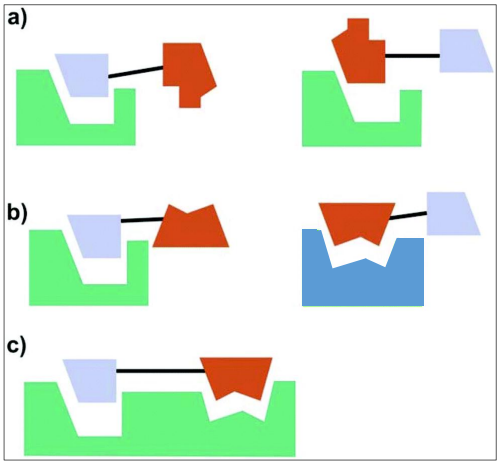

Figure 51: Categories of hybrid molecules according to their mode of action.

Bifunctional compounds are able to interfere with protein-protein interaction soffering a powerful means of influencing the function of selected proteins within the cell.

Protein-protein interactions have a central role in cellular processes. In fact, anomalous or inappropriate interactions posses the potential to induce pathological conditions while the modulation of such protein-protein interactions by organic molecules offers possibilities for the treatment of human disease.

On the base of recent results regarding the crystallographic structure of tubulin in complex with thiocolchicine,[145] we moved our attention toward the preparation of bivalent hybrid compounds linking our pironetin-dumetorine hybrid compounds and a drug able to bind β-tubulin by a linker (Figure 52).

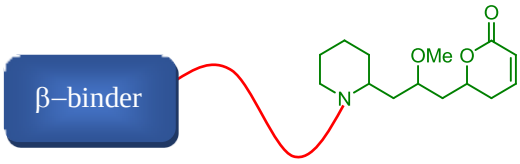

Figure 52: General structure of bivalent derivatives

[145] Marangon, J.; Christodoulou M. S.; Casagrande, F.V.M.; Tiana, G.; Dalla Via, L.; Aliverti, A.; Passarella, D.; Cappelletti, G.; Ricagno, S. *Biochem.Biophys.Res.Comm.* **2016,** *479*, 48-53.

4.5.2. Aim of the work

The first attempt for the synthesis of bivalent compound was to connect one of our hybrid compounds and deacetylthiocolchicine by a linker containing 10 carbon atoms (Figure 53).

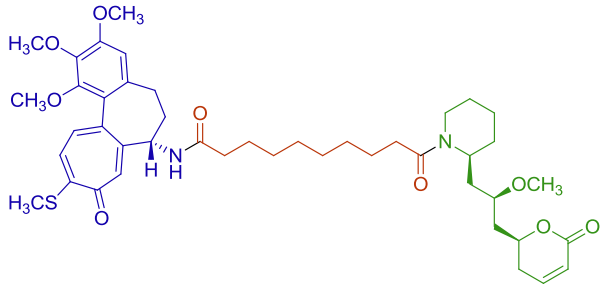

Figure 53: Structure of our first bivalent molecule. In blue deacetylthiocolchicine, in red sebacic acid and in green **86b** as hybrid compound.

As active compounds, we chose deacetylthiocolchicine because it is a potent inhibitor of tubulin polymerization that it is able to bind tubulin more rapidly than colchicine.[146]

Hydrolysis of (+)-thiocolchicine with 20% HCl yielded (+)-deacetylthiocolchicine (Figure 54),[147] that can attack a suitable spacer binding to the amino group present in position 7 as acetamide.

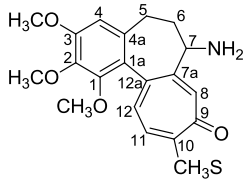

Figure 54: Deacetylthiocolchicine

Ideally, homo- and hetero-bifunctional tubulin binders should be able to simultaneously occupy two binding sites on the microtubules assembly. To do this, the three-

[146] Kang, G. J.; Getahunt, Z.; Muzaffar, A.; Brossi, A.; Hamel, *E. J. Biol. Chem.* **1990**, *265*, 10255.
[147] Velluz, L.; Muller, G. *Bull. Soc. Chim. Fr.***1955**, 194.

dimensional structure of a microtubule section was considered. From this analysis it was observed that the distances between the targeted sites within the same protofilament has to be around 40 Å, a distance that could be covered by a linker of about 50 atoms.

Future work will be the preparation of a new series of bivalent molecules that will comprise different pironetin-dumetorine hybrids and various β-tubulin binders. The chemical nature and length of the linkers between the two moieties will be varied with the aim of optimising the biological activity. The binding affinities of the prepared analogues will be measured experimentally by fluorescence quenching and compared with the suggestions deriving from computational studies.

4.5.3. Synthetic strategy

As depicted in Figure 55, two disconnections have been envisioned, in the correspondence of the amide bonds, obtainable via two condensation reactions.

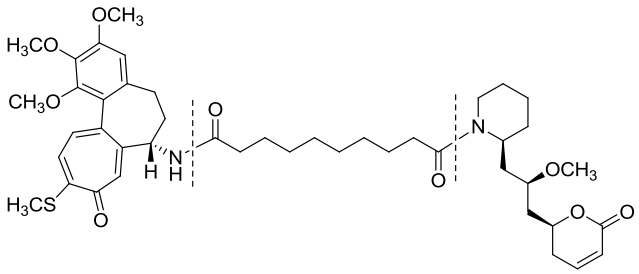

Figure 55: Disconnectionson our drug-hybrid conjugate

The first step consist in the preparation of (+)-deacetylthiocolchicine starting from (+)-thiocolchicine (Scheme 54).[148]

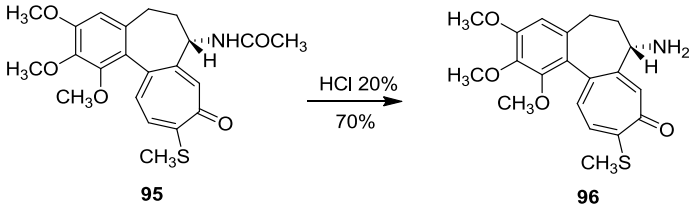

Scheme 54: Syntheis of (+)-deacetylthiocolchicine

Compound **96** was submitted to a condensation reaction with sebacic acid using BOPCl/Et_3N as activating system in CH_2Cl_2 at room temperature (Scheme 55).

[148] Shi, Q.; Verdier-Pinard, P.; Brossi, A.; Hamel, E.; Lee, K.H. *Bioorg. Med. Chem.*, **1997**, *5*, 2277-2282.

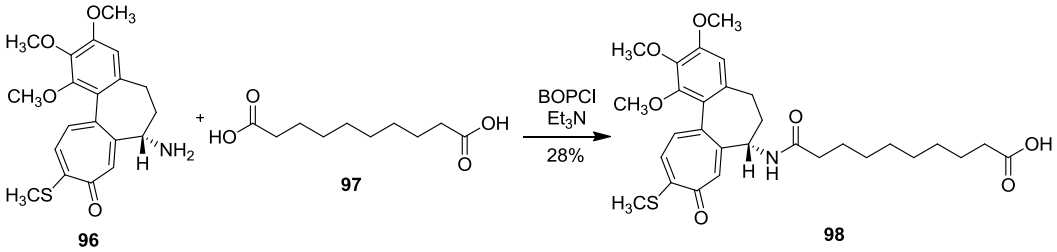

Scheme 55: Condensation between sebacic acid and compound **98**

Then we made a second condensation between **98** and hybrid copound **86b** using again BOPCl/Et_3N. NMR and mass analysis of the purified compound confirmed the structure of **99** (Scheme 56).

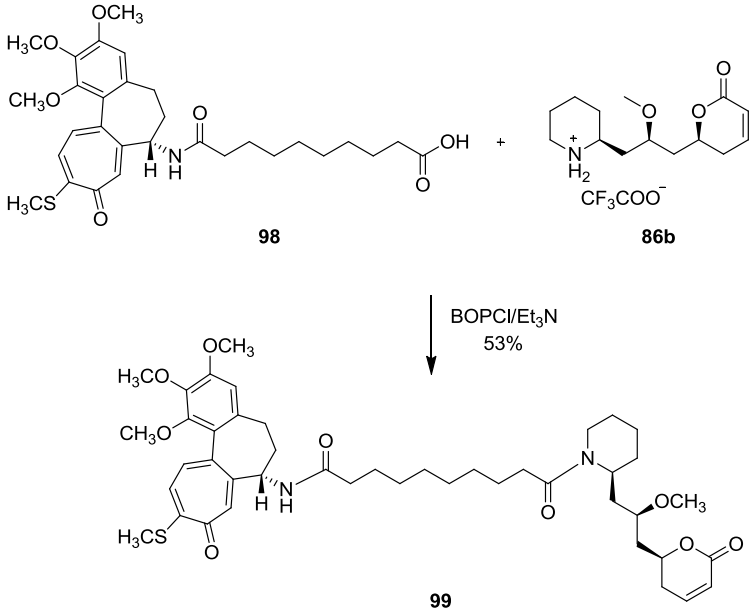

Scheme 56: Synthesis of bivalent compound

4.5.4. Biological evaluation and future work

From biological evaluation (Figure 56), we observed that compound **99** is able to inhibit tubulin polymerization process and this result encouraged us to develop new bivalent compound toward α,β-tubulin interaction.

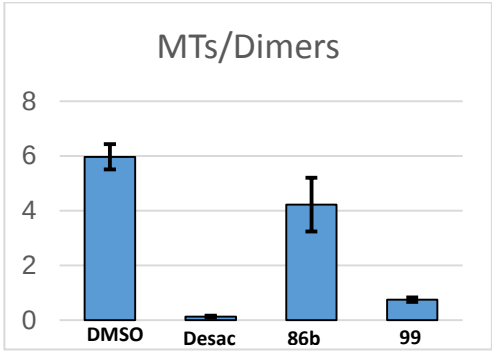

Figure 56: Desac (deacetylthiocolchicine the blu portion of bivalent compound), 86b (the green portion of bivalent compound), 99 (bivalent compound).

Furthermore we evaluated the effect of compound **99** on HeLa cells and on HepG2 cancer cell line. As reported in table 1, compound **99** is able to inhibit the growth of cancer cells but less than deacetylthiocolchicine.

Composti	HeLa (GI_{50})	HepG2 (GI_{50})
Desacetilthiocolc.	**0.0145 µM**	**0.0141 µM**
86b	**> 30 µM**	**> 30 µM**
99	**0.117 µM**	**0.41 µM**

Table 5: Desac (deacetylthiocolchicine the blu portion of bivalent compound), 86b (the green portion of bivalent compound), 99 (bivalent compound).

4.6. Experimental part

4.6.1. General information

All reactions that are sensitive to air were performed under an argon atmosphere in heatgun dried glassware. The solvents used in reactions were purchased from Fluka (dried over molecular sieves). Solvents used for extractions, thin layer chromatography (TLC) or silica gel chromatography were purchased as commercial grade and distilled. Commercially available substances were used without prior purification unless otherwise specified.

TLC were performed on aluminium sheets coated with silica gel (silica gel F254) the spots were visualised either with UV light (254 nm), or by spraying with appropriate TLC stains. Purification by flash chromatography was performed using Fluka silica gel. Solvents were evaporated with a Büchi Rotavapor together with a Büchi waterbath at 40 °C and at an appropriate pressure. Pure compounds were dried under high vacuum.

^{1}H-NMR and ^{13}C-NMR spectra were recorded on a Bruker AV-400, or an AV-500 spectrometer at room temperature. $CDCl_3$ was used as a solvent unless otherwise specified, and the chemical shifts are referenced to the residual solvent peak (for $CDCl_3$: 1H, = 7.26 ppm and 13C = 77.00 ppm) All ^{13}C spectra were measured with complete proton decoupling. The following abbreviations were used for the report of the NMR spectra: J: nucleus decoupling constant in Hz, s: singlet, d: doublet, t: triplet, q: quartet, m: multiplet. A Jasco FT/IR-6200 spectrometer was used for the acquisition of infrared resonance spectra. Frequencies are given in cm $^{-1}$.

High resolution mass spectra (HRMS) were aquired on an IonSpec (Varian) Ultima spectrometer. Melting points of pure solid products were measured on a Büchi B-540 melting point apparatus using open glass capillaries.

Optical rotation values were determined using an Anton Paar MCP 300 polarimeter. The wavelength of light used was 589 nM. The concentration of the sample used is given in g 100 cm^{-3}. Optical rotation values were recorded at 20 °C.

4.6.2. Doliculide fragments synthesis

Synthesis of compound 52

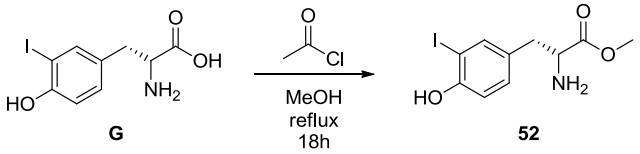

Acetyl chloride (4.7 mL, 66.4 mmol) was dissolved in MeOH (60 mL). 3-iodo-D-tyrosine (3.01 g, 9.7 mmol) was added to the solution as a solid. The reaction was stirred under reflux at 65 ºC for 18 h. The solution was concentrated under reduced pressure to yield a white-yellow solid (3.14 g, quantitative yield). This solid was used directly in the next reaction.

TLC: Rf = 0.26 (DCM/MeOH 19:1).

*Product has poor solubility and was not purified, full characterization was not made.

Synthesis of compound 53

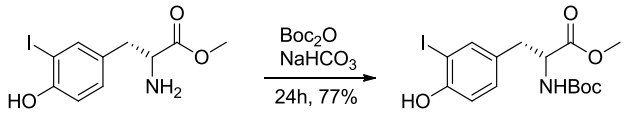

52 **53**

Compound **52** (3.14g, 9.7 mmol) was dissolved in ethanol (75 mL). Sodium bicarbonate (8.2 g, 97.7 mmol), and Boc_2O (2.28g, 10.4 mmol) were added and the solution was stirred at r.t. overnight. The solution was filtered and the filtrate was concentrated under reduced pressure to give a brown oil. The crude was purified by silica gel chromatography (hexane/EtOAc 2:1) to yield **53** as a white foam (3.15 g, 77%).

TLC: Rf = 0.40 (hexane/EtOAc 4:1)

^{1}H-NMR (400 MHz, CDCl3): δ 7.42 (s, 1H), 6.98 (dd, *J* = 8.2, 1.9 Hz, 1H), 6.86 (d, *J* = 8.2 Hz, 1H), 5.69 (s, 1H), 5.02 (bs, 1H), 4.57- 4.45 (m, 1H), 3.72 (s, 3H), 3.08-2.85 (m, 2H), 1.43 (s, 9H).

IR: $\tilde{\nu}$= 3335, 2981, 1715, 1685, 1510, 1396, 1290, 1252, 1153, 1126, 1153, 1126, 1050, 1004, 822, 567.

HRMS (ESI+): m/z calculated for $C_{15}H_{20}INO_5$ $[M+H]^+$, 422.0459, measured: 422.0459. $[a]_D^{20}$= -47.57 (c 0.35, $CHCl_3$).

Synthesis of compound 54

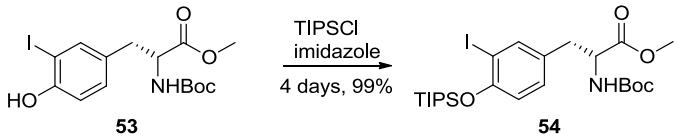

53 **54**

TIPSCl (1.8 mL, 8.43 mmol) and imidazole (1.19 g, 17.56 mmol) in dry DMF (11 mL) were stirred together. **53** (2.96 g, 7.02 mmol) was added in dry DMF (35 mL). The reaction mixture was stirred at r.t. for 4 nights. The solution was diluted with EtOAc (300 mL) and washed with water (2 x 1250 mL). The organic phase was dried over dried over anhydrous $MgSO_4$ and concentrated under reduced pressure to obtain the crude material as a yellow oily residue. The crude material was purified by silica gel chromatography (hexane/EtOAc 9:1 → 8:2) to yield **54** as a very sticky colourless oil (4.05 g, 99%).

TLC: Rf = 0.55 (hexane/EtOAc 4:1).

^{1}H-NMR (400 MHz, $CDCl_3$): δ 7.51 (d, *J* = 1.6 Hz, 1H), 6.94 (dd, *J* = 8.3, 2.2 Hz, 1H), 6.74 (d, *J* = 8.3 Hz, 1H), 4.91 (d, *J* = 8 Hz, 1H), 4.56 – 4.45 (m, 1H), 3.69 (s, 3H), 2.95-2.78 (m, 2H), 1.43 (s, 9H), 1.30-1.15 (m, 3H), 1.14 (d, *J* = 7.3 Hz, 18H).

IR (film): $\tilde{\nu}$ = 2947, 2867, 1719, 1483, 1365, 1286, 1168, 1016, 917 875, 681, 651cm^{-1}.

HRMS: **(ESI/MALDI +)**: m/z calculated for $C_{24}H_{40}INO_5Si$ $[M+Na]^+$ 600.1613, measured: 600.1611 $[a]_D^{20}$= - 36.71 (c 2.86, $CHCl_3$).

Synthesis of compound 55

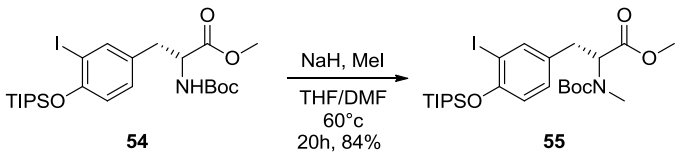

54 **55**

Compound **54** (2 g, 3.5 mmol) was dried by evaporation with toluene (high vacuum) before dissolving in a 10:1 mixture of THF: DMF (31 mL), then were added NaH 60% in oil (166 mg, 4.1 mmol) and MeI (1 mL, 17 mmol). The solution was heated at 60 °C for 20 h. After this period the mixture was cooled and then diluted with Et2O. The solution was washed with satured aqueous NH_4Cl, 20% $Na_2S_2O_3$ and brine. The organic layer was evaporated, dried over anhydrous Na_2SO_4 and concentrated to give the product **55**. Purification of the residue by flash chromatography (toluene/AcOEt 19:1 and 1% TEA) afforded 1.72 g (84 %) of **55** as a white solid.

TLC: Rf = 0.36 (toluene/EtOAc 19:1, 1% TEA).

^{1}H-NMR (400 MHz, $CDCl_3$): δ 7.58/7.57 (s, 1H), 6.98 (dd, *J* = 8.3, 2.2 Hz, 1H), 6.73 (d, *J* = 8.3 Hz, 1H), 4.85 – 4.74 (m, 1H), 4.51-4.42 (m, 1H), 3.74/3.72 (s, 3H), 3.23-3.10 (m, 1H), 2.96-2.83 (m, 1H), 2.71/2.69 (s, 3H), 1.46-1.23 (m, 12 H), 1.12/1.08 (d, *J* = 7.3 Hz, 18H).

^{13}C-NMR (101 MHz, $CDCl_3$): δ 171.9/171.6, 154.4/154.3, 139.3/139.9, 131.8/131.6, 130.1/129.8, 118.0/117.9, 80.6/80.2, 61.72, 59.70, 52.33, 34.26, 33.77, 32.75, 32.31, 28.39, 18.23, 13.32

IR (film): $\tilde{\nu}$ = 2946, 2867, 2360, 2341, 1746, 1696, 1286, 1167, 1145, 920, 882 cm^{-1}. **HRMS**: **(ESI +)**: m/z calculated for $C_{25}H_{43}INO_5Si$ $[M + Na]^+$ 592.1950, measured: 592.1956. Melting point=78-80 °C. $[\alpha]_D^{20}$ = +14.46 (c 1.68, $CHCl_3$).

Synthesis of compound 56

55 **56**

To a stirred solution of **55** (1.50g, 2.5 mmol) at 0°C, TFA (4mL) was added. The solution was warmed to 23 °C and stirred for 1 h. After this period the mixture was washed with 5% $NaHCO_3$ and brine. The organic layer was separated, dried over anhydrous Mg_2SO_4 and concentrated to give 5**6** as a sticky oil (1.7g, 97%). No Purification.

TLC: Rf = 0.50 (Hex/AcOEt 1:1, 1% TEA).

^{1}H-NMR (400 MHz, CDCl3): δ 7.57 (d, *J*= 2.1 Hz, 1H), 7.06 (dd, *J* = 8.3, 2.1 Hz, 1H), 6.77 (d, *J* = 8.3 Hz, 1H), 4.01-3.91 (m, 1H), 3.69 (s, 3H), 3.95-3.92 (m, 1H), 3.18-3.08 (m,1H), 2.72 (s, 3H), 1.38-1.21 (m, 3H), 1.12 (d, *J* = 7.3 Hz, 18H).

^{13}C-NMR (101 MHz, CDCl3): δ 168.0, 155.5, 140.13, 130.27, 127.85, 118.45, 90.80, 62.52, 53.14, 34.63, 32.22, 18.19, 13.19

IR (film): $\tilde{\nu}$= 3383, 2947, 2867, 2364, 2342, 1749, 1670, 1488, 1288, 1200, 1180, 1133, 1038, 916, 881cm^{-1}.

HRMS: (ESI/MALDI +): m/z calculated for $C_{20}H_{35}INO_3Si$ $[M+Na]^+$ 492.1425, measured: 492.1417 $[a]_D^{20}$ = - 8.04 (c 0.64, $CHCl_3$).

Synthesis of compound 58

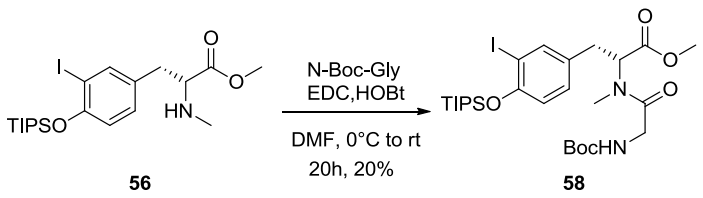

56 **58**

To the amine **56** (0.100 g, 0.2 mmol) and Boc-Gly (50 mg, 0.28mmol) in DMF at 0°C were added EDC (44 mg, 0.28 mmol) and HOBt (50 mg, 0.32mmol). The resulting solution was warmed to room temperature and stirred for 20 h. After this period the solution was quenched saturated aqueous solution NH_4Cl, diluted with AcOEt, washed with 5% HCl, 5% $NaHCO_3$ and brine. The organic layer was separated, dried over anhydrous Mg_2SO_4 and concentrated. Purification of the residue by flash chromatography (hexane/AcOEt 1:1) give **58** (30 mg, 20%). There is no TIPS protective group.

TLC: Rf= 0.55 (Hex/AcOEt 1:1, TEA 1%).

^{1}H-NMR: Complicated to interpret due to the presence of rotational isomers.

IR (film) : $\tilde{\nu}$= 3350, 2955, 2923, 2853, 2368, 2362, 2357, 2341, 2336, 1740, 1735, 1706, 1700, 1685, 1653, 1647, 1521, 1507, 1482, 1457, 1366, 1288, 1252, 1236, 1217, 1159, 1052, 1037, 1025, 759, 751

HRMS (ESI +): Calculated for $C_{18}H_{25}IN_2O_6$ $[M + H]^+$, 493.0830, found 493.0829. $[a]_D^{20}$ = 13.5 (c 0.10, $CHCl_3$)

Synthesis of compound F

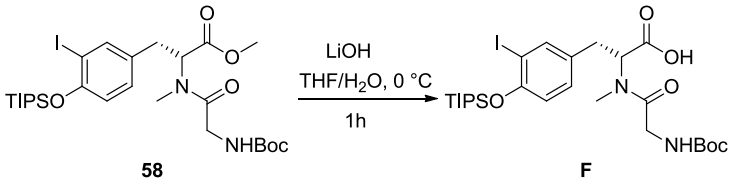

58 **F**

To a solution of dipeptide ester **58** (20 mg, 0.03 mmol) in a mixture (2:1) of THF and H_2O (1 mL) was added LiOH (3 mg, 0.075 mmol) at 0°C. The reaction mixture was continued stirring at 0°C for one hour. The reaction was acidified to pH 3.5 with aqueos $NaHSO_4$ saturated solution. The mixture was then extracted with Et_2O (x 2) and the combined organic layers were dried over $MgSO_4$, filtered, and concentrated in vacuo to afford a yellow oil, which was used immediately in the next reaction.Full characterization was not made as the product was used immediately for the next reaction.

TLC: Rf = 0.25 (AcOEt/hexane 1:1)

Synthesis of compound 61

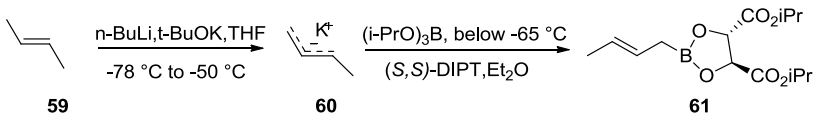

To a dry 3 necked flask, t-BuOK (3.162 g, 28.18 mmol, glovebox) and anhydrous THF (13.5 mL) were added. This solution was cooled to -78 °C. Trans-2-butene (2.42 g, 43.14 mmol) was condensed into the reaction flask from a balloon. During this addition, the solution became cloudy. Over 50 mins, *n*-BuLi (17.54 mL, 28.08 mmol) was added to the solution via a syringe pump. The solution turned a bright yellow colour. The solution was the warmed to -50 °C for 20 mins. The solution was then cooled to -78 °C and triisopropyl borate (6.47 mL, 28.075 mmol) was added over 50 min. The solution was then stirred at -72.5 °C for 15 min. The solution was then transferred to a separating funnel containing 1M HCl (53 mL). The organic layer was then extracted, using some sat. NaCl to aid separation. The aqueous layer was controlled to be pH 1 (if not used HCl 1 M). ((S,S)-DIPT) (5.87 mL, 28.08 mmol) in Et_2O (9.5 mL) was then added to the acidic solution, which was then shaken vigorously for 10 min. The phases were separated, and the aqueous phase was extracted with ether (3 x). The combined organic layers were dried over anhydrous $MgSO_4$ for two h and concentrated under reduced pressure before drying under vacuum. A crude NMR was taken and was indicative of a 2:1 DIPT: product ratio. The reaction yielded 2.5 g of **61** (19%) in 7.5 g of sticky clear oily residue. This residue was dissolved in toluene (24 mL) and stored in the freezer under argon.*Full characterisation was not made as the reagent is not pure and is highly sensitive to water and air.

Synthesis of compound 62

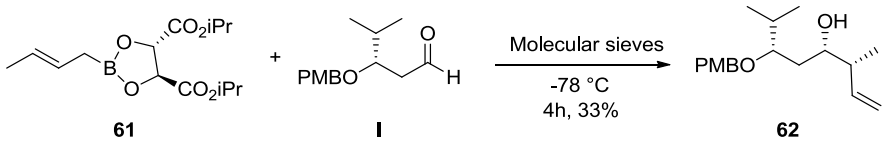

Molecular sieves (3 mg) were added to dry toluene (0.3 mL). Crude **61** in toluene was added (0.3, 0.06 mmol) and the solution was cooled to -78 °C. **I** (15 mg, 0.06 mmol) was dissolved in toluene (0.01 mL) and added dropwise to the solution. The solution was stirred for 4 h at -78 °C. The reaction was quenched with 1 M NaOH. The aqueous layer was extracted with ether (3 x). The combined organic layers were washed with $NaHCO_3$ (2 x) and brine, dried over anhydrous $MgSO_4$ and concentrated under reduced pressure. The crude material was purified by silica gel chromatography (hexane/EtOAc 10:1) to yield **62** as a slightly yellow oily residue (6 mg, 33%).

TLC: Rf= 0.30 (Hex/AcOEt 10:1).

^{1}H-NMR: (400 MHz, $CDCl_3$) δ 7.35 – 7.20 (m, 2H), 6.97 – 6.78 (m, 2H), 5.88-5.69 (m, 1H), 5.10 (d, *J* = 0.7 Hz, 1H), 5.08 – 5.02 (m, 1H), 4.49 (d, *J* = 2 Hz, 2H), 3.80 (s, 3H), 3.72-.66 (m, 1H), 3.51 – 3.38 (m, 1H), 2.43 (bs, 1H), 2.22-2.11 (m, 1H), 2.03-1.92 (m, 1H), 1.62 – 1.43 (m, 2H), 1.00 (d, *J* = 6.6 Hz, 3H), 0.95 (d, *J* = 6.8 Hz, 3H), 0.89 (d, *J* = 6.8 Hz, 3H).

^{13}C-NMR (101 MHz, $CDCl_3$): δ 159.2, 140.7, 130.8, 129.5, 120.0, 115.6, 113.8, 81.6, 71.8, 71.5, 55.2, 44.4, 33.6, 30.6, 19.1, 17.8, 16.0.

IR (film) : $\tilde{\nu}$= 3673, 2958, 2917, 1613, 1514, 1464, 1396, 1240, 1175, 1065, 1035, 909, 818cm-1.

HRMS (ESI +): m/z calculated for $C_{18}H_{28}O_3$ $[M + Na]^+$ 315.1931, measured: 315.1933. $[a]_D^{20}$ = -23.71 (c 0.165, $CHCl_3$).

Synthesis of compound E

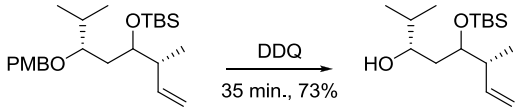

H **E**

To a solution of **H** in CH_2Cl_2 (1.6 mL) and 0.16 mL pH 7.2 buffer solution was added DDQ (16 mg, 0.07 mmol). The reaction mixture was stirred at 0°C for 35 min, when the reaction was quenched with saturated aqueous $NaHCO_3$ (1 mL). The aqueous layer was extracted with CH_2Cl_2 (3×2 mL) and the combined organic layers washed with water (2 mL). The organic layer was dried ($MgSO_4$), filtered and concentrated in vacuo. Purification of the residue by flash chromatography (hexane/AcOEt 9:1) afforded 10 mg (73 %) of **E** as a colorless oil. Full characterization was not made as the product was used immediately for the next reaction.

TLC: Rf = 0.54 (AcOEt/hexane 9:1)

4.6.3. Pironetin-dumetorine hybrid compounds

Synthesis of compound 65

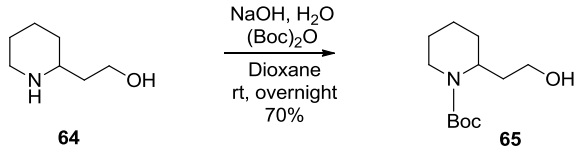

Racemic-2-(piperidin-2-yl)ethanol (2g, 15.4 mmol) was dissolved in dioxane (30 mL) at room temperature and then NaOH (15 mL) and H_2O (15 mL) were added. $(Boc)_2O$ (3.36 g, 15.4 mmol) was added to the solution cooled at 0°C. Next the solution was acidified with $KHSO_4$ until pH 2 and then extracted with EtOAc. The organic layer was washed with water, dried over anhydrous Na_2SO_4, and filtered. The solvent was evaporated under vacuum, and the residue was purified by column chromatography on silica gel (hexane /EtOAc, 7:3) to give **65** (2.5 g) as a colourless oil (70% overall yield).

^{1}H-NMR (400 MHz, $CDCl_3$,): δ 4.72-4.60 (m, 1H), 3.96-3.91 (d, *J*= 13.72 Hz, 1H), 3.62-3.56 (m, 1H), 3.39-3.31 (m, 1H), 2.65 (t, *J* = 12.83 Hz, 1H), 1.88 (d, *J* = 12.53 Hz, 1H), 1.74-1.32 (m, 16H) ppm.

^{13}C-NMR (100 MHz, $CDCl_3$): δ 156.5, 80.0, 58.5, 45.5, 39.4, 32.2, 29.1, 28.4, 25.5, 19.2 ppm.

Synthesis of compounds 66

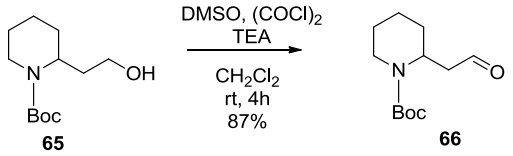

$(COCl)_2$ (0.45 mL, 5.3 mmol) was dissolved under nitrogen atmosphere in anhydrous CH_2Cl_2 (21.8 mL) the cooled at -78 °C. A solution of DMSO (0.93 mL, 13 mmol) in anhydrous CH_2Cl_2 (5.2 mL) was then added dropwise to the reaction mixture. The solution was stirred for 10 minutes at -78 °C and then a solution of **65** (1 g, 4.4 mmol) in anhydrous CH_2Cl_2 (10.4 mL), was added to the mixture. The solution was stirred for 2 hours and then TEA (7.3 mL, 22 mmol) was added. The reaction was left overnight at room temperature, then quenched with H_2O (35 mL) and HCl 1 N (18 mL) and extracted with CH_2Cl_2. The organic layer was washed with brine, dried over anhydrous Na_2SO_4, and filtered.

The solvent was evaporated under vacuum, and the residue was purified by column chromatography on silica gel (hexane /EtOAc, 7:3) to give **66** (0.860 g) as a colourless oil (87% overall yield).

^{1}H-NMR (400 MHz, $CDCl_3$,): δ 9.71 (s, 1H), 4,78 (br s, *J*=5.8 Hz, 1H), 3.98 (d, *J*=13.4 Hz,1H), 2.76-2.67 (m, 2H), 2.55-2.49 (m, 1H), 1.71-1.41 (m, 6H), 1.42 (s, 9H) ppm.

^{13}C-NMR (100 MHz, $CDCl_3$): δ 199.1, 152.9, 78.2, 44.2, 42.8, 37.5, 27.9, 27.1, 23.2, 16.8 ppm.

General procedure for synthesis of compounds 70a-73a

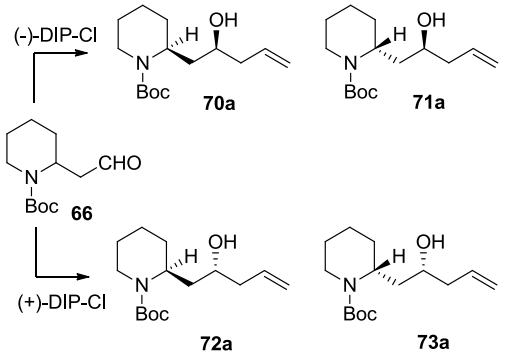

Allylmagnesium bromide (commercial 1M solution in Et_2O, 2.86 mL, 2.86 mmol) was added dropwise under nitrogen atmosphere to a solution of (-)-DIP-Cl (1.06 g, 3.3 mmol) in dry THF (13.5 mL) at -78°C. The reaction mixture was allowed to warm to 0 °C and stirred at that temperature for 1 h. The solution was then allowed to stand until magnesium chloride precipitated. The supernatant solution was then carefully transferred to another flask. After cooling this flask at −78°C, a solution of aldehyde **66** (0.500 g, 2.20 mmol) in dry THF (6.5 mL) was added dropwise. The resulting solution was further stirred at the same temperature for 1 h and then 16 h at room temperature. The reaction was quenched with NaH_2PO_4 buffer solution at pH 7 (13.5 mL), MeOH (13.5 mL) and 30% H_2O_2 (6.7 mL). After stirring for 30 minutes, the mixture was washed with saturated aqueous $NaHCO_3$ and extracted with Et_2O. The combined organic phases were dried over anhydrous Na_2SO_4, and filtered. The solvent was evaporated under vacuum, and the residue was purified by column chromatography on silica gel (hexane /EtOAc, 8:2) to give **70a** (0.311 g) and **71a** (0.234 g) as a yellow oil (51% overall yield). In order to obtain the other two diastereoisomer **72a** and **73a** the reaction is performed in the same way except for the use of (+)-DIP-Cl.

70a: **^{1}H-NMR** (400 MHz, $CDCl_3$,): δ 1.35-1.59 (m, 6H), 1.42 (s, 9H,), 1.73-1.76 (m, 1H), 2.01 (dt, *J* = 12.5, 1.8 Hz, 1H), 2.16-2.23 (m, 1H), 2.27-2.33 (m, 1H), 2.66 (dt, *J* = 12.7, 2.0 Hz, 1H), 3.39 (br s, 1H), 3.95 (br s, 1H), 4.47 (br s, 1H), 5.05 (d, *J* = 9.7 Hz, 1H), 5.08 (d, *J* = 17.4 Hz, 1H), 5.81-5.91 (m, 1H) ppm.

^{13}C-NMR (100 MHz, $CDCl_3$): δ = 19.4, 25.3, 28.6, 29.2 , 36.9, 39.3, 41.1, 46.2, 67.1, 80.2, 116.6, 135.5, 167.1 ppm.

IR: (neat) = 1674 cm^{-1}. $[\alpha]_D^{20}$= -33 (*c* 1, $CHCl_3$). **ESIMS** *m/z* $[M+H^+]^+$ calcd for $C_{15}H_{28}NO_3$: 270.21; Found: 270.72.

73a: $[\alpha]_D^{20}$= +35 (c 0.8, $CHCl_3$). **ESIMS** *m/z* $[M+H^+]^+$ calcd for C15H28NO3: 270.21; Found: 270.56.

71a: **^{1}H-NMR** (400 MHz, $CDCl_3$): δ 1.35-1.59 (m, 6H), 1.42 (s, 9H), 1.77-1.82 (m, 1H), 2.14-2.21 (m, 1H), 2.27-2.32 (m, 1H), 2.79 (dt, *J* = 12.8, 0.2 Hz, 1H), 3.65 (tt, *J* = 7.5, 2.4 Hz, 1H), 3.88-3.93 (m, 1H), 4.32 (br s, 1H), 5.08 (d, *J* = 9.8 Hz, 1H), 5.10 (d, *J* = 17.3 Hz, 1H), 5.75-5.85 (m, 1H) ppm.

^{13}C-NMR (100 MHz, $CDCl_3$): δ 18.9 , 25.5, 28.4, 28.9, 37.0, 38.8, 41.8, 48.0, 71.3, 79.6, 117.4, 135.06, 155.29 ppm.

IR: (neat) = 1674 cm^{-1} $[\alpha]_D^{20}$ = +15 (*c* 0.9, $CHCl_3$). **ESIMS** *m/z* $[M+H^+]^+$ calcd for $C_{15}H_{28}NO_3$: 270.21; Found: 270.78.

72a: $[\alpha]_D^{20}$= -13.8 (*c* 13.3, $CHCl_3$). **ESIMS** *m/z* $[M+H^+]^+$ calcd for $C_{15}H_{28}NO_3$: 269.20; Found: 269.84.

General procedure for synthesis of compounds70b-73b

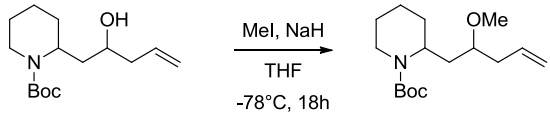

70a-73a **70b-73b**

Alcohol **70a** (0.319 g, 1.18 mmol) was dissolved in anhydrous THF (7 mL) and the solution was added dropwise to a suspensionof sodium hydride (0.095 g, 3.90 mmol) in dry THF (3 mL) cooled at -78°C and it was stirred for 1 h. Then methyl iodide (0.3 mL, 4.70 mmol) was added and the reaction mixture was stirred 1 h at -78 °C and 16 h at room temperature. The mixture was quenched with cold water (10 mL) and the aqueous layer was extracted with Et_2O. The organic layer was dried with Na_2SO_4 and the solvent was removed under vacuum. The residue was purified by column chromatography on silica gel (hexane/EtOAc, 8:2) to give **70b** (0.235g,74%) as yellow oil. In order to obtain the other compounds **71b**, **72b** and **73b** the reaction was performed in the same way.

70b:^{1}H-NMR (400 MHz, $CDCl_3$): δ 1.37-1.64 (m, 6H), 1.46 (s, 9H), 1.83-1.90 (m, 1H), 2.21-2.33 (m, 2H), 2.70 (t, *J* = 13.2 Hz, 1H), 3.11-3.17 (m, 1H), 3.35 (s, 3H), 3.97 (br s, 1H), 4.44 (br s, 1H), 5.08 (d, *J* = 17.1 Hz, 1H), 5.10 (d, *J* = 9.2 Hz, 1H), 5.73-5.83 (m, 1H) ppm.

^{13}C-NMR (100 MHz, $CDCl_3$): δ 19.4, 25.7, 25.7, 28.5, 29.5, 34.5, 37.7, 47.6, 56.9, 77.9, 79.1, 117.3, 134.5, 155.1 ppm.

IR: (neat) = 1677 cm^{-1}.$[\alpha]_D^{20}$= -36 (*c* 3.64, $CHCl_3$). **ESIMS** *m/z* $[M+H^+]^+$ calcd for $C_{16}H_{30}NO_3$: 284.22; Found: 284.45.

73b:$[\alpha]_D^{20}$= +33 (*c* 0.5, $CHCl_3$). **ESIMS** *m/z* $[M+H^+]^+$ calcd for $C_{16}H_{30}NO_3$: 284.21; Found: 284.55.

71b:^{1}H-NMR (400 MHz, $CDCl_3$): δ 1.33-1.59 (m, 6H,$(CH_2)_3$), 1.43 (s, 9H, Boc), 1.88-1.96 (m, 1H), 2.28 (dddd, *J* = 12.3, 12.3, 6.4, 1.2 Hz,1H), 2.35 (dddd, *J* = 12.3, 12.3, 6.4, 1.2 Hz), 2.78 (t, *J* = 13,3 Hz, 1H), 3.14-3.19 (m, 1H), 3.29 (s, 3H), 3.96 (m, 1H), 4.33 (br s, 1H), 5.03-5.09 (m, *2*H), 5.75-5.84 (m, 1H) ppm.

^{13}C-NMR (100 MHz, $CDCl_3$): δ 23.6, 24.9, 30.2, 33.7, 35.1, 39.2, 44.7, 47.9, 53.9, 73.9, 80.8, 118.5, 132.4, 153.9 ppm.

IR: (neat) = 1677 cm^{-1}.$[\alpha]_D^{20}$= +23.4 (*c* 2.7, $CHCl_3$). **ESIMS** *m/z* $[M+H^+]^+$ calcd for $C_{16}H_{30}NO_3$: 284.21; Found: 284.78.

72b: $[\alpha]_D^{20}$= -19 (*c* 0.9 $CHCl_3$). **ESIMS** *m/z* $[M+H^+]^+$ calcd for $C_{16}H_{30}NO_3$: 284.22; Found: 284.89.

General procedure for synthesis of compounds 74-77

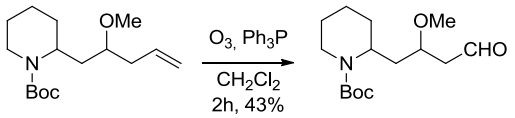

70b-73b **74-77**

Olefin **70b** (0.470 g, 1.66 mmol) was dissolved in dry CH_2Cl_2 (19 mL) and cooled to −78°C. A stream of ozone-oxygen was bubbled through the solution until persistence of the bluish color. Dry N_2 was then bubbled through the solution for 10 min at the same temperature. After addition of PPh_3 (0.870 g, 3.32 mmol), the reaction mixture was stirred for 2 h at room temperature. After the completion of the reaction the solvent was removed under vacuum. The residue was purified by column chromatography on silica gel (hexane/EtOAc, 7:3) to give **74** (0.202 g,43%) as orange oil. In order to obtain the other compounds **75**, **76** and **77** the reaction was performed in the same way.

74:^{1}H-NMR (400 MHz, $CDCl_3$): δ 1.37-1.65 (m, 6H), 1.46 (s, 9H), 1.88 (ddd, *J* = 14.0, 9.3, 4.4 Hz, 1H), 2.63 (ddd, *J* = 6.3, 4.3, 2.1 Hz, 2H), 2.75 (t, *J* = 12.7 Hz, 1H), 3.36 (s, 3H), 3.59-3.65 (m, 1H), 3.98 (br s, 1H), 4.43 (br s, 1H), 9.81 (t, *J* = 2.1 Hz, 1H) ppm.

^{13}C-NMR (100 MHz, $CDCl_3$): δ 19.1, 25.6, 28.5, 29.0, 33.6, 38.8, 48.0, 56.6, 74.4, 76.2, 79.5, 155.0, 201.4 ppm.

IR: (neat) = 1679, 1719 cm^{-1}.$[\alpha]_D^{20}$= -21.3 (*c* 3.45, $CHCl_3$). **ESIMS** *m/z* $[M+H^+]^+$ calcd for $C_{15}H_{28}NO_4$: 286.20; Found: 286.57.

77: $[\alpha]_D^{20}$= +19.1 (*c* 0.5, $CHCl_3$). **ESIMS** *m/z* $[M+H^+]^+$ calcd for $C_{15}H_{28}NO_4$: 286.20; Found: 286.97.

75: ^{1}H-NMR (400 MHz, $CDCl_3$): δ 1.37-1.66 (m, 6H), 1.44 (s, 9H), 2.09-2.19 (m, 1H), 2.59 (ddd, *J* = 16.4, 7.5, 2.8 Hz,1H), 2.75-2.82 (m, 2H), 3.32 (s, 3H), 3.64 (ddd, *J* = 12.4, 7.7, 5.1 Hz, 1H), 4.00-4.02 (m, 1H), 4.34 (br s, 1H), 9.78 (s, 1H) ppm.

^{13}C-NMR (100 MHz, $CDCl_3$): δ 19.2, 25.7 , 28.6, 29.1, 33.7, 38.8, 48.0, 56.8, 60.5, 74.3, 79.7, 155.0, 201.6 ppm.

IR: (neat) = 1678, 1719 cm^{-1}.$[\alpha]_D^{20}$= 28.8 (*c* 2.65, $CHCl_3$). **ESIMS** *m/z* $[M+H^+]^+$ calcd for $C_{15}H_{28}NO_4$: 286.20; Found: 286.77.

76:$[\alpha]_D^{20}$= -26.54 (*c* 0.5, $CHCl_3$). **ESIMS** *m/z* $[M+H^+]^+$ calcd for $C_{15}H_{28}NO_4$: 286.20 ; Found: 286.79.

General procedure for synthesis of compounds 78a-85a

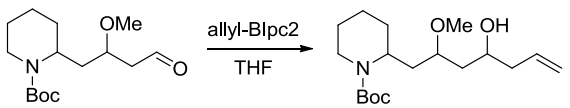

74-77 **78a-85a**

Allylmagnesium bromide (commercial 1M solution in Et_2O, 0.87 mL, 0.87 mmol) was added dropwise under nitrogen atmosphere to a solution of (-)-DIP-Cl (0.323 g, 1.01 mmol) in dry THF (5 mL) at -78°C. The reaction mixture was allowed to warm to 0 °C and stirred at that temperature for 1 h. The solution was then allowed to stand until magnesium chloride precipitated. The supernatant solution was then carefully transferred to another flask. After cooling this flask at −78°C, a solution of aldehyde **74** (0.190 g, 0.67 mmol) in dry THF (2.5 mL) was added dropwise. The resulting solution was further stirred at the same temperature for 1 h and then 16 h at room temperature. The reaction was quenched with NaH_2PO_4 buffer solution at pH 7 (5.1 mL), MeOH (5.1 mL) and 30% H_2O_2 (2.5 mL). After stirring for 30 minutes, the mixture was washed with saturated aqueous $NaHCO_3$ and extracted with Et_2O. The combined organic phases were dried over anhydrous Na_2SO_4, and filtered. The solvent was evaporated under vacuum, and the residue was purified by column chromatography on silica gel (Hexane /EtOAc, 7:3) to give **78a** (0.179 g, 82%) as a yellow oil. In order to obtain the other diastereoisomer the reaction is performed in the same way except for the use of (+)-DIP-Cl.

78a: ^{1}H-NMR (400 MHz, $CDCl_3$): δ 1.34-1.63 (m, 8H), 1.45 (s, 9H), 1.74-1.76 (m, 2H), 2.22 (t, J = 6.6 Hz, 2H), 2.72-2.78 (m, 1H), 3.35-3.41 (m, 1H), 3.36 (s, 3H), 3.78-3.84 (m, 1H),3.95 (br s, 1H), 4.33 (br s, 1H), 5.07-5.12 (m, 2H), 5.83 (ddt, J = 17.5, 10.5, 7.1 Hz, 1H) ppm.

^{13}C-NMR (100 MHz, $CDCl_3$): δ 19.3, 25.7, 28.4, 28.6, 34.5, 38.9, 40.7, 42.4, 48.0 , 56.5, 68.31, 70.3, 79.6, 117.7, 135.0, 155.1 ppm.

IR: (neat) = 1687 cm^{-1}.$[\alpha]_D^{20}$= - 21.4 (*c* 0.7, $CHCl_3$). **ESIMS** *m/z* $[M+H^+]^+$ calcd for $C_{18}H_{34}NO_4$: 328.25; Found: 328.67.

85a: $[\alpha]_D^{20}$= + 24.3 (*c* 0.1, $CHCl_3$). **ESIMS** *m/z* $[M+H^+]^+$ calcd for $C_{18}H_{34}NO_4$: 328.25; Found: 328.43.

79a:^{1}H-NMR (400 MHz, $CDCl_3$): δ 1.37-1.66 (m, 8H), 1.45 (s, 9H), 1.77-1.84 (m, 1H), 2.14-2.19 (m, 1H), 2.23 (t, *J* = 6.1 Hz, 2H), 2.80 (t, *J* = 13.2 Hz,1H), 3.29-3.40 (m, 1H), 3.34 (s, 3H), 3.81-3.87 (m, 1H),4.01 (br s, 1H), 4.30 (br s, 1H), 5.07-5.12 (m, 2H), 5.82-5.97 (m, 1H) ppm.

^{13}C-NMR (100 MHz, $CDCl_3$): δ 19.2, 25.7, 28.6, 29.5, 33.7, 39.1, 41.0, 42.2, 47.3, 56.2, 68.3, 71.2, 79.8, 117.4, 135.1, 155.3 ppm.

IR: (neat) = 1687 cm^{-1}.$[\alpha]_D^{20}$ = -9.2 (*c* 0.3, $CHCl_3$). **ESIMS** *m/z* $[M+H^+]^+$ calcd for $C_{18}H_{34}NO_4$: 328.25; Found: 328.15.

84a : $[\alpha]_D^{20}$= +10.5 (*c* 0.04, $CHCl_3$). **ESIMS** *m/z* $[M+H^+]^+$ calcd for $C_{18}H_{34}NO_4$: 328.25; Found: 328.12.

80a:^{1}H-NMR (400 MHz, $CDCl_3$): δ 1.33-1.66 (m, 8H), 1.45 (s, 9H), 1.76-1.84 (m, 1H), 2.15-2.19 (m, 1H), 2.23-2.25 (m, 2H), 2.80 (t, *J* = 13.8 Hz,1H), 3.30-3.39 (m, 1H), 3.33 (s, 3H), 3.81-3.85 (m, 1H),4.01 (br s, 1H), 4.30 (br s, 1H), 5.06-5.13 (m, 2H), 5.87 (ddt, *J* = 17.3, 10.2, 7.1 Hz, 1H) ppm.

^{13}C-NMR (100 MHz, $CDCl_3$): δ 19.3, 25.8, 28.6, 29.4, 34.4, 38.9, 40.8, 42.3, 47.8, 57.1, 68.1, 71.05, 79.7, 117.5, 135.1, 155.0 ppm.

IR: (neat) = 1687 cm^{-1}.$[\alpha]_D^{20}$= +17.8 (*c* 0.1, $CHCl_3$). **ESIMS** *m/z* $[M+H^+]^+$ calcd for $C_{18}H_{34}NO_4$: 328.25; Found: 328.24.

83a: $[\alpha]_D^{20}$= -15.7 (*c* 0.07, $CHCl_3$). **ESIMS** *m/z* $[M+H^+]^+$ calcd for $C_{18}H_{34}NO_4$: 328.25; Found: 328.18.

81a:^{1}H-NMR (400 MHz, $CDCl_3$): δ 1.31-1.66 (m, 15H),1.69- 1.84 (m, 3H), 2.16-2.29 (m, 2H), 2.64-2.82 (m, 1H), 3.33-3.47 (m, 5H), 3.89-4.02 (m, 3H), 4.27-4.42 (s, 1H), 5.04-5.15 (m, 2H), 5.75-5.91 (m, 1H) ppm.

^{13}C-NMR (100 MHz, $CDCl_3$): δ 19.3, 25.8, 28.7, 29.3, 34.2, 38.9, 40.6, 42.5, 48.01, 57.3, 68.2, 70.3, 79.5, 117.7, 135.0, 155.1 ppm.

$[\alpha]_D^{20}$ = +22.4 (c 1.4, $CHCl_3$). **ESIMS** m/z $[M+H^+]^+$ calcd for $C_{18}H_{34}NO_4$: 328.25; Found: 328.45.

82a: $[\alpha]_D^{20}$= -21.6 (c 0.02, $CHCl_3$). **ESIMS** m/z $[M+H^+]^+$ calcd for $C_{18}H_{34}NO_4$: 328.25; Found: 328.29.

General procedure for synthesis of compounds 78b-85b

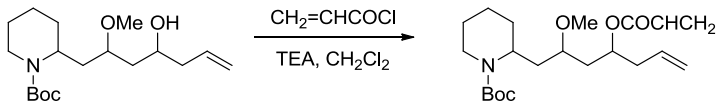

78a-85a **78b-85b**

Acryloyl chloride (014 mL, 1.71 mmol) and TEA (0.48 mL, 3.42 mmol) were added sequentially to a cooled solution (0°C) of compound **78a** (0.140 g, 0.42 mmol) dissolved in dry CH_2Cl_2 (0.73 mL). The reaction was stirred for 4 h at room temperature, then it was quenched with water (3 mL) and satd. aqueos NaCl (3 mL). the aqueous layer was extracted with CH_2Cl_2. The organic layer were dried with Na_2SO_4 and filtered. The solvent was evaporated under vacuum, and the residue was purified by column chromatography on silica gel (Hexane /EtOAc, 6:4) to give **78b** (0.118 g, 72%) as yellow oil.

78b: ^{1}**H-NMR** (400 MHz, $CDCl_3$): δ 0.86-0.97 (m, 2H), 1.45 (s, 9H), 1.51-1.72 (m, 6H), 1.88-1.98 (m, 2H), 2.33-2.45 (m, 2H), 2.70 (t, J = 13.6 Hz, 1H), 3.09-3.15 (m, 1H), 3.30 (s, 3H), 3.95 (br s, 1H), 4.44 (br s, 1H), 5.06-5.12 (m, 3H), 5.72-5.82 (m, 1H), 5.82 (dd, J = 10.6, 1.5 Hz, 1H), 6.10 (dd, J = 17.3, 10.4 Hz, 1H), 6.39 (dd, J = 17.3, 1.5 Hz, 1H) ppm.

^{13}**C-NMR** (100 MHz, $CDCl_3$): δ 19.2, 25.7, 28.5, 29.6, 34.6, 37.2, 38.7, 39.1, 47.0, 56.4, 70.6, 75.4, 78.9, 118.1, 128.6, 130.6, 133.3, 154.4, 165.6 ppm.

IR: (neat) = 1677, 1719 cm^{-1}.$[\alpha]_D^{20}$= -7.66 (*c* 0.7, $CHCl_3$). **ESIMS** *m/z* $[M+H^+]^+$ calcd for $C_{21}H_{36}NO_5$: 382.26; Found: 382.64.

85b: $[\alpha]_D^{20}$= +9.1 (*c* 0.03, $CHCl_3$). **ESIMS** *m/z* $[M+H^+]^+$ calcd for $C_{21}H_{36}NO_5$: 382.26; Found: 382.55.

79b: ^{1}**H-NMR** (400 MHz, $CDCl_3$): δ 0.82-0.94 (m, 2H), 1.35-1.59 (m, 6H), 1.45 (s, 9H), 1.86-1.97 (m, 2H), 2.30-2.44 (m, 2H), 2.79 (t, 1H, J = 12.6 Hz), 3.21 (tt, 1H, J = 12.3, 6.2 Hz), 3.26 (s, 3H), 3.97 (br s, 1H), 4.35 (br s, 1H), 5.05-5.10 (m, 2H), 5.12-5.18 (m,

1H), 5.72-5.82 (m, 2H), 5.79 (dd, *J* = 10.4, 1.5 Hz, 1H), 6.10 (dd, *J* = 17.3, 10.4 Hz, 1H), 6.38 (dd, *J* = 17.3, 1.5 Hz, 1H) ppm.

^{13}C-NMR (100 MHz, $CDCl_3$): δ 19.0, 25.6, 28.5, 28.7, 29.3, 33.5, 37.5, 39.3, 47.3, 56.8, 70.8, 75.7, 79.1, 118.2, 128.4, 130.5, 133.4, 154.7, 165.8 ppm.

IR: (neat) = 1677, 1719 cm^{-1}.$[\alpha]_D^{20}$= +20.4 (*c* 0.5, $CHCl_3$). **ESIMS** *m/z* $[M+H^+]^+$ calcd for $C_{21}H_{36}NO_5$: 382.26; Found: 382.87.

84b: $[\alpha]_D^{20}$= -15.4 (*c* 0.005, $CHCl_3$). **ESIMS** *m/z* $[M+H^+]^+$ calcd for $C_{21}H_{36}NO_5$: 382.26; Found: 382.18.

80b:^{1}H-NMR (400 MHz, $CDCl_3$): δ 0.89-0.94 (m, 2H), 1.46 (s, 9H), 1.44-2.00 (m, 8H), 2.30-2.45 (m, 2H), 2.76-2.82 (m, 1H), 3.21 (tt, *J* = 12.3, 6.2 Hz, 1H), 3.26 (s, 3H), 3.97 (br s, 1H), 4.35 (br s, 1H), 5.05-5.10 (m, 2H), 5.12-5.18 (m, 1H), 5.71-5.82 (m, 2H), 6.10 (dd, *J* = 17.3, 10.4 Hz, 1H), 6.39 (ddd, *J* = 17.3, 2.9, 1.5 Hz, 1H) ppm.

^{13}C-NMR (100 MHz, $CDCl_3$): δ 18.9, 25.6, 28.6, 28.9, 33.2, 37.0, 38.5, 39.0, 47.4, 55.7, 70.9, 75.3, 79.2, 117.9, 128.8, 130.4, 133.5, 154.8, 165.6 ppm.

IR: (neat) = 1677, 1719 cm^{-1}. $[\alpha]_D^{20}$= +12.3 (*c* 0.5, $CHCl_3$). **ESIMS** *m/z* $[M+H^+]^+$ calcd for $C_{21}H_{36}NO_5$: 382.26; Found: 382.54.

83b: $[\alpha]_D^{20}$= -16.5 (*c* 0.002, $CHCl_3$). **ESIMS** *m/z* $[M+H^+]^+$ calcd for $C_{21}H_{36}NO_5$: 382.26; Found: 382.25.

81b:^{1}H-NMR (300 MHz, $CDCl_3$): δ 1.20-1.65 (m, 19H),1.65-1.86 (m, 1H), 2.29–2.44 (m, 2H), 2.66-2.81 (m, 1H), 3.05-3.17 (m, 1H), 3.31 (s, 3H), 3.89-4.03 (m, 1H), 4.26-4.50 (m, 1H), 5.01-5.28 (m, 2H), 5.69-5.85 (m, 2H), 6.03-6.17 (m, 1H), 6.33-6.45 (m, 1H) ppm.

^{13}C-NMR (100 MHz, $CDCl_3$): δ 18.9, 25.5, 28.4, 28.7, 29.5, 34.7, 38.6, 39.1, 47.6, 57.1, 70.6, 75.6, 79.1, 117.9, 128.6, 130.4, 133.1, 165.5 ppm.

$[\alpha]_D^{20}$ = +11.4 (*c* 0.8, $CHCl_3$). **ESIMS** *m/z* $[M+H^+]^+$ calcd for $C_{21}H_{36}NO_5$: 382.26; Found: 382.91.

82b: $[\alpha]_D^{20}$= -9.4 (*c* 0.01, $CHCl_3$). **ESIMS** *m/z* $[M+H^+]^+$ calcd for $C_{21}H_{36}NO_5$: 382.26; Found: 382.59.

General procedure for synthesis of compounds 86a-93a

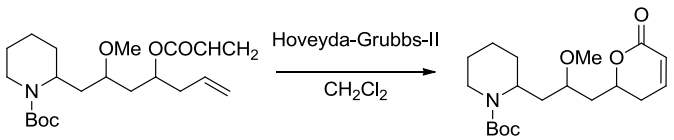

78-85 86a-93a

A solution of Hoveyda-Grubbs-II catalyst (0.014 g, 0.02 mmol) in dry CH_2Cl_2 (3.2 mL) was added dropwise to a solution of compound **78b** (0.085 g, 0.22 mmol) dissolved in dry CH_2Cl_2 (9.4 mL). The reaction was stirred for 3.5 h at room temperature, then the solvent was removed under vacuum. The residue was purified by column chromatography on silica gel (Hexane /EtOAc, 6:4) to give **86a** (0.059 g, 75%)as dark oil.

86a:^{1}H-NMR (400 MHz, $CDCl_3$): δ 1.38-1.71 (m, 6H),1.46 (s, 9H), 1.84-1.92 (m, 2H), 1.99-2.07 (m, 2H), 2.31-2.41 (m, 2H), 2.73 (t, *J* = 13.3 Hz, 1H), 3.32 (s, 3H), 3.32-3.37(m, 1H), 3.96 (br s, 1H), 4.43 (br s, 1H), 4.59 (dt, *J* = 11.4, 6.2 Hz, 1H), 6.02 (d, *J* = 9.9 Hz, 1H), 6.88 (m, 1H) ppm.

^{13}C-NMR (100 MHz, $CDCl_3$): δ 19.6, 25.8, 28.7, 28.9, 29.94, 30.2, 34.6, 40.6, 56.6, 58.0, 74.9, 75.5, 79.7, 121.7, 146.3, 155.3, 164.7 ppm.

IR: (neat) = 1677, 1721 cm^{-1}.$[\alpha]_D^{20}$ = -50.2 (*c* 0.6, $CHCl_3$). **ESIMS** *m/z* $[M+H^+]^+$ calcd for $C_{19}H_{32}NO_5$: 354.23; Found: 354.78.

93a: $[\alpha]_D^{20}$= +47.6 (*c* 0.002, $CHCl_3$). **ESIMS** *m/z* $[M+H^+]^+$ calcd for $C_{19}H_{32}NO_5$: 354.23; Found: 354.65.

87a:^{1}H-NMR (400 MHz, $CDCl_3$): δ 1.36-1.58 (m, 7H),1.44 (s, 9H), 1.91-2.15 (m, 3H), 2.32-2.38 (m, 2H), 2.76-2.82 (m, 1H), 3.24-3.31(m, 1H), 3.28 (s, 3H), 3.96 (br s, 1H), 4.35 (br s, 1H), 4.55-4.62 (m, 1H), 6.00 (d, *J* = 9.8 Hz, 1H), 6.86 (ddd, *J* = 9.2, 4.5 Hz, 1H)ppm.

^{13}C-NMR (100 MHz, $CDCl_3$): δ 19.3 (t), 25.7 (t), 28.7 (t), 29.5 (q), 29.9 (t), 30.2(t), 34.4 (t), 40.7 (t), 54.0 (q), 57.7 (d), 74.8 (d), 75.0 (d), 79.5 (s), 121.6 (d), 145.2 (d), 155.1 (s), 164.4 (s)ppm.

IR: (neat) = 1677, 1721 cm^{-1}. $[\alpha]_D^{20}$= -15.8 (*c* 0.7, $CHCl_3$). **ESIMS** *m/z* $[M+H^+]^+$ calcd for $C_{19}H_{32}NO_5$: 354.23; Found: 354.24.

92a: $[\alpha]_D^{20}$= +11.1 (*c* 0.023, $CHCl_3$). **ESIMS** *m/z* $[M+H^+]^+$ calcd for $C_{19}H_{32}NO_5$: 354.23; Found: 354.72.

88a:^{1}H-NMR (400 MHz, $CDCl_3$): δ 1.37-1.59 (m, 7H),1.46 (s, 9H), 1.92-2.17 (m, 3H), 2.32-2.40 (m, 2H), 2.74-2.83 (m, 1H), 3.23-3.27(m, 1H), 3.29 (s, 3H), 3.98 (br s, 1H), 4.36 (br s, 1H), 4.61 (td, *J* = 15.4, 6.5 Hz, 1H), 6.01 (d, *J* = 9.8 Hz, 1H), 6.87 (td, *J* = 9.2, 4.2 Hz, 1H) ppm.

^{13}C-NMR (100 MHz, $CDCl_3$): δ 19.1 (t), 25.6 (t), 28.5 (q), 28.7 (t), 28.9 (t), 29.4 (t), 33.0 (t), 38.0 (t), 47.5 (d), 55.9 (q), 75.2 (d), 75.4 (d), 79.3 (s), 121.4 (d), 145.0 (d), 155.0 (s), 164.4 (s) ppm.

IR: (neat) = 1677, 1721 cm^{-1}. $[\alpha]_D^{20}$ = -15.8 (*c* 0.4, $CHCl_3$). **ESIMS** *m/z* $[M+H^+]^+$ calcd for $C_{19}H_{32}NO_5$: 354.23; Found: 354.19.

91a: $[\alpha]_D^{20}$= +13.3 (*c* 0.001, $CHCl_3$). **ESIMS** *m/z* $[M+H^+]^+$ calcd for $C_{19}H_{32}NO_5$: 354.23; Found: 354.47.

89a:^{1}H NMR (400 MHz, $CDCl_3$): δ 1.19-1.77 (m, 17H),1.78-1.94 (m, 2H), 1.95-2.11 (m, 1H), 2.29-2.48 (m, 2H), 2.67-2.83 (m, 1H), 3.38 (s, 3H), 3.40-3.52 (m, 1H), 3.88-4.05 (m, 1H), 4.56-4.72 (m, 1H), 6.02 (dt, 1H, *J*= 9.8, 1.6 Hz), 6.84-6.92 (m, 1H) ppm.

^{13}CNMR (100 MHz, $CDCl_3$): δ19.2, 25.7, 28.6, 28.7, 29.8, 30.2, 34.5, 40.7, 56.6, 57.7, 74.8, 75.0, 79.5, 121.6, 145.0, 155.0, 164.4 ppm.

$[\alpha]_D^{20}$ = +6.8 (*c* 0. 038, $CHCl_3$). **ESIMS** *m/z* $[M+H^+]^+$ calcd for $C_{19}H_{32}NO_5$: 354.23; Found: 354.17.

90a: $[\alpha]_D^{20}$= -4.7 (*c* 0.006, $CHCl_3$). **ESIMS** *m/z* $[M+H^+]^+$ calcd for $C_{19}H_{32}NO_5$: 354.23; Found: 354.69.

General procedure for synthesis of compounds 86b-93b

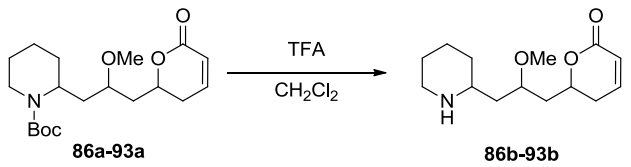

86a-93a **86b-93b**

To a stirred solution of compound **86a** (0.352 g, 1 mmol) in CH_2Cl_2 (2 mL) was added TFA (2 mL) at 0°C. The reaction mixture was stirred for 30 min. at room temperature. Upon completation the reaction was quenched with NH_4OH 5M at pH 9.The organic layer was dried with Na_2SO_4 and concentrated under reduced pressure to give **86b** (0.233g, 92%) as colorless oil.

86b: **^{1}H-NMR** (400 MHz, $CDCl_3$): δ 2.43-2.01 (m, 10H),2.32-2.38 (m, 3H), 2.80-2.85 (m, 1H), 3.02 (br s, 1H), 3.34 (br s, 1H), 3.36 (s, 3H), 3.65-3.72(m, 1H), 4.57-4.65 (m, 1H), 6.01 (dd, *J* = 10.3, 1.6 Hz, 1H), 6.88 (ddd, *J* = 9.5, 5.2, 3.1 Hz, 1H) ppm.

^{13}C-NMR (100 MHz, $CDCl_3$): δ = 23.0, 23.2, 30.0, 37.7, 38.6, 40.3, 44.9, 54.2, 57.2, 74.1, 74.8, 121.2, 145.3, 164.1 ppm.

IR: (neat) = 1730 cm^{-1}. $[\alpha]_D^{20}$= +21.7 (*c* 0.009, $CHCl_3$). ESIMS *m/z* $[M+H^+]^+$ calcd for $C_{14}H_{24}NO_3$: 254.18; Found: 254.57.

93b: $[\alpha]_D^{20}$= -21.8 (*c* 0.2, $CHCl_3$). **ESIMS** *m/z* $[M+H^+]^+$ calcd for $C_{14}H_{24}NO_3$: 254.18; Found: 254.23.

87b:^{1}H-NMR (400 MHz, $CDCl_3$): δ 1.33-1.80 (m, 8H),1.86-1.93 (m, 1H), 2.29-2.38 (m, 2H), 2.62-2.72 (m, 2H), 3.09-3.15 (m, 1H), 3.33 (s, 3H), 3.57-3.67(m, 1H), 4.02 (br s, 1H), 4.57-4.64 (m, 1H), 6.00 (dd, *J* = 9.8, 1.9 Hz, 1H), 6.84-6.88 (m, 1H) ppm.

^{13}C-NMR (100 MHz, $CDCl_3$): δ 22.0, 22.3, 29.1, 30.0, 37.7, 40.0, 45.1, 55.8, 62.1, 74.8, 75.0, 120.9, 145.8, 160.5 ppm.

IR: (neat) = 1730 cm^{-1}. $[\alpha]_D^{20}$= + 6.3 (*c* 0.001, $CHCl_3$). **ESIMS** *m/z* $[M+H^+]^+$ calcd for $C_{14}H_{24}NO_3$: 254.18; Found: 254.93.

92b: $[\alpha]_D^{20}$= -9.8 (*c* 0.5, $CHCl_3$). **ESIMS** *m/z* $[M+H^+]^+$ calcd for $C_{14}H_{24}NO_3$: 254.18; Found: 254.27.

88b: **^{1}H-NMR** (400 MHz, $CDCl_3$): δ 1.33-1.80 (m, 9H),2.12 (ddd, *J* = 7.2, 7.2, 5.7 Hz, 2H), 2.31-2.38 (m, 2H), 2.70 (dt, *J* = 14.6, 2.6 Hz, 1H), 2.84-2.88 (m, 1H,), 3.16-3.19 (m, 1H), 3.32 (s, 3H), 3.60-3.67(m, 1H), 4.30 (br s, 1H), 4.50-4.57 (m, 1H), 6.00 (d, *J* = 9.8 Hz, 1H), 6.87 (ddd, *J* = 9.4, 5.1, 3.2 Hz, 1H) ppm.

^{13}C-NMR (100 MHz, $CDCl_3$): δ 23.9, 24.5, 29.7, 31.6, 38.2, 39.3, 46.1, 54.0, 56.3, 74.1, 75.0, 121.4, 145., 164.4 ppm.

IR: (neat) = 1730 cm^{-1}. $[\alpha]_D^{20}$= +24.8 (*c* 0.005, $CHCl_3$). **ESIMS** *m/z* $[M+H^+]^+$ calcd for $C_{14}H_{24}NO_3$: 254.18; Found: 254.14.

91b:$[\alpha]_D^{20}$= -21.2 (*c* 0.8, $CHCl_3$). ESIMS *m/z* $[M+H^+]^+$ calcd for $C_{14}H_{24}NO_3$: 254.18; Found: 254.11.

89b:**^{1}H-NMR** (400 MHz, $CDCl_3$): δ 1.31-1.80 (m, 8H),2.11 (ddd, *J* = 12.9, 9.6, 6.0 Hz, 1H), 2.31-2.40 (m, 2H), 2.61-2.67 (m, 2H), 3.06-3.09 (m, 1H, *H*-CH-N), 3.26 (br s, 1H), 3.31 (s, 3H), 3.57-3.63(m, 1H), 4.53 (ddd, *J* = 12.5, 10.6, 5.3 Hz, 1H), 6.01 (d, *J* = 9.9 Hz, 1H), 6.87 (ddd, *J* = 12.9, 9.6, 6.0 Hz, 1H) ppm.

^{13}C-NMR (100 MHz, $CDCl_3$): δ 24.6 (t), 25.7 (t), 29.7 (t), 32.7 (t), 38.3 (t), 40.5 (t), 46.9 (t), 55.8 (d), 56.0 (q), 75.0 (d), 75.5 (d), 121.3 (d), 145.1 (d), 164.2 (s) ppm.

IR (neat) = 1730 cm^{-1}.$[\alpha]_D^{20}$= + 12.7 (*c* 0.001, $CHCl_3$). **ESIMS** *m/z* $[M+H^+]^+$ calcd for $C_{14}H_{24}NO_3$: 254.18; Found: 254.10.

90b: $[\alpha]_D^{20}$= -13.9 (*c* 1.0, $CHCl_3$). **ESIMS** *m/z* $[M+H^+]^+$ calcd for $C_{14}H_{24}NO_3$: 254.18; Found: 254.22.

4.6.4. Bivalent compounds

Synthesis of compound 96

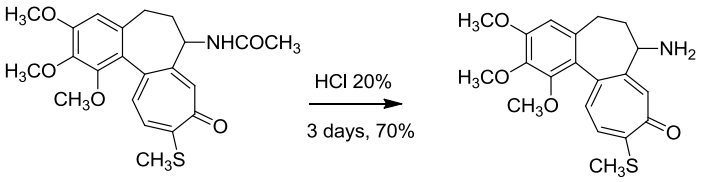

95 **96**

A solution of tiocolchicine **95** (0.500 g, 1.2 mmol) in MeOH (20 mL) and 2 N HC1 (9.5 mL) was heated at 85-90 °C with stirring for 3 days. Then the reaction mixture was cooled and the solutionwas neutralized with saturated $NaHCO_3$ solution,extracted with CH_2CI_2, and washed with brine. Theextract was dried over Na_2SO_4 and the solvent was removed under vacuum. The residue was purified by column chromatography on silica gel (CH_2CI_2 /MeOH, 9:1) and crystallization fromCH_2Cl_2/MeOH to give 0.320 g of pure **96** in an 70% yield.

^{1}H-NMR (400 MHz, $CDCl_3$): δ 7.63 (s, 1H), 7.42 (d, J = 10.5 Hz, 1H), 7.22 (d, J = 10.5 Hz, 1H), 6.54 (s, 1H), 4.01 (s, 6H), 3.73-3.63 (m, 1H), 3.66 (s, 3H), 2.43 (s, 3H), 2.51-2.38 (m, 4H).

Synthesis of compound 98

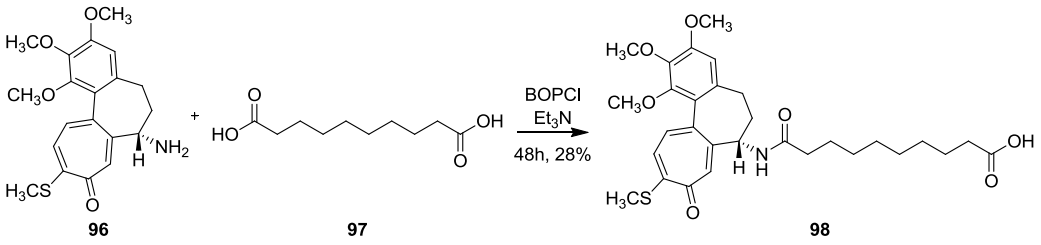

A solution of deacetylthiocolchicine **96** (0.500 g, 1.34 mmol), sebacic acid (0.271 g, 1.34 mmol), BOP-Cl (0.409g, 1.68 mmol) and Et_3N (220μL) in CH_2CI_2 (10mL) was stirring for 2 days at room temperature.The mixture was quenched with HCl 1N and the aqueous layer was extracted with CH_2Cl_2. The organic layer was dried with Na_2SO_4 and the solvent was removed under vacuum. The residue was purified by column chromatography on silica gel (EtOAc/ MeOH, 30:1) to give **98** (0.212 g, 28 %) as yellow oil.

^{1}H-NMR (400 MHz, $CDCl_3$): δ 7.58 (s, 1H), 7.34 (d, J = 9 Hz, 1H), 7.10 (d, J = 9 Hz, 1H), 6.95 (d, J = 5 Hz, 1H), 6.52 (s, 1H), 4.75-4.63 (m, 1H), 3.91 (s, 3H), 3.88 (s, 3H), 3.62 (s, 3H), 2.56-2.40 (m, 1H), 2.40 (s, 3H), 2.40-2.23 (m, 4H), 2.23-2.15 (m, 2H), 1.92-1.78 (m, 1H), 1.68-1.49 (m, 4H), 1.38-1.18 (m, 8H).

ESIMS *m/z* $[M+H^+]^+$ 558.

Synthesis of compound 99

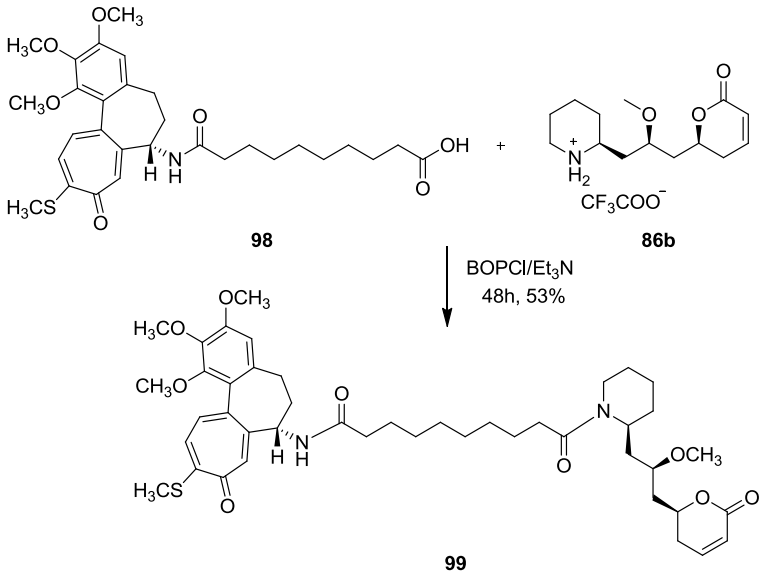

A solution of *N*-sebacoyl-*N*-deacetylthiocolchine (0.030 g, 0.05 mmol), hybrid **86b** (0.020 g, 0.05 mmol), BOP-Cl (0.016 g, 0.06 mmol) and Et_3N (15 μL) in CH_2CI_2 (1mL) was stirring for 2 days at room temperature. The mixture was quenched with HCl 1N and the aqueous layer was extracted with CH_2Cl_2. The organic layer was dried with Na_2SO_4 and the solvent was removed under vacuum. The residue was purified by column chromatography on silica gel (CH_2CI_2 /MeOH, 98:2) to give **99** (0.023 g, 53%)as dark yellow oil.

^{1}H-NMR (400 MHz, $CDCl_3$): δ 7.46 (s, 1H), 7.40 (d, J = 8.7 Hz, 1H), 7.16 (d, J = 8.7 Hz, 1H), 6.93-6.90 (m, 1H), 6.56 (s, 1H), 6.06-6.02 (m, 1H), 5.01 (bs, 1H), 4.78-4.51 (m, 2H), 4.18-4.02 (m, 1H), 3.98 (s, 3H), 3.92 (s, 3H), 3.70 (s, 3H), 3.34 (s, 3H), 3.21-3.05 (m, 1H), 2.98-2.91 (m, 1H), 2.61-2.52 (m, 2H), 2.47 (s, 1H), 2.46-2.18 (m, 11H), 1.72-1.51 (m, 5H), 1.48-1.18 (m, 17H).

$[\alpha]_D^{20}$= -115.9 (*c* 0.465, $CHCl_3$). **ESIMS** *m/z* $[M+H^+]^+$ 794.04

4.7. Biological assay

Tubulin was purified from bovine brain purchased from a local slaughterhouse, conserved before use in ice-cold PBS and used as soon as possible. According to Castoldi and Popov,[149] pure tubulin was obtained by two cycles of polymerization–depolymerization in a high-molarity PIPES buffer (1 M K-PIPES, pH 6.9, 2 mM EGTA, 1 mM $MgCl_2$), and protein concentration was determined by the MicroBCA assay kit (Pierce). To test the effects on tubulin assembly, stereoisomers were dissolved in dimethyl sulfoxide (DMSO), added at 50 μM to a reaction mixture composed of 20 μM tubulin, 10 % glycerol, 1 mM GTP in BRB80 buffer (80 mM K-PIPES, pH 6.9, 2 mM EGTA and 1 mM $MgCl_2$) and incubated for 30 min at 37 °C. As control conditions were used either unmodified thiocolchicine (10 μM) or DMSO alone were employed. At the end of polymerization, unpolymerized and polymerized fractions of tubulin were separated by centrifugation at 16500 × g for 30 min at 25 °C. The collected microtubules were resuspended in SDS-PAGE sample buffer (2 % w/v SDS, 10 % v/v glycerol, 5 % v/v β-mercaptoethanol, 0.001 % w/v bromophenol blue, and 62.5 mM Tris, pH 6.8) and the unpolymerized tubulin was diluted 3:1 with 4 X SDS PAGE sample buffer. Equal proportions of each fraction were resolved by a 7.5 % SDS-gel and stained with Coomassie blue. Densitometric analyses of stained gels were performed by using ImageJ software (National Institute of Health), and data were elaborated using STATISTICA (StatSoft Inc., Tulsa, OK). Significant differences were assessed by one-way ANOVA with Fisher LSD post hoc test. Experiments were done in triplicate and data are expressed as means ±SEM.

[149] Castoldi, M.; Popov, A. V. *Protein Expression Purif.* **2003**, *32*, 83–88

4.8. Docking Studies

Pironetin derivatives were docked in the pironetin binding site in the crystal structure of tubulin (1JFF.pdb)[150] using AutoDock 4.2 software. Pironetin binding site has been identified according to Usui *et al.*,[151] thus the grid box for ligand-protein interaction potential evaluation has been centered on Asn258. A cubic box has been employed, with 50 points per side and a grid spacing of 0.375 Å. A Lamarkian genetic algorithm was used for the docking simulations, performing 100 independent runs per molecule. In each run, a population of 50 individuals evolved along 27.000 generations and a maximum number of 25 million energy evaluations was performed. The best fit (lowest docked energy) solutions of the 100 independent runs were stored for subsequent analysis. Docked structures have been rendered using VMD.

[150] Lowe,J.; Li, H.; Downing, K. H.; Nogales, E. *J. Mol. Biol.* **2001**, *313*, 1045–1057.
[151] Usui, T.; Watanabe, H.; Natayama, H.; Tada, Y.; Kanoh, N.; Asao, T.; Takio, K.; Nishikawa, K.; Kitahara, T.; H. Osada *Chem. Biol.* **2004**, *11*, 799–806.

5. Natural products and cancer stem cells

All tissues of multicellular adult organism are constituted by mature and specialized cells and its specific stem cells that are responsible for tissue renewal and repair of damaged tissue.

Stem cells have four distinct properties respect to the other cells in the body:

1. self-renewal
2. undifferentiated and unspecialised
3. differentiation potential into specialised cells of a specif tissue
4. potential to proliferate extensively while remaining undifferentiated

The combination of these four characteristics makes stem cells unique. In addition, all these properties are often referred to as "stemness".[152]

Even if the cells in adult tissues are various, all cells originate from a single egg after fertilization of an ovule by a spermatozoid. Egg fertilization leads to the creation of totipotent stem cells, which are the precursors of every tissues of embryo, allantois, amniotic sac and placenta. After about four days, these totipotent stem cells go through several mitotic divisions to form identical cells and, after this point, they gradually lose their high proliferative potential and initiate to specialize, until they become nullipotent (Figure 57).

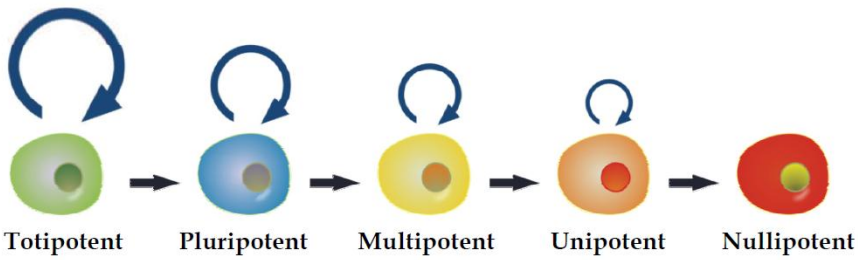

Figure 57: Diverse degree of differentiation potential of stem cells

The integrity of adult tissues is preserved by the constant replacement of cells that cyclally differentiate and die. Thus, in most adult tissues there are groups of progenitor cells that multiply and differentiate into specialized tissues of origin and, at the same

[152] Mikkers,H.; Frisèn, J. The EMBO Journal **2005**, *24*, 2715–2719.

time, maintain a reserve of undifferentiated cells. These adult progenitor cells are called *somatic stem cells* or *adult tissue-specific stem cells*.

Stem cells can divide in two different manners (Figure 58):

- symmetrically: two daughter cells share the same stem cell feature. It happens when their number (stem cell pool) needs to be extended, such as during embryonic development and after tissue damage.
- asymmetrically: one of the progeny continue to be undifferentiated, renewing the pool of stem cells, while the other daughter cells can proliferate and differentiate into specialized cells to produce new tissue mass.

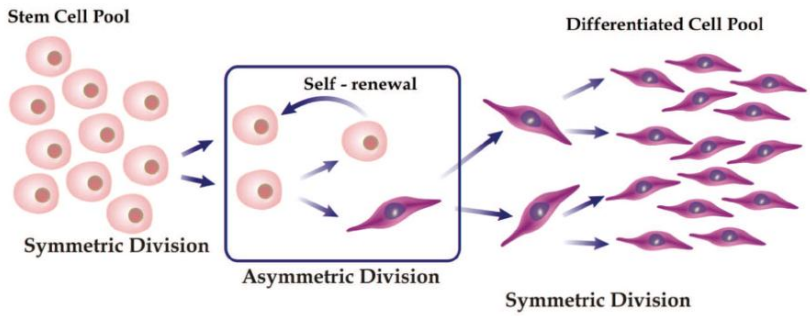

Figure 58: Stem cells asymmetrical and symmetrical division

A subset of cancer initiating cells have been identified in cancers of the hematopoietic system, breast, and brain.[153]

This kind of cells have the ability to self-renew and differentiation into a variety of mature cells and the proliferative ability to drive continued expansion of the population of malignant cells. Consequently, the properties of cancer-initiating cells and normal stem cells are closely parallel. Malignant cells with these features have been termed "cancer stem cells" to reflect their stem-like properties.

The cancer stem cells theory proposes that these cancer cells are responsible for tumor initiation, progression, maintenance, metastasis and recurrence.

[153] Singh, S. K.; Hawkins, C.; Clarke, I. D.; Squire, J.A.; Bayani, J.; Hide, T.; Henkelman, R.M.; Cusimano, M.D.; Dirks, P.B. *Nature* **2004**, *432*, 396-401.

Figure 59 shows the situations that are possible for tumors in which cancer stem cells play a central role.

In panel A is shown a primary tumor generated from mutation of a normal stem cell or progenitor cell that may create a cancer stem cell. In the second panel, during chemotherapy treatment, most of cells in a primary tumor may be destroyed, but if the cancer stem cells are not eliminated, the tumor may regrow and cause a relapse. In panel C, cancer stem cells arising from a primary tumor may migrate creating metastasis.

Based on these scenarios it is evident that it is possible to have a recurrence of the tumor if cancer stem cells have not been completely destroyed during the treatment.

It is well known that different cancers are particularly resistant to conventional chemo- and radiotherapy that usually kill the majority of cancer cells. This clinical response could reflect the targeting of the bulk of non-stem cell population. On the other hand, several specific key intracellular signaling pathways are involeved in CSCs self-renewal and proliferation processes that seem to be promising therapeutic targets.

For these reasons therapeutic strategies that specifically target cancer stem cells should eliminate tumors more effectively than current treatments and reduce the risk of relapse and metastasis. [154]

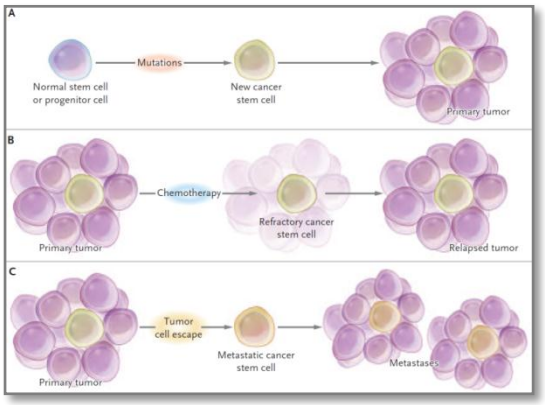

Figure 59: Situations involving cancer stem cells

[154] K, Chen; Y.H., Huang; J.L., Chen. *Acta Pharmacol Sin* **2013**, *34*, 732-740 .

In order to develop efficient treatments that can induce a long-lasting clinical response preventing tumor relapse it is important to develop drugs that can specifically target and eliminate CSCs.[155][156]

An ideal therapeutic strategy may be sensitize CSCs to radio- and chemotherapy by inhibiting their stem properties and then by promoting a direct cytotoxicity. Due to the fact that the CSCs population is driven by embryonic signaling pathways, the targeting of these pathways could lead to an efficient therapy: in this direction, several drugs for the inhibition of embryonic signaling pathways are now underdevelopment.

Natural products are efficient tools for the exploration of the chemical space because they embrace so many varied pharmacophores of wide structural diversity. Recent progress have permitted a revival of interest in natural products for the drug discovery pipeline.[157]

Many natural products have been reported that influence cellular pathways important for stem cells and cancer stem-like cells, but have not yet been tested in these cell types specifically. Thus, there are many natural compounds to be explored in cancer stem cell biology.

Natural products could have considerable importance in stem cell biology for both protection of normal tissue against the side effects of cancer radio- and chemotherapy and for tissue regeneration (Figure 60). Well-known anticancer drugs kill the bulk of differentiated cancer cells, but leave quiescent and undifferentiated cancer stem-like cells untouched. This population of cancer stem-like cells could be responsible for tumor relapse even after chemotherapy. In the past few years the results obtained with natural products were promising, as several molecules have been described to attack cancer stem-like cells. In addition, many of these natural products improve the efficacy of chemo- and radiotherapy, making them ideal partners for combination therapy

[155] C., Yang; K., Jin; Y., Tong; W.C., Cho *Med. Oncol.* **2015**, *32*, 170.
[156] P.A., Sotiropoulou; M.,Christodoloulou; A., Silvani; C.,Herold-Mende; D., Passarella *Drug discovery today* **2014**, *19*, 1547-1562 .
[157] Harvey, A.L.; Edrada-Ebel, R.A.; Quinn, R.J. *Nat. Rev. Drug Discov.* **2015**, *14*, 111.

treatments. The field of treating cancer stem-like cells with natural products is still at the beginning, but it can be predictable to develop into a rapidly growing area of research.

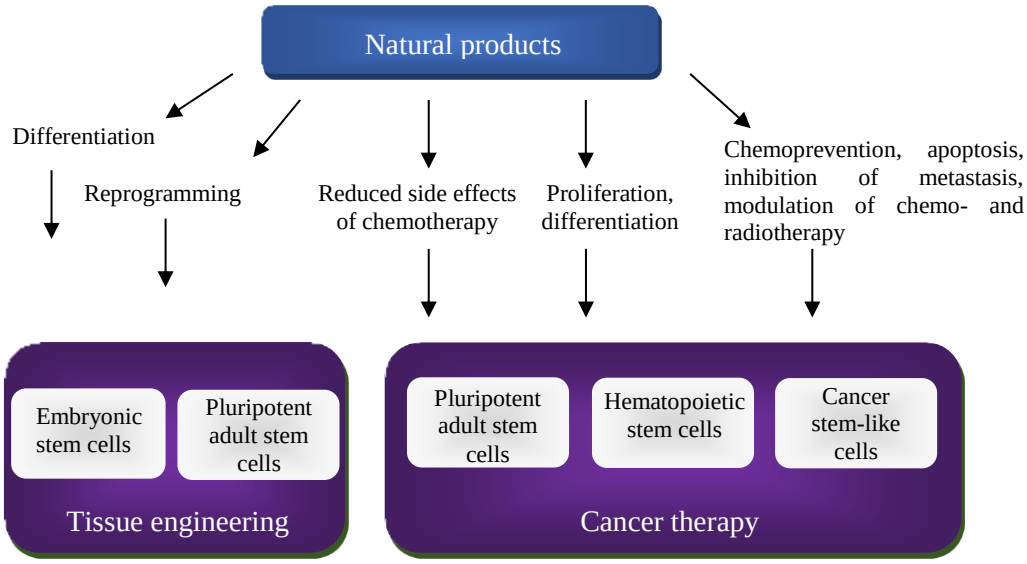

Figure 60: Therapeutical potential of natural products towards stem cells

In a review recently published from our research group, [158] we summarize the natural products that demonstrate activity against CSCs (forty-nine different natural products are reported in Figure 61).

Some of these natural products, grouped into several structural classes (such as flavonoids, polyketides, terpenes, alkaloids and many others), are here described.

[158] Marucci, C.; Christodoulou, M.S.; Pieraccini, S.; Sironi, M.; Dapiaggi, F.; Cartelli, D.; Calogero, A. M.; Cappelletti, G.; Vilanova, C.; Gazzola, S.; Broggini, G.; Passarella, D.*Eur. J. Org. Chem.* **2016**, 2029-2036

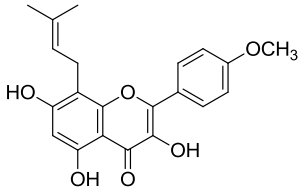

100
Icaritin

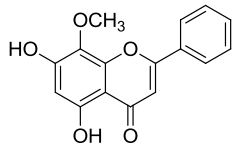

101
Wogonin

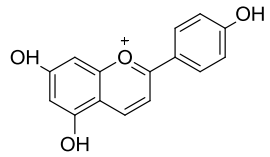

102
Apigeninidin

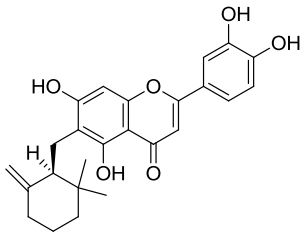

103
Ugonin J

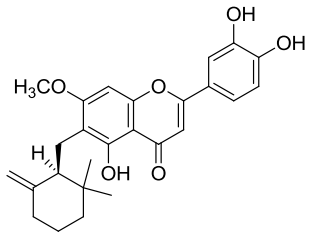

104
Ugonin K

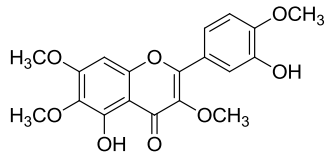

105
Casticin

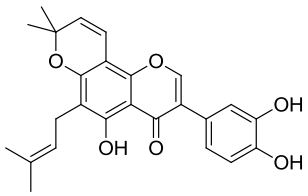

106
Pomiferin

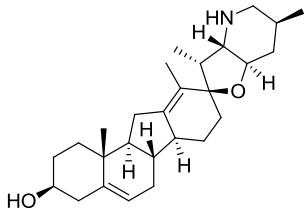

107
Cyclopamine

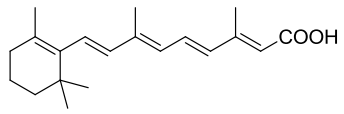

108
All-trans-retinoic acid

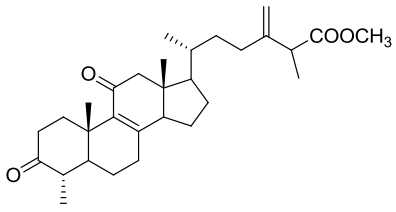

109
Methylantcinate A

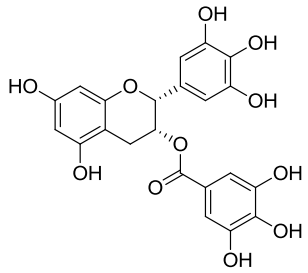

110
Epigallocatechin-3-gallate

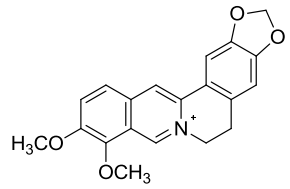

111
Berberine

(continues)

(continued)

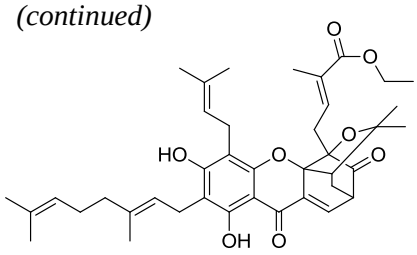

112
Compound 2

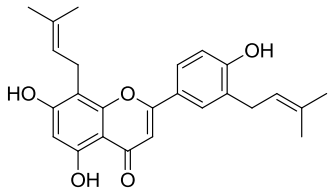

113
Broussoflavonol

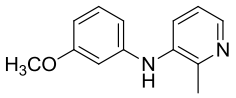

114
Harmine

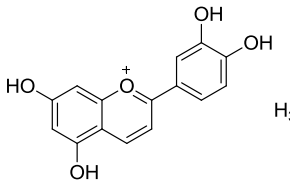

115
Luteolinidin

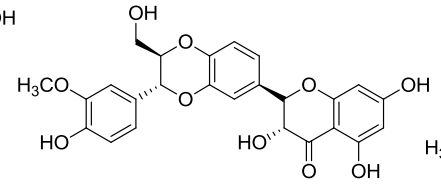

116
Silibinin

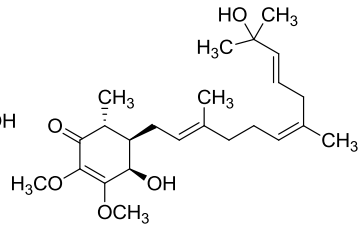

117
Antraquinolol B

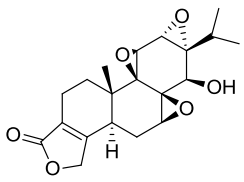

118
Triptolide

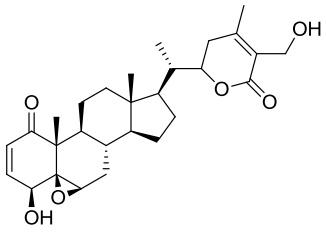

119
Withaferin A

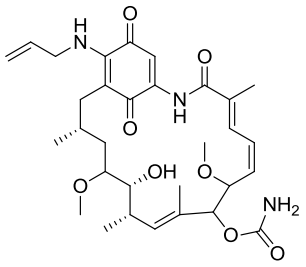

120
Tanespimycin

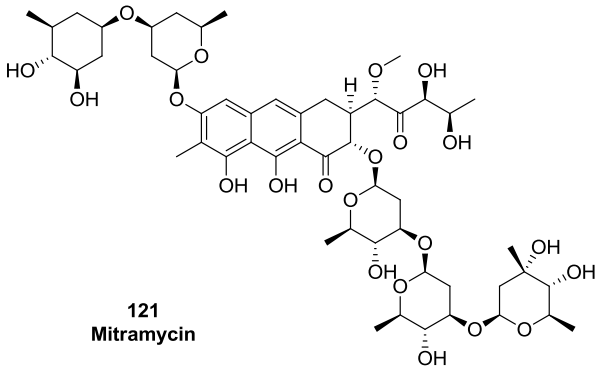

121
Mitramycin

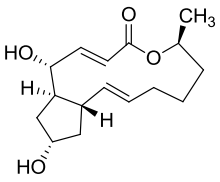

122
Brefeldin A

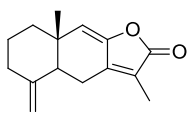

123
Atractylenolide I

(continues)

(continued)

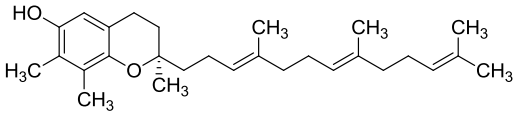

124
Gamma-tocotrienol

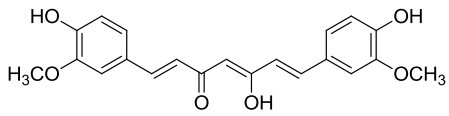

125
Curcumine

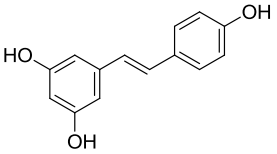

126
Resveratrol

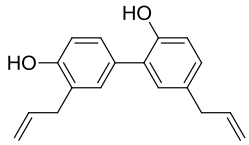

127
Honokiol

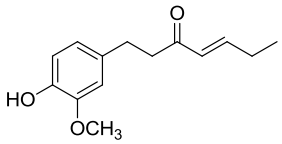

128
6-Shogaol

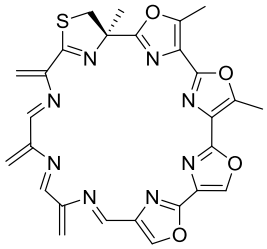

129
Telomestatin 1

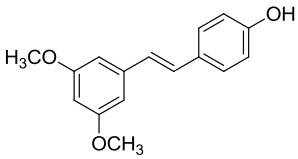

130
Pterostilbene

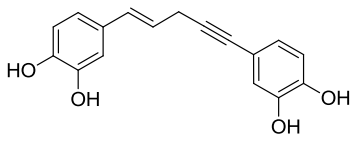

131
Rooperol

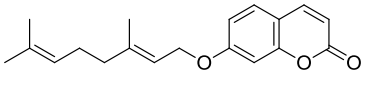

132
Auraptene

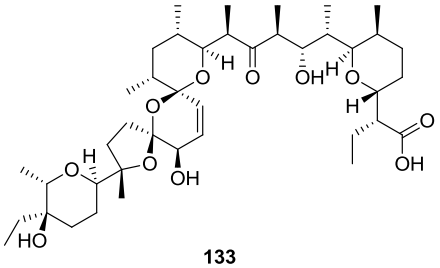

133
Salinomycin

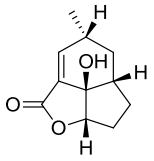

134
Galiellalactone

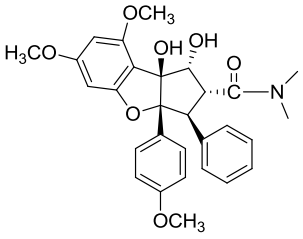

135
Rocaglamide

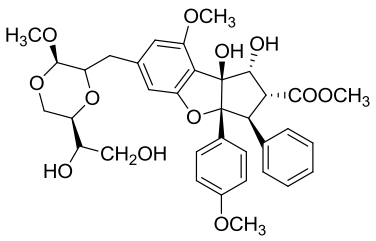

136
Silvestrol

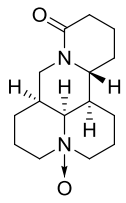

137
Oximatrine

(continues)

(continued)

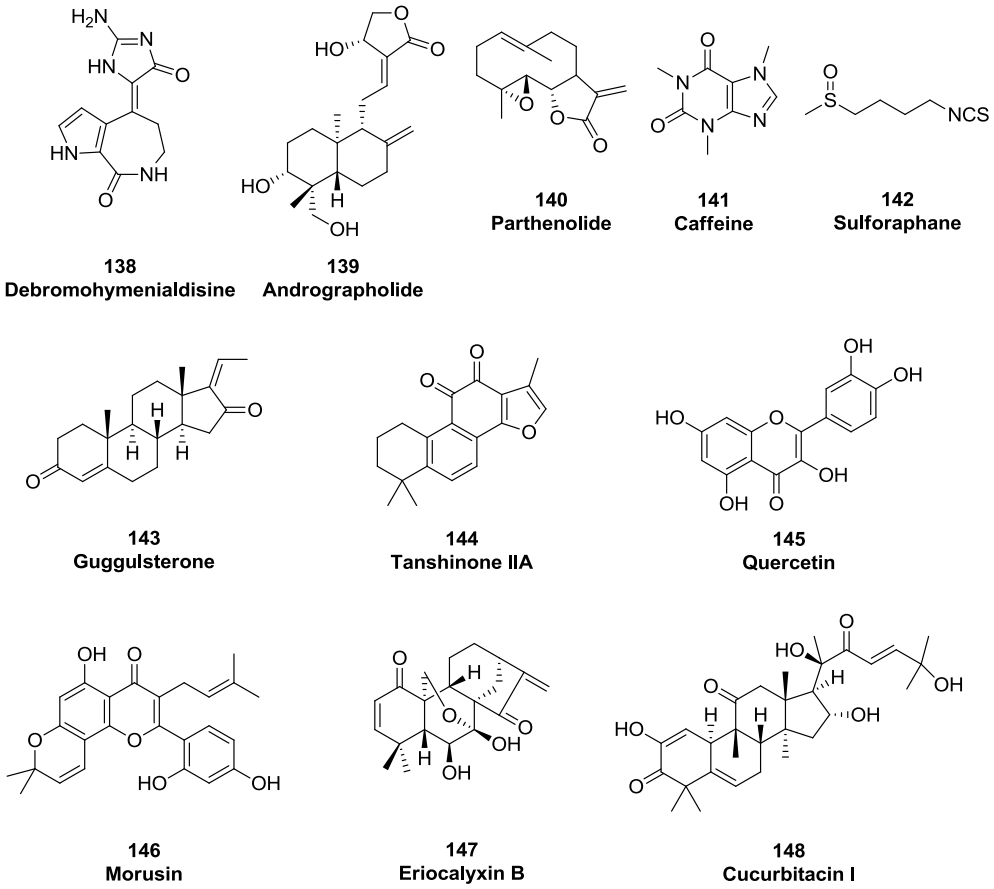

Figure 61: Natural compounds that target CSCs

Flavonoids

Icaritin (**100**), a prenylflavonoid isolated from plants of the genus *Epimedium*, possesses many biological and pharmacological activities, such as stimulation of neuronal and cardiac differentiation, growth inhibition of human prostate carcinoma PC-3 cells, neuroprotective effects and estrogen-like properties.[159] Icaritin is able to inhibit the growth of breast CSCs and/or progenitor-like cells in a different way from the well-known antiestrogen tamoxifen.

[159] Guo, Y.; Zhang, X.; Meng, J.; Wang, Z.Y. **2011**, *658*, 114-122

Icaritin induces continued activation of ERK signaling, cell cycle arrest and apoptosis.

Wogonin (**101**),[160] obtained from extraction of an herbal material of *Scutellaria baicalensis,* is used for the treatment of different types of cancer of diverse organs. The inhibition of CSCs growth is possible by a pharmaceutical composition, which is formed by wogonin, a pharmaceutically acceptable carrier and also a therapeutic agent such as a cytotoxic agent. Wogonin can also be used in combination with radiotherapy or immunotherapy. The expression of ABCG2, ALDHA1 and β catenin was revealed after the treatment with the extract of *S. Baicalensis*.

Apigeninidin (**102**) and luteolinidin (**115**), which are two constituents of the 3-deoxyanthocyanidin subclass of flavonoids, are isolated from *Sorghum bicolor*.[161] These molecules have been reported to have a cytotoxic activity towards various cancer cell lines, such as liver, colon and leukemia.

Phenolic extract of the sweet *sorghum* pith and dermal layer were analyzed and revealed the presence also of flavonoids, stilbenoids and phenolic acids which possess effective *in vitro* and *in vivo* anticancer activities.

The majority of 3-deoxyanthocyanidins is in the dermal layer extract than in the pith one. As a result, the dermal layer extract shows a potent *in vitro* anti-cancer activity against the colon cancer cell line: HCT116 and colon CSCs. In addition, luteolinidin inhibits colon CSCs proliferation more than apigeninidin.

Epigallocathechin-3-gallate (**110**), the most abundant catechin in green tea, is able to inhibit self-renewal capacity and the migration of nasopharyngeal CSCs by attenuating NF-κB p65 activity.

Broussoflavonol B (**113**)[162] was isolated from the plant *Broussonetia papyrifera (Moraceae),* which contains different types of flavonoids some of which showed strong antimicrobial, antifungal, antioxidant properties and tyrosinase inhibition. Recently broussoflavonol B has been reported to inhibit the growth of ER-positive breast cancer cells and also of ER-negative breast cancer stem-like cells. It induces the differentiation

[160] Hsieh ,H.M.; Lee, C.Y.; Shen, C.C.; Wang, C.T. US patent 100131944, **2013**.
[161] Massey, A.R.; Reddivari, L.; Vanamala, J. *J. Agric. Food Chem.***2014**, *62*, 3150-3159
[162] Matsumoto, J.; Fujimoto, T.; Takino, C.; Saitoh, M.; Hano, Y.; Fukai, T.; Nomura, T. *Chem. Pharm. Bull.* **1985**, *33*, 3250–325.

of these cells and this could be one of the mechanisms used to limit the growth of ER-negative breast cancer stem like cells.

Ugonins J and K (**103-104**), identified as the main two cyclohexylmethyl flavonoids constituents of the rhizomes of *H. zeylanica*, inhibit propagation of breast CSCs in mammosphere cultures and in tumor xenografts.

Recently, activation of p53, which in turn led to reduction of NANOG, was found to mediate the suppressive effect of ugonin J for the propagation of breast CSCs. Overexpression of NANOG arrests the suppressive effect of ugonin J. Rhizomes of *H. zeylanica* can be utilized as a complementary medicine for reducing CSC-mediated breast cancer relapse.

Casticin (**105**) is the main active compound of *Fructus Viticis Simplicifoliae*, which is used in traditional Chinese medicine for the treatment of different types of tumors. This compound inhibits self-renewal of glioma stem-like cells, but the effects of casticin on lung cancer stem-like cells and its mechanisms of action remain unknown.

Pomiferin (**106**), extracted from the fruit of the *Maclura pomifera*, shows *in vitro* antitumor effects on various types of tumor cell lines from kidney, prostate, breast, lung and colon.[163] Compound **106** acts on gliomas stem cells by down-regulating stemness-associated genes[20] and could be used as a therapeutic agent in the future.

Compound 2 (**112**)[164] is a new gamboge derivative able to inhibit proliferation of both CSCs and non-CSCs derived from neck and head squamous cell carcinoma. Gamboge is a natural anti-cancer medicine that possesses pharmacological effects different from those of traditional chemotherapeutical drugs. Compound 2 acts on CSCs by suppressing the activation of EGF/EGFR signal pathway leading to down-regulation of multiple stem cell-related proteins. For these reasons, it could be a candidate for use in long-term and recurrent cancer drug therapies.

Silibinin (**116**), a flavonolignan isolated from the milk thistle *Silybum marianum*, demonstrated pro-apoptotic, anti-proliferative and anti-inflammatory activities.

[163] Son, I.H.; Chung , I.M.; Lee, S.I.; Yang, H. D.; Moon, H.I. *Bioorg. Med. Chem. Lett.* **2007**, *17*, 4753–4755

[164] Deng, R.; Wang, X.; Liu, Y.; Yan, M. ; Hanada, S. ; Xu, Q. ; Zhang, J. ; Han, Z. ; Che, W. ; Zhanf, P. *J. Cell. Mol. Med*. **2013**, *17*, 1422-1433

Silibinin could interfere with kinetics of CSC by shifting CSC cell division to an asymmetric type via the targeting of the various signals associated with the survival and multiplication of colon CSC pool.[165]

Alkaloids

Three different alkaloids have been reported to be active against different CSC lines. Harmine (**114**) inhibits the self-renewal and promotes the differentiation of glioblastoma stem-like cells. It is able to decrease the tumorigenicity of glioblastoma CSCs (this feature was confirmed *in vivo*).[166] Glioblastoma CSCs are also the targets of the well-known cyclopamine (**107**) alkaloid that is able to limit significantly drug resistance of CD34+ leukemic cells to cytarabine.

Recently it was demonstrated that cyclopamine- and paclitaxel-squalene conjugates self-assemble to generate hetero-nanoparticles that have shown combined activities in the treatment of ovarian and glioblastoma CSCs.[167]

Berberine (**111**) is an alkaloid isolated from *Coptis chinensis*, *Hydrastis canadensis* and other species of the family *Berberidaceae*.[26] It shows anti-inflammatory and anti-bacterial properties, and has been formulated into liposomes for targeted delivery to the mitochondria of breast CSCs. These liposomes are able to cross the CSC membrane, inhibit the ABC transporters (ABCC1, ABCC2, ABCC3 and ABCG2) and selectively accumulate in the mitochondria. Moreover, the pro-apoptotic protein BAX was activated, while the anti-apoptotic protein BCL-2 was inhibited, resulting in cell apoptosis.

Terpenoidic derivatives

Seven different terpene or terpenoid compounds have been reported to arrest the proliferation of various types of CSC. Retinoic acids (all-trans) (**108**) are potent differentiating agents. These natural products induce *in vitro* differentiation of stem-like glioma cells and, consequently, are able to induce therapy-sensitizing effects, to impair

[165] Kumar, S.; Raina, K.; Agarwal, C.; Agarwal, R. *Oncotarget* **2014**, *5*, 4972-4989
[166] Liu, H.; Han, D.; Liu, Y.; Hou, X.; Wu, J.; Li, H.; Yang, J.; Shen, C.;Yang, G.; Fu, C.; Li , X.; Che, H.; Ai, J.; Zhao, S. *J. Neuro.Oncol.* **2013**, *112*, 39-48
[167] Fumagalli, G.; Mazza, D.; Christodoulou, M. S.; Damia, G.; Ricci, F.; Perdicchia, D.; Stella, B.; Dosio, F.; Sotiropoulou, P. A.; Passarella, D. *ChemPlusChem* ***2015***, *80*, 1380-1383

the secretion of angiogenic cytokines and disrupt stem-like glioma cells motility. The anti-cancer effects of all *trans* retinoic acids are associated with downregulation of Wnt/β-catenin signaling.

Methyl antcinate A (**109**) is an ergostane-type triterpenoid extracted from the fruiting bodies of *Antrodia camphorate*. It may be a powerful anti-metastasis agent and could amplify the expression of p53, which is a tumor supressor able to block the self-renewal capability of breast CSCs.[168] Compound **109** is able to suppress the expression of Hsp27 in breast CSC-like cells and to inhibit their self-renewal capability.

Another natural product isolated from *Antrodia camphorate* is Antroquinonol B (**117**).[169] This compound could inhibit the survival of various cancer cells including breast, hepatic, lung and prostate cancer. These different types of cancer can be treated with a medicinal formulation composed by antroquinonol B, antroquinonol C and the pharmaceutically accepted carriers, for example water, diluents and many others. The inhibitory effects on CSCs could be increased through a co-administration of the chemotherapy drugs, such as cisplatin or taxol, and the *A.camphorata* extracts.

Triptolide (**118**), the major active substance in *Tripterygium wilfordii Hook f.*, is a diterpenoid triepoxide currently being tested in a phase I trial for its safety. It possesses pro-apoptotic, anti-inflammatory, and tumor-repressing effects when inhibiting NFAT, topoisomerase, proteasome activity, NF-κB signaling and heat-shock response.

Withaferin A (**119**), a bioactive compound extracted from the plant *Withania somniferia*, has been recently demonstrated to be used as a possible anti-cancer compound showing the ability to prevent tumor growth, angiogenesis and metastasis.[170]

It is able to suppress tumor growth, target cells expressing CSC markers and to inhibit Notch1 and its downstream signaling genes (Hes1 and Hey1) that play a key role in self-renewal and maintenance of CSCs. These features have been confirmed through the treatment of mice bearing human orthotopic ovarian tumors.

[168] Cicalese, A.; Bonizzi, G.; Pasi, C.E.; Faretta, M.; Ronzoni,S.; Giulini,B.; Brisken, C.; Minucci, S.; Di Fiore P.P.; Pelicci P. G.Cell **2009**,*138*, 1083–1095

[169] Huang, C.C.; Chen, C.C.; Chen, L.G. US patent 100136825, **2013**

[170] Stan, S.D.; Hahm, E.R.; Warin, R.; Singh, S.V. *Cancer Res.* **2008**, *68*, 7661–7669

Gamma tocotrienol (**124**) is one of the four isoforms of tocotrienols, which are components of the vitamin E family. It inhibits prostate cancer cell invasion and makes the cells sensitive to docetaxel induced apoptosis. These features suggest that gamma tocotrienol may be an efficient therapeutic agent against advanced stage prostate cancer. Tocotrienol has been shown to regulate different signaling pathways, such as PI3K and NF-κB, but the exact mechanisms underlying its antitumor effects are not known. Gamma tocotrienol treatment downregulates protein expression of prostate CSC markers CD44 and CD133 in prostate cancer cells and it is able to suppress their spheroid formation capacity and also interferes with their ability to form tumors *in vivo*.

Atractylenolide I (**123**), a constituent of the sesquiterpene lactone class, is isolated from *Rhizoma Atractylodis Macrocephalae*.[171] This compound acts in inhibiting cancer cell proliferation and in inducing apoptosis through inactivation of the Notch pathway. Atractylenolide I treatment led to the reduction of expressions of Jagged1, Notch1 and its downstream effector Hes1/ Hey1. In addition, **123** is able to inhibit the self-renewal capacity of gastric stem-like cells by suppression of their sphere formation capacity and cell viability.

Polyketides

The macrocyclic tanespimycin (**120**) is a derivative of the antibiotic geldanamycin. It eliminates lymphoma CSCs both *in vitro* and *in vivo* by disrupting the transcriptional function of HIF1a, a client protein of HSP90. Tanespimycin selectively induced apoptosis and led to elimination of the colony-formation capacity of mouse lymphoma CSCs and human AML CSCs. However, low concentrations of tanespimycin failed to eliminate highly proliferative lymphoma and AML cells (non CSCs), in which the AKT-GSK3 signaling pathway is constitutively active. The heat shock transcription factor HSF1 is highly expressed in non CSCs, but it is weakly expressed in lymphoma CSCs. Nevertheless, siRNA-mediated attenuation of HSF1 abrogated the colony-formation ability of both lymphoma and AML CSCs.[172] Another macrocyclic compound,

[171] Ma, L.; Mao, R.; Shen, K.; Zheng, K.; Li, Y.; Liu, J.; Ni, L. *Biochem. Biophys. Res. Comm.* **2014**, *450*, 353-359

[172] Newman, B.; Liu, Y.; Lee, H.F.; Sun, D.; Sun, D.; Wang, Y. *Cancer Res.* **2012**, *72*, 4551–4561

telomestatin (**129**), has been demonstrated to make less effective the maintenance of glioma stem cells (GSCs) by inducing apoptosis *in vitro* and *in vivo*. Telomestatin treatment also inhibited the migration potential of GSCs.

Mithramycin (**121**), a polyauroleic acid isolated from *Streptomyces*, is another useful antibiotic. This compound was initially evaluated as an anticancer agent in patients with cancer during the 1960s and 1970s. The use of mithramycin was discontinued due to its excessive toxicity. Recently, mithramycin showed efficacy in repressing ABCG2 and in inhibiting stem cell signaling in thoracic malignancies.[173]

Brefeldin A (**122**) is a lactone antibiotic first isolated from the fungus *Eupenicillium brefeldianum.* It inhibits the transport of secreted and membrane proteins from endoplasmic reticulum (ER) to Golgi apparatus, leading to disruption of Golgi function, accumulation of unfolded and incompletely processed proteins in ER and, finally, the induction of ER stress. Brefeldin A shows various effects including reducing CSCs activities, inducing anoikis and inhibiting the migration capacity of the human breast cancer MDA-MB-231 cells.[174] Western blotting analysis showed that these effects of brefeldin A might be mediated by the down regulation of the breast CSC marker CD44 and the anti-apoptotic proteins Bcl-2 and Mcl-1, in addition to the reversal of epithelial-mesenchymal transition.

Salinomycin (**133**) is an antibiotic isolated from *Streptomyces albus*. The activity of salinomycin is probably due to the interference with the Wnt/β-catenin signaling pathway, with the ABC drug transporters and other CSC pathways. Salinomycin is able to eliminate effectively CSCs and to induce partial clinical regression of heavily pre-treated and therapy-resistant cancers, as demonstrated by pre-clinical trials using human xenografts in mice and a few pilot clinical studies. The ability of salinomycin to kill both CSCs and therapy-resistant cancer cells identify the compound as a promising and potent antitumor drug.

Galiellalactone (**134**) is a hexaketide metabolite produced by the fungus *Galiella rufa* that possesses promising features for the development of anti-prostate cancer drugs. It is

[173] Zhang, M.; Mathur, A.; Zhang, Y.; Xi, S.*et al. Cancer Res.* **2012**, *72*, 4178–4192
[174] Tseng, C.N.; Hong, Y.R.; Chang, H.W. *et al. Molecules* **2014**, *19*, 17464-77

a highly potent and selective inhibitor of IL-6 signaling through STAT3, and is believed to inhibit STAT3 signaling by blocking the binding of activated STAT3 to DNA. The effects of galiellalactone on ALDH-expressing prostate cancer cells have been studied to explore the expression of ALDH as a marker for cancer stem cell-like cells in human prostate cancer cell lines. Galiellalactone treatment decreased the proportion of ALDH+ prostate cancer cells and induced their apoptosis. The gene expression of ALDH1A1 was downregulated *in vivo* in galiellalactone-treated DU145 xenografts.[175]

Cinnamic acid derivatives

Six different compounds sharing a polyphenolic structure have been used to inhibit different types of CSC. Among these, curcumin (**125**) has been reported to be effective against different types of tumors: colon (in combination with dasatinib), breast and brain (in combination with paclitaxel). A difluorinated derivative was shown to be active against colon cancer stem-like cells.[176] Resveratrol (**126**), a controverted sirtuin activator, has been reported to inhibit pancreatic CSC characteristics in both humans and KrasG12D transgenic mice when inhibiting pluripotency-maintaining factors and epithelial–mesenchymal transition.[177]

Honokiol (**127**), used in traditional Chinese medicine for the treatment of various disorders, possesses a biphenolic backbone. It has been demonstrated to be a potent inhibitor of colon cancer growth and it is also able to target CSCs by inhibiting the γ-secretase complex and the Notch signaling pathway. Recently honokiol has been demonstrated to eliminate oral CSCs by the inhibition of their EMT, suppression of Wnt/β-catenin signaling and apoptosis induction.[178]

6-Shogaol (**128**) and pterostilbene (**130**) are natural products that act by increasing the sensitivity of basal CSCs to chemotherapeutic drugs and the anticancer activity of paclitaxel.

[175] Hellsten, R.; Johansson, M.; Dahlman, A.; Sterner, O.; Bjartell, A. *PLoS One* **2011**, *6*, e22118
[176] Kanwar, S.S.; Yu, Y.; Nautiyal, J.; Patel, B.B.; Padhye, S.; Sarkar, F.H.; Majumdar, A.P.N. *Pharm. Res.* **2011**, *28*, 827–838
[177] Shankar, S.; Nall, D.; Tang, S.N.; Meeker, D.; Passarini, J.; Sharma, J.; Srivastava,K.R. *PLoS ONE* **2011**, *6*, e16530
[178] Yao, C.J.; Lai, G.M.; Yeh,C.T., *et al. Evid. Based Complement. Alternat. Med.* **2013**, Article ID 146136

6-shogaol and pterostilbene decrease the expression of the surface antigen CD44 on basal CSCs and promote β-catenin phosphorylation through the inhibition of the Hedgehog/Akt/GSK3β pathway.

Rooperol (**131**), the aglycone of hypoxoside, is the major phenolic constituent of the African potato, *Hypoxis hemerocallidea* (Fish. & C.A. Mey). In the last decade, it has been demonstrated that the hypoxoside derivative has pro-apoptotic effect on different types of cancer cell lines.[76] Rooperol-induced cell death involves cell cycle arrest and increases the expression levels of $p21^{Waf1/Cip1}$ and active caspase-3. This compound kills pluripotent cancer stem-like cells in a selective fashion.

Auraptene (**132**) is a coumarin derivative extracted from the fruits of edible plants belonging to the *Rutaceae* family. Genovese and Epifano performed studies[179] in order to elucidate the mechanisms of action and the pharmacological effects of this natural product. They showed that auraptene inhibits the formation and growth of colonospheres of the FOLFOX-resistant colon cancer HT-29 cells *in vitro* at a concentration of 10 μM. The corresponding parental cells were also treated with auraptene. The inhibition in the growth and colonospheres formation in FOLFOX-resistant HT-29 was related to a concomitant decrease in phospho-epidermal growth factor receptor. These results suggest that auraptene could prevent the re-emergence of CSCs.

Miscellaneous

Rocaglamide (**135**) and silvestrol (**136**), which are flavagline compounds isolated from the plant genus *Aglaia*, demonstrated toxic effect toward leukemia cells. A recent study[180] demonstrated that rocaglamide and silvestrol preferentially kill phenotypically and functionally defined leukemia stem cells, while sparing normal stem and progenitor cells. These compounds are significantly more toxic to leukemia cells as single agent or in combination with other anti-cancer drugs than clinically available translational inhibitors.

The plant compound isothiocynate sulforaphane (**142**) is present in high concentration in *Brassica oleracea* and other cruciferous vegetables. This natural product showed

[179] Epifano, F.; Genovese, S.; Miller, R.; Majumdar, A.P.N. *Phytother. Res.* **2013**, *27*,784–786
[180] Callahan, K.P.; Minhajuddin, M.; Corbett, C. *et al. Leukemia* **2014**, *28*, 1960–1968

interesting activity against three different types of CSCs. One of the first contributions in this field reported the inhibitory activity of sulforaphane against breast CSCs and the downregulation of the Wnt/β-catenin self-renewal pathway.[181] More recently, sulforaphane has been reported to regulate the self-renewal of pancreatic CSCs through the modulation of the Sonic Hh–GLi pathway[182] and to inhibit downstream targets of GLi transcription by suppressing the expression of pluripotency-maintaining factors (Nanog and Oct-4), and PDGFRα and Cyclin D1. As a result, sulforaphane has been highlighted as an inexpensive, safe and effective alternative for the management of pancreatic cancer.

Plant extracts

Berberis libanotica, specifically its roots, has been used in traditional herbal Lebanese medicine for rheumatic and neuralgic diseases.

Berberis are characterized by the presence of different type of secondary metabolites with important biological activities. *Berberis* extracts was found to induce cell cycle arrest at the G0-G1 inter phase. In fact, a high increase in the G0-G1 peak was seen in response to treatment with the *berberis* extract, suggesting an arrest at the G0-G1 phase. Since other studies have been demonstrated that the anti-proliferative effect of alkaloid-rich plant extracts is due to G2-M arrest rather than G0-G1 arrest, as in the *berberis* extract, more studies should be done at the molecular level in order to clarify the altered pathways in response to *berberis* treatment.

Bitter melon (*Momordica charantia*) is a tropical and subtropical vine, widely grown in Africa and Asia.

Methanolic extracts of bitter melon revelaed great efficacy on both colon cancer stem and progenitors cells.[183]

In particular, extracts are able to inhibit the growth of colon CSCs *in vitro* by inducing autophagy.

[181] Li, Y.; Zhang, T.; Korkaya, H. *et al*. *Clin. Cancer. Res.* **2010**, *16*, 2580-90
[182] Li, S.H.; Fu, J.; Watkins, D.N.; Srivastava, R.K.; Shankar, S. *Mol. Cell. Biochem.* **2013**, *373*, 217-227
[183] Kwatra, D.; Subramaniam, D.; Ramamoorthy, P. *et al. Evid. Based. Complement. Alternat. Med.* **2013**, Article ID 702869, 14 pages

We concluded that the natural products here reported could become lead compounds for the design of new analogues due to their structural and chemical diversity. The development of a single “magic bullet” that will eliminate CSCs and therefore prevent the development of metastasis, drug resistance, and relapse is an attractive purpose.

6. Conclusions

During my three years of PhD, I've been focusing my attention on the study of natural products as building blocks and lead compounds for active pharmaceutical ingredients production. The research activity regarded seven different topics that could be grouped in four main fields:

- Natural products and large scale production of Active Pharmaceutical Ingriedients (API)
  - ✓ Industrial synthesis of vincamine
  - ✓ Synthesis of lignan derivatives
  - ✓ Synthesis of cytisine derivatives
- Isolation and structural characterization of natural products
  - ✓ Isolation and structural elucidation of natural products from *Voacanga africana*
- Natural products as lead compounds
  - ✓ Synthesis of doliculide analogue
  - ✓ Pironetin-dumetorine hybrid compounds
- Natural products and cancer stem cells

These topics have in common the natural products as critical point, underling the importance of Nature as a source for medicinal products.
It is clear that nature will continue to provide interesting inspirations for the discovery, design and synthesis of new drug leads.

7. Acknowledgments

This research work was performed thanks to a scholarship financed by Linnea SA, a high-quality manufacturer of botanical exracts and pharmaceutical ingredients of natural origin for use in the pharmaceutical, nutraceutical and cosmetic industries.
I want to thanks COST Action CM1407 (Challenging Organic Synthesis Inspired By Nature: From Natural Product Chemistry To Drug Discovery) for the financial support for international collaboration with Prof. Karl-Heinz-Altmann (ETH-Zurich).